
UNIVERSITAT POLITÈCNICA DE VALÈNCIA

Programa de Doctorado en Matemáticas

Centro de Tecnologías Físicas: Acústica, Materiales y Astrofísica



Research of the acoustic phenomenon produced by isolated scatterers and its applicability as a noise reducing device in transport infrastructures. Search for an optimised and sustainable design.

Memoria presentada por:

M^a DEL PILAR PEIRÓ TORRES

Para optar al Grado de Doctor por la

UNIVERSITAT POLITÈCNICA DE VALÈNCIA

Dirigida por los Doctores

Dr. JUAN VICENTE SANCHEZ PÉREZ

Dr. FRANCISCO JAVIER REDONDO PASTOR

Dr. JUAN JOSÉ MARTÍN PINO

Valencia, enero de 2021

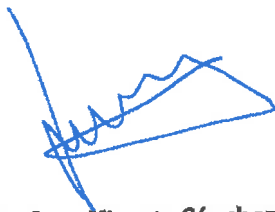


Dr. JUAN VICENTE SÁNCHEZ PEREZ, Catedrático del Departamento de Física Aplicada de la Universitat Politècnica de València, y Dr. FRANCISCO JAVIER REDONDO PASTOR, Profesor Titular del Departamento de Física Aplicada de la Universitat Politècnica de València, y Dr. JUAN JOSÉ MARTÍN PINO, Jefe de Laboratorio de Materiales de la empresa BECSA, S.A.U.

CERTIFICAN: que la presente memoria "*Research of the acoustic phenomenon produced by isolated scatterers and its applicability as a noise reducing device in transport infrastructures. Search for an optimised and sustainable design.*" Ha sido realizada bajo su dirección por Dña. M^a del Pilar Peiró Torres, en el Departamento de Física Aplicada de la Universitat Politècnica de València, y constituye su tesis para optar al grado de Doctor.

Y para que así conste, presentan la referida tesis, firmando el presente certificado.

Valencia, octubre de 2020



Fdo. Dr. Juan Vicente Sánchez Pérez



Fdo. Dr. Francisco Javier Redondo Pastor



Fdo. Dr. Juan José Martín Pino



Agradecimientos

En primer lugar, me gustaría agradecer al Director del Departamento de Innovación y Nuevas Tecnologías D. Francisco José Veá Folch, por apostar por mí y por este proyecto, y apoyarme en la consecución de esta tesis desde el primer momento. También a Dña. Mireia Ballester Ramos, por guiarme tanto en mi integración en la empresa como respecto a los procedimientos de la misma, por tener una paciencia infinita en mi proceso de aprendizaje.

Agradecer a mis tutores Dr. Juan Vicente Sánchez Pérez y Dr. Francisco Javier Redondo Pastor, por la oportunidad que me han brindado. A Juan Vicente por ofrecerme desarrollar esta tesis en su grupo de investigación y acogerme desde el primer momento como uno más. A ambos por ayudarme SIEMPRE, por enseñarme TODO lo que sé de acústica y continuar guiándome hasta el último momento de redacción de la presente memoria de tesis. También quería mencionar la ayuda que me ha ofrecido siempre el Dr. Sergio Castiñeira Ibáñez, sin cuyos conocimientos y enseñanzas, no me habría sido posible realizar el trabajo, las simulaciones y ensayos experimentales que he precisado para el desarrollo de esta tesis. Asimismo, agradecer el apoyo del resto del grupo de investigación Sonic Crystals Technologies, al Dr. Jose M^a Bravo Plana-Sala y al Dr. Marcelino Ferri García.

A mis padres por apoyarme en esta y todas las aventuras que he iniciado. A mi madre por empujarme a seguir formándome siempre. A mi hermano Víctor por sus consejos. Y a Paco por aceptar el pacto de cuatro años encargándose de todo aquello a lo que yo no he alcanzado, por las tardes de parque, extraescolares y tutorías, por las noches de baños y cuentos, en definitiva por ser papá y mamá durante mucho tiempo. Y a Fran y Blanca más que agradecerles me gustaría pedirles disculpas, perdón por el tiempo perdido, por los veranos empleados en estancias internacionales, por las noches invertidas en la tesis, por los fines de semana de trabajo, por el estrés no manejado adecuadamente. Pedir perdón por las promesas incumplidas, por el “mañana tendré tiempo”, por el “mamá ya no se irá más” y recordarles que a mamá le gusta pasar tiempo con ellos y espera hacerlo algo más a partir de ahora.

Finalmente agradecer al Ministerio de Ciencia e Innovación por la ayuda concedida dentro del programa Doctores Industriales. Asimismo, a mi tutor en empresa Dr. Juan José Martín Pino, por posibilitar la realización de esta investigación dentro de la empresa BECSA. Al Departamento de Física Aplicada de la Universitat Politècnica de València, a la Comisión Académica del Programa de Doctorado de Matemáticas y al Centro de Tecnologías Físicas: Acústica, Materiales y Astrofísica.

Y también por qué no, a este “bicho” que nos ha tenido encerrados tantos meses, gracias COVID-19 por encerrarme en casa a escribir. No todo tenía que ser malo... Ahora sí, vete por donde has venido.

A todos, GRACIAS



A Paco, Fran y Blanca
con todo mi cariño



RESUMEN INGLÉS

Control of environmental noise is a major concern for advanced societies because of the resulting problems for citizens' health. One of the most widespread solutions for controlling noise in its transmission phase is the use of acoustic screens.

The emergence of new materials made up of arrays of isolated acoustic scatterers, called sonic crystals, is revolutionizing the field of acoustic screening. In recent years, acoustic screens based on sonic crystals have positioned themselves as a viable alternative to traditional acoustic screens, as they offer multiple advantages over current traditional solutions. This Doctoral dissertation compiles the advances in the field of acoustic screening using this type of sonic crystals.

However, there is still active research in this area which needs to be addressed and studied in order to apply this technology as noise reduction devices in transport infrastructures. Therefore, during the PhD student's training period, we have researched the acoustic phenomena produced by isolated scatterers in order to better understand the physical phenomena behind the latest designs of this type of screen.

One of these researches led to the discovery of interferences between the effects of resonance and multiple scattering of sonic crystals when occurring in nearby frequency ranges. Also we have designed a new noise reduction device based on sonic crystals, using multi-objective optimization tools, which would block and diffuse the noise. This new designing tool identified the need for a comparative study of the most commonly used simulation methods to estimate the performance of devices based on sonic crystals. Finally, we have carried out a psychoacoustic study that determined the perception of the annoyance reduction provided by acoustic screens based on sonic crystals and traditional barriers, determining whether the objective parameters that evaluate their performance match to the subjective response of the users.

RESUMEN ESPAÑOL

El control de ruido ambiental es una preocupación de primera magnitud para las sociedades avanzadas, debido a los problemas derivados que ocasionan en la salud de los ciudadanos. Una de las soluciones más extendidas para el control del ruido en su fase de transmisión es la utilización de pantallas acústicas.

La aparición de nuevos materiales formados por redes de dispersores acústicos aislados, denominados cristales de sonido, está revolucionando el campo del apantallamiento acústico, posibilitando el avance tecnológico de esta área. Así, en los últimos años, las pantallas acústicas basadas en cristales de sonido se han posicionado como una alternativa viable a las pantallas acústicas tradicionales, puesto que ofrecen múltiples ventajas frente a las soluciones actuales. En el presente trabajo se muestra primeramente una recopilación de los avances realizados en el campo del apantallamiento acústico mediante esta tipología de pantallas.

No obstante, aún existen líneas de investigación abiertas en esta área, que es necesario abordar para conseguir el objetivo de aplicar esta tecnología como atenuadores de sonido en las infraestructuras de transporte. Durante el periodo de formación de la doctoranda, se ha trabajado en algunas de las líneas de investigación activas en este campo del apantallamiento acústico.

Una de estas investigaciones condujo al descubrimiento de interferencias entre los efectos de la resonancia y la dispersión múltiple de los cristales de sonido cuando estos efectos se producen en rangos de frecuencia cercanos. También hemos diseñado un nuevo dispositivo de reducción de ruido basado en cristales de sonido, utilizando herramientas de optimización multiobjetivo, que permitan apantallar y reflejar de forma difusa el ruido. El empleo de esta nueva herramienta de diseño identificó la necesidad de realizar un estudio comparativo de los métodos de simulación más utilizados para estimar el rendimiento de los dispositivos basados en cristales de sonido. Por último, hemos realizado un estudio psicoacústico para determinar la percepción de la reducción de molestia que proporcionan las pantallas acústicas basadas en cristales de sonido y las barreras tradicionales, determinando si los parámetros objetivos que evalúan su rendimiento coinciden con la respuesta subjetiva de los usuarios.

RESUMEN VALENCIANO

El control de soroll ambiental és una preocupació de primera magnitud per a les societats avançades, a causa dels problemes derivats que ocasionen en la salut dels ciutadans. Una de les solucions més esteses per al control del soroll en la seua fase de transmissió en la utilització de pantalles acústiques.

L'aparició de nous materials formats per xarxes de dispersors acústics aïllats, denominats cristalls de so, està revolucionant el camp de l'apantallament acústic, possibilitant l'avanç tecnològic d'esta àrea. Així, en els últims anys, les pantalles acústiques basades en cristalls de so s'han posicionat com una alternativa viable a les pantalles acústiques tradicionals, ja que oferixen múltiples avantatges enfront de les solucions actuals. En el present treball es mostra primerament una recopilació dels avanços realitzats en el camp de l'apantallament acústic per mitjà d'esta tipologia de pantalles.

No obstant això, encara hi ha línies d'investigació obertes en esta àrea, que és necessari abordar per a aconseguir l'objectiu d'aplicar esta tecnologia com a atenuadors de so en les infraestructures de transport. Durant el període de formació de la doctoranda, s'ha treballat en algunes de les línies d'investigació actives en este camp de l'apantallament acústic.

Una d'estes investigacions va conduir al descobriment d'interferències entre els efectes de la ressonància i la dispersió múltiple dels cristalls de so quan estos efectes es produïxen en rangs de freqüència pròxims. També hem dissenyat un nou dispositiu de reducció de soroll basat en cristalls de so, utilitzant ferramentes d'optimització multiobjectiu, que permeten apantallar i reflectir de forma difusa el soroll. L'ús d'esta nova ferramenta de disseny va identificar la necessitat de realitzar un estudi comparatiu dels mètodes de simulació més utilitzats per a estimar el rendiment dels dispositius basats en cristalls de so. Finalment, hem realitzat un estudi psicoacústic per a determinar la percepció de la reducció de molèstia que proporcionen les pantalles acústiques basades en cristalls de so i les barreres tradicionals, determinant si els paràmetres objectius que avaluen el seu rendiment coincideixen amb la resposta subjectiva dels usuaris.

Index

1. Acoustic screens.....	12
1.1.- Introduction. Problem and noise control engineering.	12
1.2.- Physical principles.	13
1.3.- Good practices in the installation of acoustic screens. Legislation.	15
1.4.- Typologies of acoustic screens.....	17
1.5.- Research lines in the field of acoustic screens.....	22
2. Acoustic screen based on Sonic Crystals.....	23
2.1.- Sonic Crystals. Definition	23
2.2.- Application of Sonic Crystals to acoustic screens.	25
2.3.- Advantages and disadvantages of using Sonic Crystals for the design of acoustic screens.	27
2.4.- Current research lines on Sonic Crystals screens.....	29
3. References.....	30
4. Research areas developed in the thesis.....	38
4.1.- Open noise barriers based on sonic crystals. Advances in noise control in transport infrastructures.....	39
4.1.1.- Abstract.....	39
4.1.2.- Introduction	39
4.1.3.- Description of first and second generation of Sonic Crystals Acoustic Screens.	41
4.1.4.- Acoustic standardization and determination of the structural efforts in a wind tunnel	42
4.1.5.- Advantages of SCAS	45
4.1.6.- Conclusions	45
4.1.7.- References	46
4.2.- Interferences in locally resonant Sonic metamaterials formed from Helmholtz resonators.	49
4.2.1.- Abstract.....	49
4.2.2.- Discussion.....	49
4.2.3.- References	55
4.3.- Sonic Crystals Acoustic Screens and Diffusers.....	58
4.3.1.- Abstract.....	58
4.3.2.- Introduction	58
4.3.3.- Theoretical considerations.....	60

4.3.4.- Results and discussion	64
4.3.5.- Conclusions	71
4.3.6.- References	72
4.4.- Insertion loss provided by Sonic crystal acoustic screen – assessment of different estimation methods.....	75
4.4.1.- Abstract.....	75
4.4.2.- Introduction	75
4.4.3.- Simulation Methods Under Study.....	76
4.4.4.- Simulation Scheme and calculations.....	78
4.4.5.- Results and Discussion	81
4.4.6.- Conclusions	85
4.4.7.- References	86
4.5.- Correlation between objective and subjective assessment of noise barriers.	89
4.5.1.- Abstract.....	89
4.5.2.- Introduction	89
4.5.3.- Testing methodology	93
4.5.4.- Results of the listening test.....	100
4.5.5.- Discussion.....	106
4.5.6.- Conclusions	109
4.5.7.- References	110
5. Discussion.....	115
6. Conclusions.....	116
7. Further research.....	118

1. Acoustic screens

1.1.- Introduction. Problem and noise control engineering.

Noise can be defined as any sound that disturbs or is an unpleasant listening sensation for the receiver. This type of environmental pollution has special characteristics making it different from other types of pollution. It is a "clean" pollution, meaning that it disappears completely when the source ceases; and yet can be very disturbing to a large group of receivers while it lasts. As an example, a single motorbike riding at night through city streets can disturb the sleep of many citizens.

For decades, in developed societies there has been a growing awareness about noise pollution generated by human activity. As higher standard of living creates higher level of noise by factors such as industrial activity, entertainment, mobility, leading to a greater annoyance associated with the noise. There is a demand for development of techniques and devices to control this kind of pollution in order to achieve a quiet environment in advanced societies.

The main source of noise produced by human activity is due to the transport of passengers and goods. In particular, the activity which produces the most noise is road transport, followed by air and rail transport. Other noise-generating activities are industrial, building sites and activity of citizens. Focusing on the main source of noise, road transport, the main factor which determines the level of noise is traffic density, but other factors such as the state of the vehicle, the types of vehicles, the speed at which they are driven, or the type of road surface also play a role.

The disturbance caused by noise has been present since ancient times. There are documents that indicate that in the Roman Empire, in the time of Julius Caesar, there was awareness about noise and its interaction with the sleep disturbance of the citizens. Because of this, Rome and other cities in Italy had regulations in place to try to mitigate the night-time noise that chariots made when circulating on the cobbled Roman roads [1]. Much later, at the end of the 19th century, the invention of the combustion engine brought about a revolution in transport, but it also created noise problems that were evident at the beginning of the 20th century [2]. It was not until the 1960s, however, that the first noise barriers began to be installed in the United Kingdom, made up of wood or earth mounds [1].

Nowadays, environmental noise is a major problem with health consequences for those exposed to it. The World Health Organization (WHO) published a guide on the acceptance of environmental noise in 1980 [3], and the Organization for Economic Cooperation and Development concluded that traffic noise did not cause immediate risks of hearing loss, but did cause other negative health effects [4]. Indeed, exposure to excessive noise levels can lead to changes in blood pressure, gastrointestinal disorders, hypertension, circulatory and cardiac disorders, etc. [5]

The publication of the WHO recommendations on limitations of environmental noise, which determined the exposure levels above which noise could present a risk to health, marked a change in society's position towards the sources of noise emission referred above. The levels were set at 55dB_{L_{Aeq}} during the day and 35dB_{L_{Aeq}} during the night inside

dwellings to facilitate rest, which meant, depending on the insulation of the dwellings, an outdoor level during night of approximately $45\text{dB}_{L_{Aeq}}$ [3]. This was a starting point for the development of all the noise regulations that would be gradually developed at a European scale initially, and later adapted at a national scale by each of the member countries.

Thus, after this WHO publication, noise was already considered, within environmental pollution, as a serious problem to be tackled by the different Administrations, focusing on urban areas as the most conflictive zones. Noise control is a multidisciplinary task in which many actors are involved, both politicians who dictate the legislation in this respect and sociologists, doctors, scientists and of course engineers. The control measures that may be implemented can be of various types, administrative, educational, informative and technical.

Focusing on technical noise control measures, these can be classified according to the noise transmission phase in which they operate. The control of high noise levels can either be done at the sound source, in the noise transmission phase from the source to the receiver, or be done at the receiver.

Some of the measures taken to reduce the problem at the source include improving vehicle technology by developing quieter engines, controlling traffic by reducing densities or speeds, or in the case of rolling noise, using porous asphalt or asphalt with rubber or plastic aggregates that absorb and partially mitigate the noise emitted. [6, 7, 8, 9]

With regard to the measures for action in the receiver, these are mainly focused on the progress made in improving materials to try to achieve better sound insulation of buildings, or on improving the design of external facades.

Finally, among the measures that act in the phase of transmission of noise from the source to the receiver, there is the implementation of an appropriate urban planning, separating those uses that are sources of noise from residential areas, increasing the distances between different urban uses through the planning of green areas, open spaces, or even compatible uses or activities. However, when this adequate urban planning has not been previously carried out, the most commonly used action is the installation of acoustic barriers. In this document we will focus on the development of these noise reducing devices, designed using new materials called Sonic Crystals (SCs).

1.2.- Physical principles.

We define screen or acoustic barrier as that element placed between the source and the receiver, which attenuates the sound in its transmission phase, interposing itself in the line of advance of the acoustic waves.

The physical working of the barrier can be explained in the following way, as shown in Figure 1: When we interpose an acoustic barrier in the noise transmission line from the source to the receiver, a large part of the acoustic energy is reflected back to the source of the noise, part of the direct noise that reaches the barrier is transmitted through it, part is absorbed if the barrier has absorbent materials, and a good part of the incident energy is diffracted by the upper or lateral edges of the barrier. If the barrier has devices that allow

this, the reflected sound could also be diffused towards the source of the sound in all directions, avoiding specular reflections.

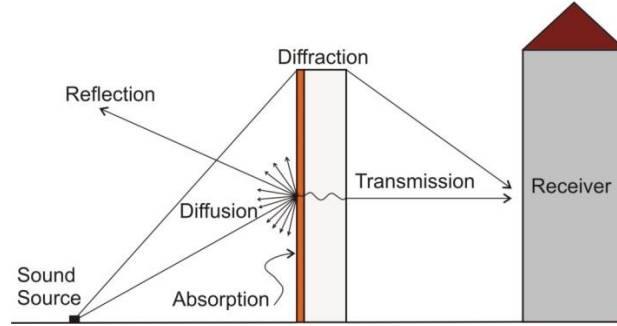


Figure 1: Diagram of the acoustic performance of a screen

Traditional acoustic barriers are made up of continuous walls and base their effectiveness on the mass law, considering that the energy transmitted through them is negligible if materials with densities greater than 20 kg/m^2 are used for their construction. The effectiveness of acoustic barriers varies with the frequency of the noise they screen, being low frequencies the most difficult to screen. In order to be able to evaluate the noise control capability of these devices, standards describe and regulate the ways in which this frequency attenuation is grouped into a "single number", weighing the importance of the different sound frequencies with respect to both the response of the human ear through the use of "A" isophonic curves, and with respect to the standardised traffic noise spectrum [10].

The indices defined in the standard are, first of all, those that quantify the airborne noise isolation of a barrier [11], calculated by the formula:

$$DL_R = -10 \log \left| \frac{\sum_{i=1}^{18} 10^{0,1L_i} 10^{-0,1R_i}}{\sum_{i=1}^{18} 10^{0,1L_i}} \right| \quad (1)$$

Being R_i the sound reduction index in the i^{th} third octave band and L_i the sound pressure level within the i^{th} one-third octave band of the A-weighted traffic spectrum, as defined in the standard [10].

Secondly, the standard [12] also defines the overall sound absorption capability of the screens, such as:

$$DL_\alpha = -10 \log \left| 1 - \frac{\sum_{i=1}^{18} \alpha_{si} 10^{0,1L_i}}{\sum_{i=1}^{18} 10^{0,1L_i}} \right| \quad (2)$$

Being α_{si} the sound absorption coefficient within the i^{th} third octave band.

However, the insulation capability that a noise barrier can provide will depend not only on these intrinsic characteristics defined previously by the above indices, but also on other factors such as the dimensions of the barrier, its location with respect to the source and receiver, the type of noise it is intended to screen, the type of ground or the topography of the adjacent area. To determine the acoustic performance of these devices taking into account these extrinsic factors, the index called insertion loss is usually used, defined as the difference between the sound pressure level before and after the screen has been installed:

$$IL = LP_{before} - LP_{after} = 20 \log \left| \frac{P_{direct}}{P_{inter}} \right| \quad (3)$$

This index expresses the relationship between the direct sound pressure reaching the receiver (P_{direct}), before the screen is installed, and the pressure reaching the receiver after it is interposed (P_{inter}), as indicated in the corresponding standard [13].

These insertion losses evaluate the screening capability of the acoustic screens, which would always be limited due to different factors, but mainly due to the diffraction produced at the edges of the screens [14]. Due to the loss of acoustic performance produced by this diffraction, as mentioned in section 1.4 of this document, the reduction of this phenomenon represents one of the main lines of research in the field of acoustic barriers.

On the other hand, and in order to increase the effectiveness of traditional acoustic barriers, attempts have been made to incorporate into these devices other noise control mechanisms in addition to reflection.

The acoustic absorption that some of the barriers offer in their performance is mainly due to the fact that they incorporate absorbent material on the surface that is exposed to the noise source, thus providing a considerable increase in their acoustic performance. The most effective and used are the metallic acoustic barriers composed of sandwich panels of sound absorbent material such as rock wool protected by means of a perforated steel panel on the side exposed to the noise source.

Other mechanisms also used in the barriers to increase their acoustic performance are the installation of Helmholtz resonators that attenuate the noise at specific frequencies, or acoustic diffusers that prevent specular reflections.

1.3.- Good practices in the installation of acoustic screens. Legislation.

Only those screens that have been previously certified can be placed in public road infrastructures. For the certification of this type of device, there are standards that have been developed over the last few decades.

All these standards have been drawn up by The European Committee for Standardization (CEN) since 1997. Specifically for this area, it is the CTN135/SC6 committee that is continuously reviewing the standards that are applicable for the certification of noise reduction devices that are placed on roads. Railway management bodies usually publish their own guidelines for screens installed in this other type of infrastructure. All the regulations applicable to the certification of noise-reducing devices can be consulted in publications which include the state of the art [15].

As mentioned above, these standards define the test methodology that determines the frequency acoustic performance and the formulas to group this acoustic performance into a "single number". However, as mentioned in the previous section, when determining the real effectiveness of a screen, attention must be paid to other extrinsic factors such as the place where the screen is located with respect to the noise source and the receiver, the environment of the screen, etc.

These extrinsic variables are analysed prior to the installation of the noise reducing devices, when the acoustic adaptation project is being drafted. This project defines the necessary protection for the receiver and, based on this, the necessary insulation that the barrier must provide, its height, length and location in order to try to guarantee the acoustic protection of the dwellings adjacent to the noise source, as well as the resistant calculations of the structure and the foundation of the barriers, which must withstand the loads to which the structure is subjected on a long-term basis.

The distance of the barriers from the sound source and the height of the buildings to be protected will determine the height of the noise reduction devices. An excessively high sound barrier can be a visually intrusive element, and will usually require large volumes of foundation due to the wind load it has to withstand. For this reason, it is sometimes necessary to carry out a detailed study of locations that minimise their height. Thus, options such as the installation of intermediate barriers in the central reservations of double lane roads must be studied, which could allow these devices to be brought closer to the source of noise, and in this way minimise the barrier heights required to ensure noise protection at the highest flats of the buildings adjacent to these infrastructures.

In order to calculate the foundation required for the placement of the barriers, it is necessary to know not only the loads that the device must support, but also the characteristics of the ground where it will be installed, since these factors will determine the volume of the foundation and its structure. In some cases, where the wind load to be supported is very high, it may even be necessary to use deep foundations made up of steel or concrete piles. These foundations are of vital importance for the stability of the barriers, and constitute a very important part of the implementation cost.

But it is not only the acoustic performance and the structural calculation that must be taken into account when determining the type of barrier to be placed. It is increasingly necessary to take into account environmental criteria. In this sense, the standards committee is in the process of approving the regulations on sustainability, which will help to determine how to evaluate and classify the environmental impact of noise-reducing devices.

Other aspects to be taken into account when placing acoustic barriers are their impact on the landscape, the interruption of breezes, microclimates, the passage of birds and wild species, or the visual impact, all of which have an impact and a reduction in the landscape which must also be taken into account. A noise barrier, even if it achieves its purpose of reducing noise, will not be successful if it does not achieve the acceptance of the population which it is intended to protect. This is one of the reasons why noise barriers should be integrated with their environment, not deteriorate it.

It is therefore important to consider how the installation of the barriers will affect the urban environment and citizens, since sometimes the best acoustic results are in contrast to the generation of a suitable urban environment. Thus, it should be taken into account that the reason for placing this type of device is to provide quality environments to the areas where they are placed. If the installation of acoustic barriers is opposed to this objective, resulting in a negative quality experience (acoustic or visual), the use of other

types of barriers or other noise control measures should be considered, always seeking compromise solutions.

Furthermore, the cost, both of manufacturing and of implementing the barriers, is a very important condition when it comes to projecting this type of device. Generally, better solutions (more effective and with less impact on the landscape) require higher costs, so it will be necessary to arrive at solutions of designs and materials that make the improvement of the acoustic and visual environment compatible, but with a reasonable cost.

Finally, the durability of the acoustic devices must be guaranteed in the long term, as stated in the current standards, with regard to both acoustic and non-acoustic characteristics [16, 17]. The maintenance required by these devices and the monitoring of the recommendations provided by the manufacturers must be taken into account in order to guarantee adequate structural and acoustic resistance throughout the service life of the screens.

In summary, for the successful placement of an acoustic screen, the following general requirements must be taken into account [1]:

- It must be acoustically effective.
- It must achieve the structural requirements.
- It must achieve durability requirements.
- It must achieve safety requirements
- It must achieve the environmental requirements.
- It must have a minimal impact on the landscape and be accepted by the neighbouring population.
- It must be adapted to the environment where it is placed.
- It must require minimum maintenance.
- Its manufacturing and installation cost must be competitive with other solutions on the market.

To achieve these objectives, the market offers a wide variety of screen types.

1.4.- Typologies of acoustic screens.

There are different classifications of acoustic screens depending on their shape (vertical, cantilever, tunnel...), on their integration with the existing environment between the transport infrastructure and the area to be protected (buildings, plants...), or on the materials they are made of (concrete, wood, metal, plastic, earth mounds, vegetation...). Based on the classification criteria according to the control mechanisms used by the screens, we find four main typologies: **reflective screens, absorbent screens, reactive screens and other new typologies**. In this section we will describe the most commonly used of each of these typologies. Within the reflective ones, transparent and concrete screens will be described; within the absorbent screens, the metallic ones with sandwich panels will be described, which also have reflective characteristics; and finally, the reactive screens and other new typologies that are currently emerging as a result of the technology development in this area will be described.

Reflective screens

Reflective screens are those whose main mechanism for acoustic screening is the reflection of the sound that is produced due to the change in impedance of the medium through which the wave is transmitted. Thus, most of the sound is reflected and is conducted back to the noise source and some is diffracted by the edges. Because of this, its performance is limited. However, it is the only type of traditional acoustic screen that can offer transparency of vision. These acoustic screens can be made of any rigid material such as wood, concrete, plastic, etc. Within this type of screen, we will describe in this section the transparent ones and the concrete ones, as the most used.

Transparent acoustic screens

Transparent screens are reflective screens used to minimise the landscape impact of barriers, even if only partially.



Figure 2: Transparent acoustic screen.

They are composed of laminated glass, acrylic, polycarbonate, methacrylate or any other material that presents transparency and adequate resistance. The acrylic or combined option is the most commonly used to prevent damage in the event of an accident or vandalism.

The main disadvantage, apart from their limited acoustic performance, is the fact that the birds do not detect them, so it is common for them to hit the screens in flight. In order to avoid this problem, many road administrations have designed different graphics on the screens so that the birds can detect the barrier, but reducing its transparency. In some countries, such as Portugal, it is very common to draw the figure of a bird of prey in order to scare off the rest of the birds.

Another characteristic to take into account when placing these types of barriers is the maintenance they require. Cleaning them is essential to prevent them from degrading the urban environment in a short time, and from causing the opposite effect to that expected from their installation. In addition, acrylic materials lose transparency over time. Therefore, when these are placed, it will be necessary to plan the places of access so that the cleaning and maintenance teams can carry out their work safely.

Concrete acoustic screens

Concrete barriers are considered to be reflective due to the density of the material they are made of. Concrete is also a very versatile and mouldable material that allows the construction of different textures on the surface of the screen. In some cases, the concrete used is porous concrete, so it can present certain characteristics of partial sound absorption, providing a new mechanism for noise control and slightly improving the effectiveness of the screens.



Figure 3: Concrete acoustic screen.

Prefabricated reinforced concrete panels are commonly used, which allow the barriers to be assembled quickly, or reinforced concrete panels executed on site by using formwork can also be applied. These concrete panels are usually used in combination with metal or concrete structures that make up the resistant structure of the whole, thus allowing the installation of large screen heights.

These barriers are suitable for urban environments, due to the industrial aspect of concrete. In other rural environments, they can be used in combination with bush or trees to give them a more organic appearance which improves their integration with the landscape.

Absorbent screens

Absorbing screens are those that present a porous material on the side exposed to the road traffic in order to provide certain absorption of the noise. This porous material can be mineral wool (the most effective) or any other absorbent material. These sound absorption properties, in combination with rigid materials, provide screens with high acoustic performance.

To ensure durability and maintain the acoustic properties of the absorbent material, it must be protected from the weather by means of a perforated metallic panels or some type of geotextile.

Also considered as absorbent screens are those that are made of rigid materials manufactured in such a way that they have small pores to give them certain absorbent characteristics, as is the case with those made of porous concrete. Here we will describe the most commonly used, the metallic acoustic screens combined with rock wool.

Metallic acoustic screens

Metal, of different types, is the material normally used to protect the absorbent material used in this type of barrier, although there are also metal barriers that are only reflective.



Figure 4: Metallic acoustic screen.

Due to its lightness and resistance to corrosive processes, aluminum is one of the most commonly used metals. However, other metals with anti-corrosion treatments are also used, such as galvanised steel.

In the last decades, the use of this type of screens has become extremely widespread as it has high acoustic performance, structural advantages and minimal maintenance. The corrosive processes that can occur with screws and welding joints represent the greatest disadvantage of this type of barrier, especially if they are exposed to adverse weather or aggressive environments such as coastal areas, where their use is not so recommended.

Reactive screens

These barriers incorporate different noise control mechanisms on the side exposed to the noise source, such as diffusers or resonant cavities.

Diffusers provide the opportunity to vary the direction of the reflected sound, and to cause the reflection to occur in a diffuse rather than a specular manner. This can be essential to avoid multiple reflections that could drive the sound into the areas to be protected.

Resonant cavities on the side exposed to traffic are also used, which attenuate the sound at a specific frequency. These cavities resonate at one frequency or another depending on their geometric characteristics. In this way, some frequencies are not transmitted through the screen, nor are they sent back to the sound source.

These mechanisms, combined with reflection as the main mechanism, increase the effectiveness of the acoustic screens.

New acoustic screens

Currently, the degree of technological evolution in the field of noise barriers cannot be considered high if we attend to the low number of publications in scientific journals in the last 15 years regarding this topic. Nevertheless, and thanks to the advance of other technologies that are integrated into these devices, it is possible to incorporate new

functionalities, the development of new geometric designs and the use of new materials. Thus, the advance of photovoltaic technology would allow the introduction of new functionalities in this type of device; the design of new geometries would be possible with a detailed study of the location of the screens, and the introduction of new materials such as SCs would make it possible to develop new screens with better acoustic features that could be better than those of the currently available screens.

Thus, and since the acoustic barriers are made up of vertical walls of many flat square meters located at the roadside, these could represent a large surface area that could be used to obtain photovoltaic energy if they were properly oriented. For this reason, there are already developments which attempt to implement photovoltaic panels in the acoustic screens, although these are still in an experimental phase [18].

Another recent innovation in the area of acoustic shielding is the use of low-level barriers. In order to achieve similar, or even better, acoustic performance than traditional acoustic barriers, low-height acoustic screens must be placed very close to the source of the noise; due to this, their application is limited to rail transport, screening out rolling noise. [19].



Figura 5. Low height screen placed in railway infrastructure.

Acoustic screens based on SCs involve the incorporation of new materials for screening. This type of screen will be further developed in later sections of this document.



Figure 6: Sonic Crystal Acoustic Screen.

1.5.- Research lines in the field of acoustic screens

Noise barriers are the most commonly used noise reduction devices in the transmission phase from the source to the receiver. As mentioned in previous sections, the acoustic performance of these barriers depends largely on the surface mass of the barrier.

Many investigations have been carried out to increase the acoustic performance of traditional barriers, either by tilting the reflective panels, adding absorbent or diffusing materials, or by varying their geometry and location.

The installation of tilted barriers enables the acoustic protection of the last heights of adjacent buildings, requiring lower heights of acoustic screens and, furthermore, solves the possible problems of multiple reflections that reduce their performance [20]. However, the solution is expensive and requires large volumes of foundations. Other solutions to control reflected sound are the inclusion of absorbent material in the vertical walls, or the use of surfaces that diffuse the sound [21], although the experimental results provided little improvement in acoustic performance.

In any case, one of the major problems of the acoustic screening strategy is edge diffraction, which allows a good part of the acoustic energy to reach the receiver, thus reducing the effectiveness of this type of device. Due to this, the main research line developed in the field of acoustic barriers is based on the inclusion of special devices on the edges of the screens, or the modification of the shape of the tops to try to minimise the effect of edge diffraction and increase the performance of these devices [22, 23, 24, 25, 26]. Motivated by this great variability of edge devices, the methodology by which their effectiveness was evaluated was standardised [27].

However, with the exception of some Y- or T-shaped devices with reactive surfaces, which have achieved up to 10 dB improvement [28, 29], the rest of the devices developed have provided little improvement over the straight edges of traditional barriers. Other strategies used to minimise this effect have been the installation of absorbent material at the edges of the screens [30] or the installation of active cancellation devices [31]. Something more interesting seems to be the line of research that proposes that the barriers have irregular border edges in order to obtain wave fronts of different phases that can interact between them in a destructive way. Several papers have been conducted on this promising line of research [32, 33], although subsequent "in situ" tests have shown that the improvement was only 2 dB over traditional forms [34]. Also, other work has analysed the placement of resonant cavities at the edges, designed for a certain frequency to try to minimise this diffraction [35].

Despite the extensive literature that is published about the design of these types of edge devices, their use has not been widespread in practice, perhaps because the ratio of effectiveness achieved to the cost of installation is too low.

2. Acoustic screen based on Sonic Crystals.

2.1.- Sonic Crystals. Definition

We can define sonic crystal (SC) as a heterogeneous material consisting of two media, acoustic scatterers arranged in a periodic array and a host medium in which they are embedded. These two media have different physical properties. Thus, both the density of the materials that make them up and the speed of sound propagation are different. These differences in physical properties between the two media make possible a physical phenomenon called multiple scattering.

Multiple scattering is related with the transmission properties of these new materials and occurs when a wave that is transmitted on the host medium impinges on a SC and then is reflected due to the acoustic scatterers that compose it [36]. Thus, the field that impinges on each scatterer will be formed by the combination of the fields scattered by the other scatterers and the incident wave. This physical phenomenon, based on Bragg's law, makes possible the existence of forbidden bands of propagation, that is, frequency ranges in which the waves are not transmitted through the SC. These forbidden bands are called **bandgaps (BG)**.

The application of SCs to acoustic screens could be done with any type of crystal (monodimensional, two-dimensional or three-dimensional) but, for technical reasons, the most commonly used are two-dimensional crystals. Within the two-dimensional crystals, different shapes of scatterers could be adopted, the simplest being those formed by cylinders. These scatterers are symmetric on any axis of the section perpendicular to the generatrix. Thus, these SCs present a periodicity along the x and y axes, and there is no variation of properties in the z axis.

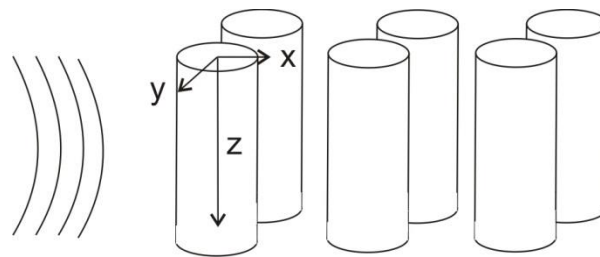


Figure 7: Bidimensional sonic crystal formed by cylindrical scatterers.

The acoustic scatterers are the **bases** of the crystal, i.e. nodes of rigid material that have a higher impedance than the fluid medium (air) in which they will be arranged in a **crystalline lattice**.

The **Bravais lattices** specify the way in which the bases are periodically arranged in space. In two dimensions these arrays are five (square, hexagonal, rectangular centred, rectangular primitive and oblique). Figure 8 shows the most commonly used arrays in two-dimensional SCs, the square and the hexagonal one, the latter being usually referred to in this area as the triangular array.

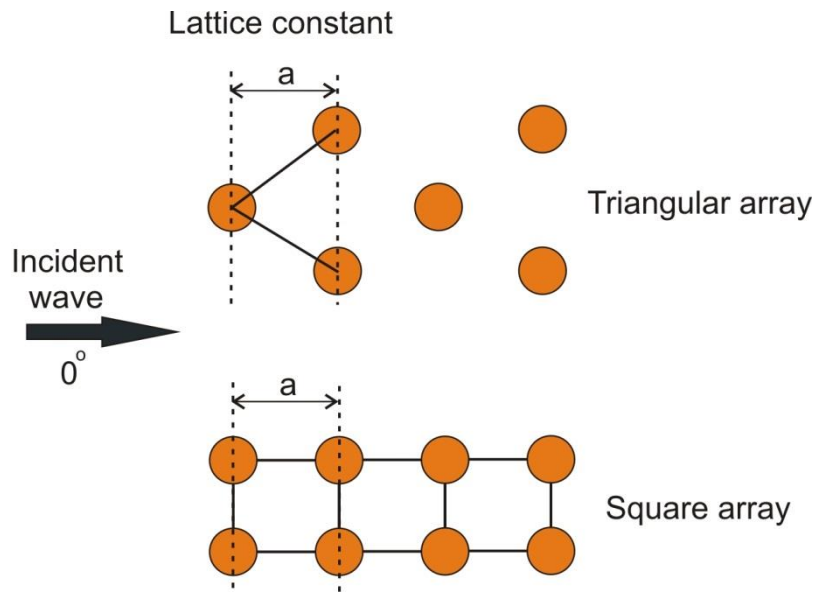


Figure 8. Bidimensional sonic crystals, triangular and square.

The **lattice constant** (a) is defined as the distance between the rows of scatterers perpendicular to the incidence direction of the wave. (figure 8).

As indicated, there are frequency bands that are not transmitted through a SC. The position of these noise attenuation bands in the frequency spectrum, which we will call the Bragg frequency (f_{Bragg}), will be established by the lattice constant according to the Bragg law. In the case of SCs, the scatterers are not punctual, but they have a certain volume. This makes it possible for the attenuation not only to occur for a single frequency but to extend over the frequencies adjacent to the Bragg frequency around which the attenuation band will appear. Thus, the Bragg frequency only indicates approximately the frequency around which the BG occurs. The BG has a certain height and width (Figure 9), and this affects the frequencies adjacent to the Bragg frequency to a smaller degree.

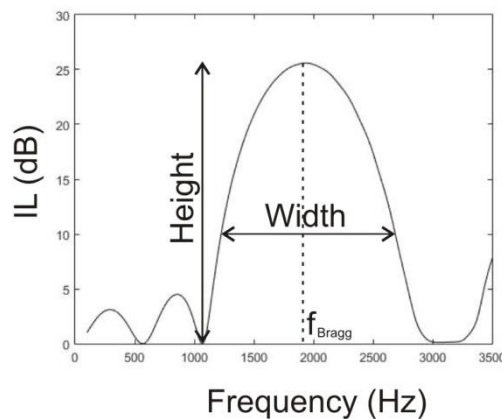


Figure 9 Insertion Loss (dB) vs frequency (Hz) of a SC.

The height and width of the BG depends on several factors. The **filling fraction** is defined as the fraction between the volume occupied by the scattering medium, and the total volume of the crystal. This filling fraction will establish the width of the BGs. The height of

the BG will depend on the number of rows that make up the SC. It has been demonstrated that an arrangement of 3 rows of scatterers would be enough to obtain remarkable BGs [37].

2.2.- Application of Sonic Crystals to acoustic screens.

Since the existence of BG was discovered and demonstrated in the propagation of acoustic waves through periodic scatter arrays due to a mechanism called multiple scattering [38], several research groups have tried to apply this physical phenomenon to the design of noise reduction devices [39]. In fact, by using bidimensional SCs and appropriate lattice constant and filling fractions, some of the studies were able to obtain insertion losses of up to 25 dB [40, 41] for specified frequency ranges.

Firstly, it was necessary to investigate the theoretical aspects of the physical phenomenon, so the studies focused on observing and trying to understand the phenomenon of wave propagation through SCs. Thus, a large number of articles were devoted to the study of the physical properties of waves transmission and reflection in SCs [42, 43, 44, 45].

Indeed, the existence of this new noise control mechanism, multiple scattering, made it possible the use of SCs as acoustic screens. Thus, the first work that experimentally demonstrated that these new materials could be used as acoustic screens in free field conditions dates from 2002 [46]. Experimental analyses of sound transmission in SCs formed by arrays of 2D cylinder had already been carried out [39], demonstrating the existence of BG in the audible frequency range [47].

Based on these results, research efforts have focused on studying the best designs for scatterers that would allow for less transmission, i.e. higher insertion losses. Thus, different scatterer geometries were tested, square [48], rectangular [49], triangular [50] and cylindrical [51], the latter being the used most in the design of screens based on SCs due to their high symmetry. The influence of the size of the scatterers and the variation of the filling fraction have been studied [51, 52, 53], as well as the number of rows of scatterers that need to be implemented to obtain appreciable attenuations [54, 55].

To predict the acoustic performance of this type of screen, it has been necessary to develop several mathematical techniques and analytical models to estimate the propagation properties in SCs and enable more effective designs. Using bidimensional models, semi-analytical simulation methods based on the theory of Multiple Scattering (MS) have been developed to predict the propagation of the waves that interact with the SC [56].

There are other numerical methods that allow us to predict the acoustic performance of these new SCs-based acoustic screens that include more complex acoustic scatter designs. Thus, the use of these other methods made it possible to simulate new forms of scatterers, the incorporation of porous-elastic materials in them [57], the simulation of thermoviscose losses, and made it possible to increase the accuracy of the results. Numerical domain discretization methods were used such as the Finite Element Method (FEM) [58], a mesh method that solves the problem by discretizing the continuous medium into various connected finite elements. This methodology has also been used to simplify the calculations, transforming real three-dimensional problems into the sum of two two-

dimensional models [58, 59]. Another methodology that has made it possible the use of iteration techniques was the Finite Difference Time Domain (FDTD) method [60], a technique that works in time domain and allows with a single simulation to obtain results for a wide range of frequencies. To predict and evaluate the acoustic performance of SCs, new simulation methods have also been developed, such as the Boundary Element Method (BEM) [61, 62], which instead of meshing the whole domain, discretises only the boundary elements, thus requiring only the approximation of the geometry and variables of the problem at the boundary of the model, simplifying the calculation in complex geometries. And finally the Method of Fundamental Solutions (MFS) has been developed [55, 63, 64], which, in contrast to other methods, simplifies mathematical formulation and its implementation even more, since it is based on a linear overlapping of fundamental solutions to approximate the solution of the problem without using meshing.

Thus, once the possibility of using SCs in the design of noise control devices was confirmed, and the calculation tools were made available, research efforts were focused on increasing the attenuation capability of these screens, not only to increase the level of the attenuation, but also to increase the attenuated frequency range [65]. Standardised acoustic characterisation tests [54] have shown that the use of multiple scattering as the only noise control mechanism is not sufficient to design screens that can compete acoustically with traditional barriers.

Many strategies have been implemented to achieve the objective of extending the attenuation obtained to wider frequency ranges, either by acting on the type of array or by modifying the design of the acoustic scatterers. In the first case, new arrays of acoustic scatterers have been employed [66, 67, 68], using arrays in fractal scatterer structures [36], and also combining these fractal structures with optimization strategies to determine optimal filling fraction [69]. An attempt has also been made to attenuate a wider frequency range by modifying the scatterer array through the application of genetic optimisation algorithms [70, 71, 72]. In the second case, the design of the acoustic scatterers has been modified by including other noise control mechanisms. Thus, resonant cavities and absorbent materials were added to the scatterers [73, 74, 75, 76]. The possibility of incorporating multiple coupled resonators has also been studied [77] and the working of periodic arrays of 2D resonators has been analysed [59], demonstrating the possibility of using this type of material as an acoustic filter for low frequencies [78]. And as previously introduced, the incorporation of recycled rubber [79] or other absorbent materials in the scatterers [80].

Another line of research developed, and as was being carried out with traditional acoustic screens, consisted of analysing edge diffraction in this type of screen, using numerical models that separated the effects of multiple dispersion and edge diffraction to facilitate their analysis [81]. On the other hand, also in the case of SCs-based acoustic screens, an attempt has been made to reduce their visual impact by reducing their height [82, 83].

Finally, with a scatter design using resonance and absorption (Figure 13), the first SCs-based acoustic screen device has been certified according to standardised airborne sound insulation and absorption tests [84].

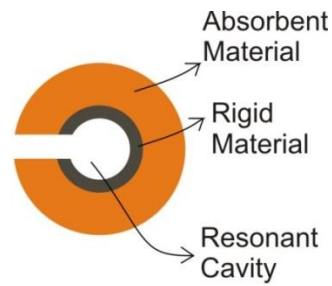


Figure 11. Multi-physics acoustic scatterer section

Some studies have also been carried out on the effect of wind on these screens, determining the reduction in the loads transmitted to the foundation in SCs-based acoustic screens, and comparing the results with those obtained in traditional barriers [85], concluding that the reduction in these efforts in the case of SCs-based screens is significant. Another advantage over traditional acoustic barriers has also been highlighted by studying in detail the interaction of SCs with sand, showing that this type of device would not cause dunes to form and demonstrating the viability of their implementation in desert areas [86].

Other applications for SCs have recently been explored, even proposing them to reduce specular reflections for aerospace applications [87].

Much progress has been made since studies began on the structures of simple cylindrical scatterers, up to the multi-physical scatterers with which this type of screen is currently designed. However, there is still a long way to be gone before SCs-based acoustic screens can be implemented in transport infrastructures, as there is not much work involving full-scale or real environment acoustic tests [65], which would demonstrate the viability of the product. The work included in this thesis report attempts to follow part of this way.

2.3.- Advantages and disadvantages of using Sonic Crystals for the design of acoustic screens.

As mentioned in previous sections, theoretical and experimental studies have shown the viability of the application of SCs in the design of acoustic screens with an acoustic performance comparable to traditional barriers. In this section, the advantages of using these new materials in the design of acoustic screens will be explained, as well as the disadvantages they present with respect to the installation of traditional acoustic barriers.

First of all, the most important feature that distinguishes acoustic screens designed with this new material from traditional ones, which are made up of continuous walls, is indeed the "open" nature of the SC. This open design offers a permeability to both wind and water that makes it possible to place them in locations where it would not be possible to use traditional barriers.

Due to the wind permeability of SCs-based screens, the loads transmitted to the foundation by this force are much lower than those of traditional barriers [85]. This advantage is very important for the placement of acoustic screens in areas with strong wind regimes, such as in the case of viaducts where the transmission of loads to the structure due

to wind load is so important that it prevents the installation of traditional barriers. Or for those locations where the aerodynamic loads that the vehicles themselves generate on their surroundings are so high that the effort calculations result in costly deep foundations, as is the case with high-speed trains [88, 89]. These open screens would make it possible to reduce the volume of the foundation.

On the other hand, its open nature also offers water permeability which is an advantage over traditional barriers when they are placed in flood-prone areas, or next to ravines and streams, where easy and quick water evacuation is required in the event of torrential rain. In many locations, the installation of traditional barriers makes it difficult to drain rainwater from transport infrastructures. To avoid this, the continuity of the installation of the barriers is interrupted in order to facilitate the evacuation of water, which drastically reduces their acoustic performance. However, the use of SCs-based acoustic screens allows for the evacuation of water while maintaining the acoustic performance of the device.

Another important advantage of SCs-based acoustic screens is that they incorporate a new noise control mechanism. Thus, these new screens, in addition to the mechanisms already used by traditional screens (reflection and, in some cases, absorption and resonance), also employ multiple scattering. This makes it possible to design acoustic screens “ad hoc”, allowing designs to be “tuned” to specific noise problems. Reflection and absorption are mechanisms that do not allow their effectiveness to be adjusted to the frequency of the noise they are designed to attenuate. Resonance does allow some adaptation to these frequencies, but the multiple scattering gives these screens a versatility with which traditional acoustic barriers cannot compete.

A major problem with traditional acoustic barriers is the aesthetic aspect. These traditional barriers can generate a certain amount of rejection on the part of the population, as they degrade the landscape in the area where they are placed and can generate a certain sensation of isolation. This typology of acoustic screens has a very careful design and aesthetic aspect that can produce greater acceptance by the population, as shown by their artistic origin, since the first experimental test that demonstrated the existence of the physical phenomenon was carried out on a sculpture by Eusebio Sempere [38].

Another advantage derived from the design composed of insulated acoustic scatterers is that, by having different elements, it offers greater possibilities of action in the face of the problem of diffraction of the upper edge [59]. As mentioned above, this effect minimises the effectiveness of the acoustic screens. These screens would make possible designs with scatterers at different heights, which could more effectively reduce this effect.

Among the disadvantages of this new type of screen is, firstly, the greater occupation space at the side of the infrastructure compared to the space required by traditional acoustic barriers. The cleaning work required is also a disadvantage, as the space between the scatterers must be kept free of obstacles and dirt, not only to maintain its permeability but also to ensure its effectiveness. However, the main disadvantage they present may be the low or even no attenuation achieved in some frequency bands. Because of this, many lines of research are focused on the study of solutions that try to affect a greater number of

frequency bands. Lastly, a final disadvantage is the higher manufacturing cost compared to traditional acoustic barriers, although the technological difference of these solutions may well be worth the extra cost.

2.4.- Current research lines on Sonic Crystals screens.

At present, research on the application of SCs to acoustic wave control devices is still active, with the aim of obtaining more technologically advanced devices. The most important lines where work is currently underway will be outlined below.

The physics behind the behaviour of SCs has been studied for more than 25 years and new effects are still being discovered today, which allow new applications of SCs to be obtained, such as the application to the development of invisibility covers [90], lenses [91], windows [92], silencers in ducts, diffusers [93, 94], reducing the effects of seismic waves [95] etc. Thus, in the field of acoustic screens, research continues in this area in order to gain a more in-depth understanding of the physical functioning of SCs and to achieve more technologically advanced and effective screens, or those with new functionalities.

In addition, the development of simulation methods based on new numerical techniques has allowed the simplification of the process of checking the effectiveness of SCs-based screens, improving the design processes. Thus, in order to develop these devices, powerful calculation tools are now available that allow the acoustic performance of the devices to be predicted before any prototype is manufactured. The validation of these methods by means of comparison with experimental results has enabled progress to be made in research, since by means of numerical results researchers were able to predict the performance of different designs, thus reducing the costs of research and the time taken to obtain results. Also, these numerical methods have allowed the emergence of iterative design techniques that test a large number of configurations and select the best ones, thus offering optimisation tools that make it possible to achieve the best, most efficient designs [71].

Another interesting line of research for acoustic screens is the study of the reduction of diffraction by the edge. As previously mentioned, the design based on isolated acoustic dispersions offers greater possibilities of action against this problem. This is an active line of research that aims to obtain designs that offer greater acoustic performance than traditional barriers.

Also, the challenge of achieving SCs-based screens that provide effective attenuation across the entire spectrum of standardised traffic noise has been noted above. To this target, work is being done not only on the design of the scatterers, but also on the geometry of the array, and the possibility of adding active noise control elements has even been analysed.

Finally, focusing on the case of SCs-based acoustic screens, it would be important to know the subjective response of citizens to this new type of acoustic barrier. This point is of particular interest in order to find out whether this new product would be well received by users. This line of research, which is very active in other areas of acoustic devices [96, 97] must also be taken into account by researchers and developers of SCs-based screens.

3. References

- [1] Kotzen, B., & English, C. (2014). Environmental noise barriers: a guide to their acoustic and visual design. CRC Press.
- [2] The Motor Cars (Excessive Noise) Regulations (1929). No 416, HMSO, London.
- [3] World Health Organization. (1980). Environmental health criteria 12: Noise. Geneva: WHO.
- [4] Organisation for Economic Co-operation and Development (1995) Roadside Noise Abatement, OECD, Paris, p.20
- [5] Cohn, L. F. (1981). Highway noise barriers. NCHRP Synthesis of Highway Practice, (87).
- [6] Lastra-González, P., Calzada-Pérez, M. A., Castro-Fresno, D., Vega-Zamanillo, Á., & Indacoechea-Vega, I. (2016). Comparative analysis of the performance of asphalt concretes modified by dry way with polymeric waste. *Construction and Building Materials*, 112, 1133-1140.
- [7] Morcillo López, M. A., Hidalgo, M. E., & Pastrana, M. D. C. (2019, September). LIFE SOUNDLESS: New Generation of Eco-friendly Asphalt With Recycled Materials. In *INTER-NOISE and NOISE-CON Congress and Conference Proceedings* (Vol. 259, No. 2, pp. 7852-7862). Institute of Noise Control Engineering.
- [8] Real, T., Zamorano, C., Hernández, C., García, J. A., & Real, J. I. (2016). Static and dynamic behavior of transitions between different railway track typologies. *KSCE Journal of Civil Engineering*, 20(4), 1356-1364.
- [9] Licitra, G., Moro, A., Teti, L., Del Pizzo, A., & Bianco, F. (2019). Modelling of acoustic ageing of rubberized pavements. *Applied Acoustics*, 146, 237-245.
- [10] EN 1793-3:1998 Road traffic noise reducing devices. Test method for determining the acoustic performance. Normalized traffic noise spectrum.
- [11] EN 1793-2:2018 Road traffic noise reducing devices. Test method for determining the acoustic performance. Intrinsic characteristics of airborne sound insulation under diffuse sound field conditions.
- [12] EN 1793-1:2017 Road traffic noise reducing devices. Test method for determining the acoustic performance. Intrinsic characteristics of sound absorption under diffuse sound field conditions.
- [13] CEN TS 16272-7:2015 Railway applications – Track – Noise barriers and related devices acting on airborne sound propagation – Test method for determining the acoustic performance – Part 7: Extrinsic characteristics – in situ values of insertion loss.
- [14] Maekawa, Z. (1968). Noise reduction by screens. *Applied acoustics*, 1(3), 157-173.
- [15] Clairbois, J. P., & Garai, M. (2015). The European standards for roads and railways noise barriers: state of the art 2015. In *Proc Euronoise*.

-
- [16] EN 14389-2: 2015 Road traffic noise reducing devices - Procedures for assessing long term performance - Part 2: Non-acoustical characteristics.
- [17] EN 14389-1: 2015 Road traffic noise reducing devices - Procedures for assessing long term performance - Part 1: Acoustical characteristics.
- [18] Vallati, A., de Lieto Vollaro, R., Tallini, A., & Cedola, L. (2015). Photovoltaics noise barrier: acoustic and energetic study. *Energy Procedia*, 82, 716-723.
- [19] Jolibois, A. (2013). A study on the acoustic performance of tramway low-height noise barriers: gradient-based numerical optimization and experimental approaches (Doctoral dissertation, Paris Est).
- [20] Slutsky, S., & Bertoni, H. L. (1998). Analysis and programs for assessment of absorptive and tilted parallel barriers. *Transportation Research Record*, 1176, 13-22.
- [21] May, D. N., & Osman, N. M. (1980). Highway noise barriers: new shapes. *Journal of Sound and vibration*, 71(1), 73-101.
- [22] Defrance, J., & Jean, P. (2003). Integration of the efficiency of noise barrier caps in a 3D ray tracing method. Case of a T-shaped diffracting device. *Applied Acoustics*, 64(8), 765-780.
- [23] Watts, G. (1993). Acoustic performance of new designs of traffic noise barriers. TRL Published Article, (PA 2191).
- [24] Watts, G. R. (1996). Acoustic performance of a multiple edge noise barrier profile at motorway sites. *Applied Acoustics*, 47(1), 47-66.
- [25] Watts, G. R., Morgan, P. A., & Surgand, M. (2004). Assessment of the diffraction efficiency of novel barrier profiles using an MLS-based approach. *Journal of Sound and Vibration*, 274(3-5), 669-683.
- [26] Umnova, O., Attenborough, K., & Linton, C. M. (2006). Effects of porous covering on sound attenuation by periodic arrays of cylinders. *The Journal of the Acoustical Society of America*, 119(1), 278-284.
- [27] EN 1973-4: 2015 Road traffic noise reducing devices. Test method for determining the acoustic performance. Intrinsic characteristics. In situ values of sound diffraction
- [28] Fujiwara, K., Hothersall, D. C., & Kim, C. H. (1998). Noise barriers with reactive surfaces. *Applied acoustics*, 53(4), 255-272.
- [29] Shima, H., Watanabe, T., Mizuno, K., Iida, K., & Matsumoto, K. (1996). Noise reduction of a multiple edge noise barrier. In *Inter-Noise 96 (Noise control: the next 25 years, Liverpool, 30 July-2 August 1996)* (pp. 791-794)
- [30] Economou, E. N., & Sigalas, M. M. (1993). Classical wave propagation in periodic structures: Cermet versus network topology. *Physical Review B*, 48(18), 13434.

-
- [31] Sigalas, M. M., Economou, E. N., & Kafesaki, M. (1994). Spectral gaps for electromagnetic and scalar waves: Possible explanation for certain differences. *Physical Review B*, 50(5), 3393.
- [32] Mizuno, K., Sekiguchi, H., & Iida, K. (1984). Research on a Noise Control Device: 1st Report, Fundamental Principle of the Device. *Bulletin of JSME*, 27(229), 1499-1505.
- [33] Iida, K., Kondoh, Y., & Okado, Y. (1984). Research on a device for reducing noise. *Transportation Research Record*, 983, 51-54.
- [34] Watts, G. R., & Morgan, P. A. (1996). Acoustic performance of an interference-type noise-barrier profile. *Applied Acoustics*, 49(1), 1-16.
- [35] Norris, R. C., Hamel, J. S., & Nadeau, P. (2008). Phononic band gap crystals with periodic fractal inclusions: Theoretical study using numerical analysis. *Journal of Applied Physics*, 103(10), 104908.
- [36] Castiñeira Ibáñez, S. (2015). Análisis y modelado de la fenomenología ondulatoria asociada al diseño de barreras acústicas basadas en conjuntos de dispersores aislados. Homologación de dispositivos (Doctoral dissertation).
- [37] García-Raffi, L. M., Romero-García, V., & Sánchez-Pérez, J. V. (2010, June). Determination of the thickness of sonic crystal acoustic barriers using evanescent modes. In *INTER-NOISE and NOISE-CON Congress and Conference Proceedings* (Vol. 2010, No. 10, pp. 1527-1535). Institute of Noise Control Engineering.
- [38] Martínez-Sala, R., Sancho, J., Sánchez, J. V., Gómez, V., Llinares, J., & Meseguer, F. (1995). Sound attenuation by sculpture. *Nature*, 378(6554), 241-241.
- [39] Sánchez-Pérez, J. V., Caballero, D., Martínez-Sala, R., Rubio, C., Sánchez-Dehesa, J., Meseguer, F., ... & Gálvez, F. (1998). Sound attenuation by a two-dimensional array of rigid cylinders. *Physical Review Letters*, 80(24), 5325.
- [40] Robertson, W. M., & Rudy III, J. F. (1998). Measurement of acoustic stop bands in two-dimensional periodic scattering arrays. *The Journal of the Acoustical Society of America*, 104(2), 694-699.
- [41] Chen, Y. Y., & Ye, Z. (2001). Theoretical analysis of acoustic stop bands in two-dimensional periodic scattering arrays. *Physical Review E*, 64(3), 036616.
- [42] Gupta, A. (2014). A review on sonic crystal, its applications and numerical analysis techniques. *Acoustical Physics*, 60(2), 223-234.
- [43] Morandi, F., Marzani, A., De Cesaris, S., D'Orazio, D., Barbaresi, L., & Garai, M. (2016). I cristalli sonici come barriere antirumore Sonic crystals as tunable noise barriers. *Rivista Italiana di Acustica*, 40(4), 1-19.. (In italian)
- [44] Sanchis, L., Cervera, F., Sánchez-Dehesa, J., Sanchez-Perez, J. V., Rubio, C., & Martínez-Sala, R. (2001). Reflectance properties of two-dimensional sonic band-gap crystals. *The Journal of the Acoustical Society of America*, 109(6), 2598-2605.

-
- [45] Sanchis, L., Håkansson, A., Cervera, F., & Sánchez-Dehesa, J. (2003). Acoustic interferometers based on two-dimensional arrays of rigid cylinders in air. *Physical review B*, 67(3), 035422.
- [46] Sanchez-Perez, J. V., Rubio, C., Martinez-Sala, R., Sanchez-Grandia, R., & Gomez, V. (2002). Acoustic barriers based on periodic arrays of scatterers. *Applied Physics Letters*, 81(27), 5240-5242.
- [47] Romero-García, V., Garcia-Raffi, L. M., & Sánchez-Pérez, J. V. (2011). Evanescent waves and deaf bands in sonic crystals. *Aip Advances*, 1(4), 041601.
- [48] Romero-García, V., Lagarrigue, C., Groby, J. P., Richoux, O., & Tournat, V. (2013). Tunable acoustic waveguides in periodic arrays made of rigid square-rod scatterers: Theory and experimental realization. *Journal of Physics D: Applied Physics*, 46(30), 305108.
- [49] Rubio, C., Castiñeira-Ibáñez, S., Uris, A., Belmar, F., & Candelas, P. (2018). Numerical simulation and laboratory measurements on an open tunable acoustic barrier. *Applied Acoustics*, 141, 144-150.
- [50] Alagoz, S. (2014). A sonic crystal diode implementation with a triangular scatterer matrix. *Applied acoustics*, 76, 402-406.
- [51] Martins, M., Godinho, L., & Picado-Santos, L. (2013). Numerical evaluation of sound attenuation provided by periodic structures. *Archives of Acoustics*, 38.
- [52] Sharma, G. S., Skvortsov, A., MacGillivray, I., & Kessissoglou, N. (2019). Acoustic performance of periodic steel cylinders embedded in a viscoelastic medium. *Journal of Sound and Vibration*, 443, 652-665.
- [53] Jean, P., & Defrance, J. (2015). Sound propagation in rows of cylinders of infinite extent: Application to sonic crystals and thickets along roads. *Acta Acustica united with Acustica*, 101(3), 474-483.
- [54] Morandi, F., Miniaci, M., Marzani, A., Barbaresi, L., & Garai, M. (2016). Standardised acoustic characterisation of sonic crystals noise barriers: Sound insulation and reflection properties. *Applied Acoustics*, 114, 294-306.
- [55] Godinho, L., Redondo, J., & Amado-Mendes, P. (2019). The method of fundamental solutions for the analysis of infinite 3D sonic crystals. *Engineering Analysis with Boundary Elements*, 98, 172-183.
- [56] Romero-García, V., Sánchez-Pérez, J. V., & Garcia-Raffi, L. M. (2011). Analytical model to predict the effect of a finite impedance surface on the propagation properties of 2D sonic crystals. *Journal of Physics D: Applied Physics*, 44(26), 265501.
- [57] Ke, G., & Zheng, Z. C. (2016). Sound propagation around arrays of rigid and porous cylinders in free space and near a ground boundary. *Journal of Sound and Vibration*, 370, 43-53.

-
- [58] Sánchez-Pérez, J. V., Rubio-Michavila, C., & Castiñeira-Ibáñez, S. (2015). Towards the development of a software to design acoustic barriers based on sonic crystals: An overlapping model. In *Proceedings of Euronoise (Vol. 2015)*.
- [59] Castiñeira-Ibáñez, S., Rubio, C., & Sánchez-Pérez, J. V. (2015). Environmental noise control during its transmission phase to protect buildings. Design model for acoustic barriers based on arrays of isolated scatterers. *Building and Environment*, 93, 179-185.
- [60] Miyashita, T. (2005). Sonic crystals and sonic wave-guides. *Measurement Science and Technology*, 16(5), R47.
- [61] Gao, H. F., Matsumoto, T., Takahashi, T., & Isakari, H. (2013). Analysis of band structure for 2D acoustic phononic structure by BEM and the block SS method. *CMES-Comp. Model. Eng*, 90(4), 283-301.
- [62] Sigalas, M., Kushwaha, M. S., Economou, E. N., Kafesaki, M., Psarobas, I. E., & Steurer, W. (2005). Classical vibrational modes in phononic lattices: theory and experiment. *Zeitschrift für Kristallographie-Crystalline Materials*, 220(9-10), 765-809.
- [63] Godinho, L., Amado-Mendes, P., Pereira, A., & Soares Jr, D. (2018). An efficient MFS formulation for the analysis of acoustic scattering by periodic structures. *Journal of theoretical and computational acoustics*, 26(01), 1850003.
- [64] Godinho, L., Soares Jr, D., & Santos, P. G. (2016). Efficient analysis of sound propagation in sonic crystals using an ACA-MFS approach. *Engineering Analysis with Boundary Elements*, 69, 72-85.
- [65] Fredianelli, L., Del Pizzo, A., & Licitra, G. (2019). Recent developments in sonic crystals as barriers for road traffic noise mitigation. *Environments*, 6(2), 14.
- [66] Yablonovitch, E. (1987). Inhibited spontaneous emission in solid-state physics and electronics. *Physical review letters*, 58(20), 2059.
- [67] John, S. (1987). Strong localization of photons in certain disordered dielectric superlattices. *Physical review letters*, 58(23), 2486.
- [68] Kushwaha, M. S., Halevi, P., Martinez, G., Dobrzynski, L., & Djafari-Rouhani, B. (1994). Theory of acoustic band structure of periodic elastic composites. *Physical Review B*, 49(4), 2313.
- [69] Castiñeira-Ibáñez, S., Romero-García, V., Sánchez-Pérez, J. V., & Garcia-Raffi, L. M. (2010). Overlapping of acoustic bandgaps using fractal geometries. *EPL (Europhysics Letters)*, 92(2), 24007.
- [70] Romero-García, V., Fuster, E., García-Raffi, L. M., Sánchez-Pérez, E. A., Sopena, M., Llinares, J., & Sánchez-Pérez, J. V. (2006). Band gap creation using quasiordered structures based on sonic crystals. *Applied physics letters*, 88(17), 174104.
- [71] Herrero, J. M., García-Nieto, S., Blasco, X., Romero-García, V., Sánchez-Pérez, J. V., & Garcia-Raffi, L. M. (2009). Optimization of sonic crystal attenuation properties by ev-MOGA

multiobjective evolutionary algorithm. *Structural and Multidisciplinary Optimization*, 39(2), 203.

[72] Romero-García, V., Sánchez-Pérez, J. V., García-Raffi, L. M., Herrero, J. M., García-Nieto, S., & Blasco, X. (2009). Hole distribution in phononic crystals: Design and optimization. *The Journal of the Acoustical Society of America*, 125(6), 3774-3783.

[73] Hu, X., Chan, C. T., & Zi, J. (2005). Two-dimensional sonic crystals with Helmholtz resonators. *Physical Review E*, 71(5), 055601.

[74] Lee, H. M., Lim, K. M., & Lee, H. P. (2018). Environmental and sound divergence effects on the performance of rectangular sonic crystals with Helmholtz resonators. *Journal of Vibration and Control*, 24(12), 2483-2493.

[75] Fuster-Garcia, E., Romero-García, V., Sánchez-Pérez, J. V., & Garcia-Raffi, L. M. (2007). Targeted band gap creation using mixed sonic crystal arrays including resonators and rigid scatterers. *Applied physics letters*, 90(24), 244104.

[76] Romero-García, V., Sánchez-Pérez, J. V., & Garcia-Raffi, L. M. (2011). Tunable wideband bandstop acoustic filter based on two-dimensional multiphysical phenomena periodic systems. *Journal of applied physics*, 110(1), 014904.

[77] Cavalieri, T., Cebrecos, A., Groby, J. P., Chaufour, C., & Romero-García, V. (2019). Three-dimensional multiresonant lossy sonic crystal for broadband acoustic attenuation: Application to train noise reduction. *Applied Acoustics*, 146, 1-8.

[78] Romero-García, V., Krynkin, A., Garcia-Raffi, L. M., Umnova, O., & Sánchez-Pérez, J. V. (2013). Multi-resonant scatterers in sonic crystals: Locally multi-resonant acoustic metamaterial. *Journal of Sound and Vibration*, 332(1), 184-198.

[79] Sánchez-Dehesa, J., Garcia-Chocano, V. M., Torrent, D., Cervera, F., Cabrera, S., & Simon, F. (2011). Noise control by sonic crystal barriers made of recycled materials. *The Journal of the Acoustical Society of America*, 129(3), 1173-1183.

[80] Umnova, O., Attenborough, K., & Linton, C. M. (2006). Effects of porous covering on sound attenuation by periodic arrays of cylinders. *The Journal of the Acoustical Society of America*, 119(1), 278-284.

[81] Castiñeira-Ibáñez, S., Rubio, C., & Sánchez-Pérez, J. V. (2013). Acoustic wave diffraction at the upper edge of a two-dimensional periodic array of finite rigid cylinders. A comprehensive design model of periodicity-based devices. *EPL (Europhysics Letters)*, 101(6), 64002.

[82] Thorsson, P. J. (2000). Optimisation of low-height noise barriers using the equivalent sources method. *Acta Acustica united with Acustica*, 86(5), 811-820.

[83] Jolibois, A., Defrance, J., Koreneff, H., Jean, P., Duhamel, D., & Sparrow, V. W. (2015). In situ measurement of the acoustic performance of a full scale tramway low height noise barrier prototype. *Applied Acoustics*, 94, 57-68.

-
- [84] Castiñeira-Ibáñez, S., Rubio, C., Romero-García, V., Sánchez-Pérez, J. V., & Garcia-Raffi, L. M. (2012). Design, manufacture and characterization of an acoustic barrier made of multi-phenomena cylindrical scatterers arranged in a fractal-based geometry. *Archives of Acoustics*, 37, 455-462.
- [85] Castiñeira-Ibáñez, S., Romero-García, V., Sánchez-Pérez, J. V., & García-Raffi, L. M. (2015). Periodic systems as road traffic noise reducing devices: prototype and standardization. *Environmental Engineering & Management Journal (EEMJ)*, 14(12).
- [86] Bravo, J. M., Buchón-Moragues, F., Redondo, J., Ferri, M., & Sánchez-Pérez, J. V. (2019). Integrated Photogrammetric-Acoustic Technique for Qualitative Analysis of the Performance of Acoustic Screens in Sandy Soils. *Sensors*, 19(22), 4881.
- [87] Garcia-Raffi, L. M., Salmeron-Contreras, L. J., Herrero-Dura, I., Picó, R., Redondo, J., Sánchez-Morcillo, V. J., ... & Romero-García, V. (2018). Broadband reduction of the specular reflections by using sonic crystals: A proof of concept for noise mitigation in aerospace applications. *Aerospace Science and Technology*, 73, 300-308.
- [88] Luo, J., & Yang, Z. (2010, May). Research on the noise barrier height change of the monoline viaduct affecting the aerodynamic characteristic of high speed train. In 2010 International Conference on Intelligent Computation Technology and Automation (Vol. 3, pp. 161-164). IEEE.
- [89] Soper, D., Gillmeier, S., Baker, C., Morgan, T., & Vojnovic, L. (2019). Aerodynamic forces on railway acoustic barriers. *Journal of Wind Engineering and Industrial Aerodynamics*, 191, 266-278.
- [90] Ergin, T., Stenger, N., Brenner, P., Pendry, J. B., & Wegener, M. (2010). Three-dimensional invisibility cloak at optical wavelengths. *science*, 328(5976), 337-339.
- [91] Espinosa, V., Sánchez-Morcillo, V. J., Staliunas, K., Pérez-Arjona, I., & Redondo, J. (2007). Subdiffractive propagation of ultrasound in sonic crystals. *Physical Review B*, 76(14), 140302.
- [92] Lee, H. M., Wang, Z., Lim, K. M., Xie, J., & Lee, H. P. (2020). Novel plenum window with sonic crystals for indoor noise control. *Applied Acoustics*, 167, 107390.
- [93] Redondo, J., Sánchez-Pérez, J. V., Blasco, X., Herrero, J. M., & Vorländer, M. (2016). Optimized sound diffusers based on sonic crystals using a multiobjective evolutionary algorithm. *The Journal of the Acoustical Society of America*, 139(5), 2807-2814.
- [94] Redondo, J., Picó, R., Sánchez-Morcillo, V. J., & Woszczyk, W. (2013). Sound diffusers based on sonic crystals. *The Journal of the Acoustical Society of America*, 134(6), 4412-4417.
- [95] Xu, F., Yang, Z., He, X., & Zhen, L. (2020). An underground barrier of locally resonant metamaterial to attenuate surface elastic waves in solids. *AIP Advances*, 10(7), 075121.

[96] Hongisto, V., Oliva, D., & Rekola, L. (2018). Subjective and objective rating of the sound insulation of residential building façades against road traffic noise. *The Journal of the Acoustical Society of America*, 144(2), 1100-1112.

[97] Hongisto, V., Oliva, D., & Keränen, J. (2014). Subjective and objective rating of airborne sound insulation–living sounds. *Acta Acustica united with Acustica*, 100(5), 848-863.

4. Research areas developed in the thesis

The research work developed in this doctoral thesis report covers some of the lines of research mentioned in the previous section.

These works are included in the publications attached in the following sections.

4.1.- Open noise barriers based on sonic crystals. Advances in noise control in transport infrastructures.

4.1.1.- Abstract

Noise control is an environmental problem of first magnitude nowadays. In this work, we present a new concept of acoustic screen designed to control the specific noise generated by transport infrastructures, based on new materials called sonic crystals. These materials are formed by arrangements of acoustic scatterers in air, and provide a new and different mechanism in the fight against noise from those of the classical screens. This mechanism is usually called multiple scattering and is due to their structuring in addition to their physical properties. Due to the separation between scatterers, these barriers are transparent to air and water allowing a reduction on their foundations. Tests carried out in a wind tunnel show a reduction of 42% in the overturning momentum compared to classical barriers. The acoustical performance of these barriers is shown in this work, explaining the new characteristics provided in the control of noise. Finally, an example of these barriers is presented and classified according to acoustic standardization tests. The acoustic barrier reported in this work provides a high technological solution in the field of noise control.

4.1.2.- Introduction

Environmental noise, defined as an unpleasant outdoor sound generated by transport, industry and human activities in general, is one of the main environmental problems of the industrialized countries [1].

Furthermore, this noise problem is linked with some health problems such as stress, fatigue, sleep disturbance, cardiovascular disorders or hearing loss [2, 3]. Cities are considered as critical places where this problem is magnified and where conflict of interests appear, because high noise levels are created due to human activities and where low noise levels are necessary to enable people to rest. Schafer introduced the concept of urban soundscape as the complete range of sounds that characterize a city [4]. The main contribution to this urban soundscape is supplied by noise transport.

According to UE, more than 55 dBA in night hours and 65 dBA in day should not be exceeded. However, the EUEurostat says that higher noise levels are suffered during the day by 20% of EU citizens and during the night by 30%. These noise problems can involve important sanitary cost of around 0.35% of UE PIB.

Generally, noise control can be carried out in one of the three phases of noise propagation: (i) at noise source; (ii) at transmission phase; (iii) at noise reception.

The main solution to reduce noise levels in its transmission is the use of acoustic barriers (ABs) [5]. These barriers are built between the source of noise and the receiver. The transmitted noise travels from the source to the receiver in a straight line, and it is interrupted by the AB placed between them, which reduces the noise level by means of different acoustic mechanisms. These classic ABs are made by a continuum rigid material with a minimum superficial density of 20 kg/m² [6]. The acoustic effect of ABs can be explained as follows: They reflect or scatter back towards the source a portion of the

transmitted acoustical energy and other portion of the noise energy is absorbed by the material of the barrier. Other portion is transmitted through the barrier or diffracted from the barrier's edge (Fig. 12a). This diffraction can be considered as one of the main factors that decreases the effectiveness of the barriers [2, 5]. In fact, this is one of the main research lines in the field of classical ABs, focused on reducing this diffraction effect over the top edge, by designing new profiles far away from the simple edge of the classical ones in order to increase their efficiency. [7, 8, 9, 10].

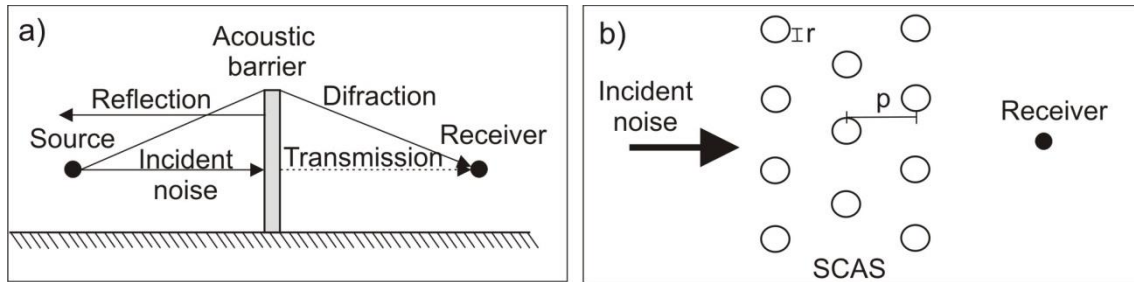


Figure 12: (a) Scheme of a classical acoustic barrier; (b) Plan view of a Sonic Crystal Acoustic Screen.

However, the use of ABs involves some disadvantages. First, the state of technology in the field of ABs nowadays does not guarantee a specific protection for each noise problem. There are not ABs which be able to distinguish the noise which have to be controlled. For that reason the same screen is used to protect different noises, it does not matter if it is a truck noise or an ambulance siren warning. Second, the placement of continuous walls presents two kinds of problems. On the one hand, classical ABs are not permeable to wind or water, as a consequence, a large volume of foundations is needed to support the heavy efforts produced, especially for large barrier heights. The heavy wind load can also produce some structural problems in viaducts with ABs installed in the case of a high speed trains, as Luo and Yang demonstrated in 2010 [11]. On the other hand, these continuous walls in cities present aesthetic and communication problems due to the existence of a solid and continuous barrier [6] related to both breakdown of the cityscape and the physical isolation of the acoustically protected areas.

Thus, the placement of classical barriers in certain places can involve high costs from technical and economical points of view. For all these drawbacks, installation of classical ABs could be inappropriate in urban areas for transport infrastructures noise control.

In the last decade, the discovery of new materials has enabled the development of new devices to noise control. Sonic Crystals (SC) can be defined as periodic arrays of cylindrical acoustic scatterers with radius r separated by a predetermined lattice constant p , and embedded in air [12] as can be seen at figure 1b. SC add a new noise control mechanism based on the well-known Bragg interferences due to a multiple scattering (MS) process [13], different from those previously known. As a consequence, there are frequency ranges, related to the periodicity of the medium, where the propagation of the waves is forbidden through the crystal, [14, 15]. These ranges of frequencies are called band gaps (BG).

The acoustic barriers based on SC are usually called Sonic Crystals Acoustic Screens (SCAS), and the first prototype was designed and constructed by Sánchez-Pérez et al. (2002) [16].

The goal of this work is to explain the working of SCAS, as well as the design and development of an advanced barrier based on these materials explaining the advantages on its use compared to the classical ABS. The paper is organized as follows: In section 4.1.3 we develop a brief introduction of SCAS, explaining their development and their noise control properties. The standardization tests for road traffic noise of the constructed prototype and its behavior in a wind tunnel are developed in section 4.1.4. Section 4.1.5 shows advantages of SCAS compared to ABs. Finally, section 4.1.6 summarizes the main results of the work.

4.1.3.- Description of first and second generation of Sonic Crystals Acoustic Screens.

The first SCAS was theoretically proposed by Kushwaha in 1997 [17], and the first prototype was designed and constructed by Sánchez-Pérez et al. (2002) [16]. These devices were designed using the existence of Bragg interferences as the unique attenuation mechanism, and were formed by a set of rigid scatterers embedded in air (Figure 13a).

The distance between the scatterers, the diameter of the cylinders or the angle of incidence of the wave on the structure, among other parameters, determine the size and the position of the BG in the range of frequencies. However, the mere use of BG as the unique mechanism to avoid the transmission of waves, is not enough to ensure a good performance of a SCAS.

To improve the noise control capabilities of SCAS, other noise control features was proposed by Romero-García et al. (2011a) [18]. Thus, resonances or absorption mechanisms are used in the design of the scatterers, resulting in multiphysical phenomena scatterers. These scatterers are formed by a core made of rigid cylinders with a slot along its entire length, and wrapped in a layer of absorbent material. Its inner acts as an acoustic resonant cavity because the core can be considered acoustically rigid and contribute to the multiple scattering (MS) phenomenon. Its external part, with absorbent material, gives a baseline of noise attenuation. Also the resonant cavities produce attenuation peaks due to the resonances. Thus, three noise control mechanisms are involved in the design of the multi-physical scatterers: BG, absorption and resonances. SCAS that use other noise control mechanisms apart from the BG, as the exposed previously, are called SCAS of 2nd generation, and provide high technological procedures to the industrial field of ABs.

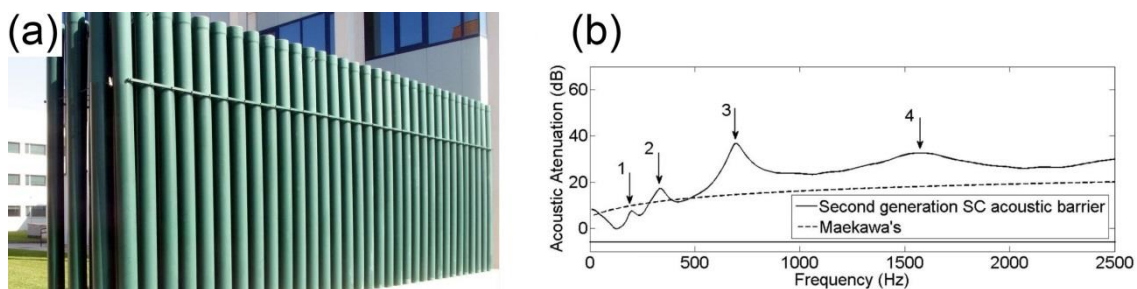


Figure 13: (a) Example of first generation SCAS; (b) Simulated attenuation spectrum of the SCAS.

An example of the attenuation performance of the second generation SCAS can be seen in the numerical simulation presented in Figure 13b. One can observe the attenuation peaks due to the different mechanisms named before: (i) the attenuation peaks due to the resonant cavity (1) (2), which position in the frequency range depends on the volume of the resonators. We have used in the design cylinders with two different diameters for adding two resonance peaks placed at different frequencies of the spectrum; (ii) the attenuation peaks due to the periodicity of the array correspond to the BG of the array (3) (4); (iii) the threshold of attenuation due to the effect of the absorbent used in every cylinder of the structure appears from 500 Hz onwards. Also in this figure the theoretical attenuation level for a classical AB with the same height and width using the Maekawa's method [19] can be observed, in order to compare the acoustic response of both kind of barriers. An increasing of the attenuation in most of the analyzed frequencies can be seen. In fact, this new generation allows the design of specific ABs for specific noise problems acting in the position of these peaks in the range of frequencies, as it will be explained in the following section.

This design of a second generation of SCAS is protected under Spanish patents [20, 21]

4.1.4.- Acoustic standardization and determination of the structural efforts in a wind tunnel

Acoustic standardization

We have applied to SCAS the acoustical standardization tests that determine the level of protection against noise. These tests are the only ones available in the European Standards to evaluate ABs. All tests have been carried out in a laboratory approved for this type of testing.

In order to characterize acoustically the second generation of SCAS, two acoustics tests have been carried out in a laboratory approved. The standards EN 1793:1997 relative to road traffic noise reducing devices, test method for determining the acoustic performance has been used to characterize our barrier: (i) EN 1793-1:1997 Intrinsic characteristics of sound absorption [22]; (ii) EN 1793-2:1997 Intrinsic characteristics of airborne sound insulation. These two first standards define the performed tests related with the noise absorption and their behaviour with regard to the spread or airborne noise [23]. Finally (iii) EN 1793-3:1997 Normalized traffic noise spectrum, is used as a reference to obtain a ranking of barriers on the basis of their acoustic characteristics [24]. Although these tests are not designed to evaluate this kind of barriers, the obtained results were promising.

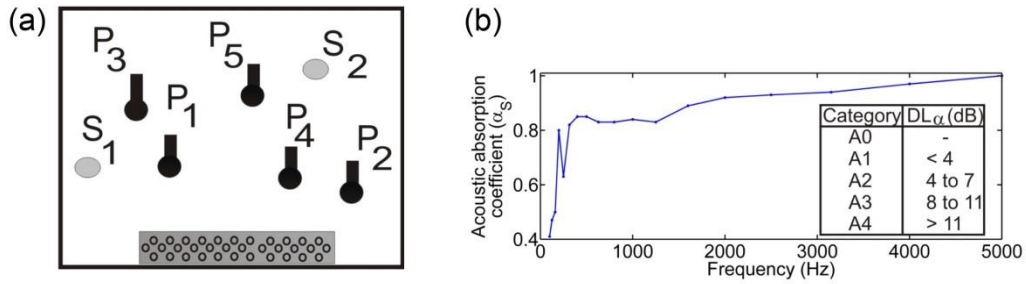


Figure 14: (a) Scheme of arrangement of the instrumental used (two sources and five microphones) in the test given by EN 1793-1:1997 norm. ; (b) Variation of α_S as a function of the frequency.

To carry out the first test, five microphones have been placed at points P1, P2, P3, P4 and P5 faced the device, and two omnidirectional sound sources are used placed in the positions S1 and S2 as can be seen in Figure 3a and as this standard specifies.

The goal of this test is to classify the barrier with regard to its acoustic absorption characteristics through experimental measurements in a reverberant chamber, obtaining the evaluation index of the acoustic absorption (DL_α):

$$DL_\alpha = -10 \log \left| 1 - \frac{\sum_{i=1}^{18} \alpha_{si} 10^{0,1L_i}}{\sum_{i=1}^{18} 10^{0,1L_i}} \right| \quad (2)$$

Where L_i is the noise level for each third octave band of the normalized traffic noise spectrum (dB) given by the standard EN 1793-3:1997. [24]

In our case $DL_\alpha=8\text{dB}$, which corresponds to the A3 category; it was almost the highest category, regarding its acoustic absorption characteristics as it can be seen at figure 14b.

The second test were carried out in a transmission chamber, and the sample was installed in the same way as it will be used in practice, as can be seen at figure 15a.

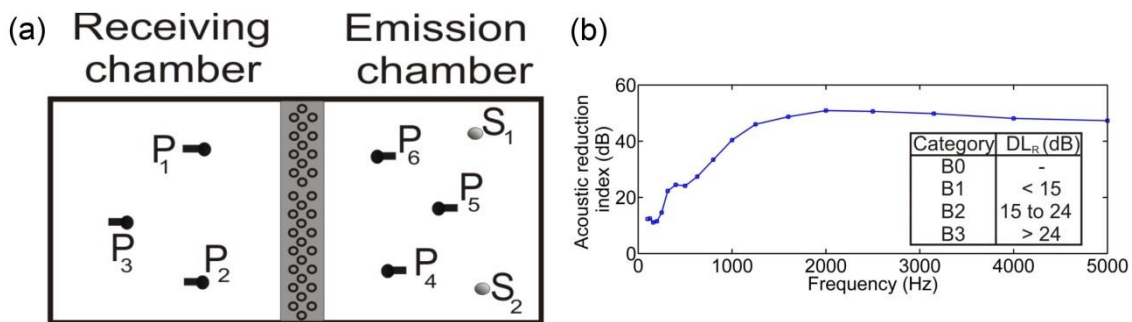


Figure 15: (a) Scheme of arrangement of the experimental set up used (two sources and five microphones) in the test given by EN 1793-2:1997; (b) Experimental values of the index R.

This test checks the intrinsic characteristics of the barrier relative to the airborne sound insulation, which is defined by the evaluation index of the airborne sound insulation according to the standard EN-ISO 10140:2011 (ISO, 2010) DL_R (dB) [25]. The value of this index enables us to classify the capability of airborne sound insulation of the barrier using the following expression:

$$DL_R = -10 \log \left| \frac{\sum_{i=1}^{18} 10^{0,1L_i} 10^{-0,1R_i}}{\sum_{i=1}^{18} 10^{0,1L_i}} \right| \quad (1)$$

Where L_i is the noise level for each third octave band of the normalized traffic noise spectrum (dB) given by the standard EN 1793-3:1997 [24].

In our case $DL_R=22$ dB, which corresponds to the category B2, almost the highest category (Figure 15b). This is the value that allows us to classify the capability of airborne sound insulation of the checked barrier.

Then we conclude that, under the acoustical point of view, these open noise barriers based on sonic crystals can compete with the traditional ones formed by continuous walls. In any case, the constructive interaction of the different mechanisms of sound attenuation involved in SCAS makes possible to select the range of frequencies where each one of the different mechanism mainly contributes.

Determination of the structural effort in a wind tunnel

Several laboratory experiments in a wind tunnel have been carried out to estimate the values of wind efforts in SCAS and to compare them with corresponding to a classical AB formed by a wall (figure 16a). This test could give information about the size of their foundations or the efforts transmitted to the ground, because it depends basically on this kind of load. [26]

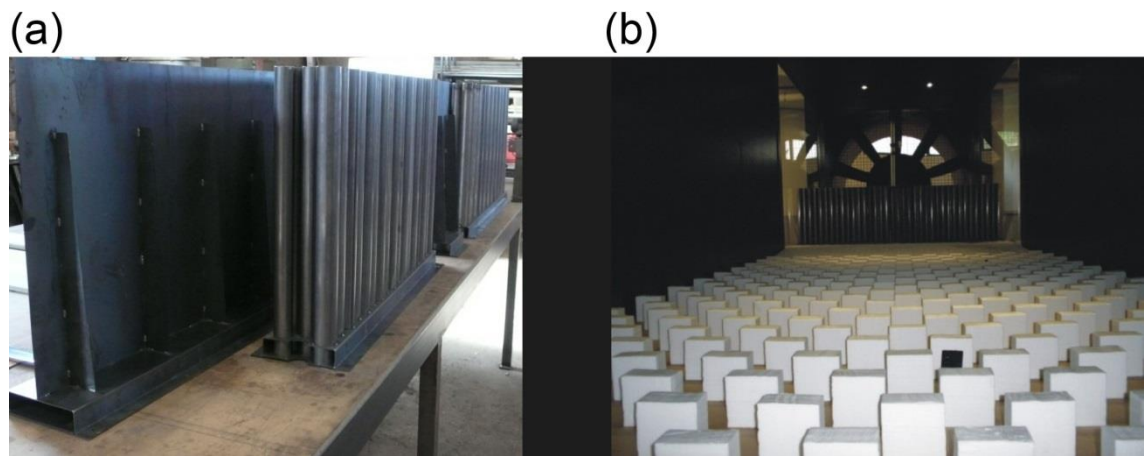


Figure 16. (a) Partial view of the scale model of both classical AB and SCAS; (b) View of the arrangement of obstacles inside the wind tunnel

We have to consider the action of the wind on both ABs and SCAS as it was generated by the atmospheric pressure field. According to the Spanish Technical Building Code [27], we have considered here a ground roughness corresponding to urban or industrial areas as can be seen at figure 16b. Thus, we have simulated typical flow conditions, assuming an area with uniform buildings.

We have used a precision balance AMTI MC36 to measure the wind efforts on both barriers. This balance allows the measurement of forces in the three directions of the space. In this test we measured both the force in the wind direction and the corresponding overturning momentum on the bases of the barriers. To determinate the size of the foundations is necessary know the variations of these efforts with the wind speed.

Thus, we obtained the efforts on the model in a real-time conditions, and applying criteria of similarity and scale, the values of the actions on the model.

Taking into account the obtained results we can conclude that SCAS supports smaller efforts than the classical AB. In fact, there is an average around 42% of reduction for both the drag efforts and the overturning momentum.

This is an important structural factor since the placement of acoustic barriers in certain places is restricted by the huge efforts transmitted to the structure, allowing the use of SCAS in situations where until now it was not possible the use of classical AB due to structural problems, such as viaducts. And also this characteristic can lead to significant foundation reduction in this kind of devices compared to classical ABs.

4.1.5.- Advantages of SCAS

The SCAS of 2nd generation are based on a more advanced design of multiphenomena scatterers, in which three different noise control mechanisms are involved. On the one hand, the use of resonators allows the existence of two different resonance peaks, which position in the range of frequencies can be shifted by changing the geometry of the resonators. On the other hand, the distance between scatterers in the array used allows the existence of BG, which location in the range of frequencies can be again determined by changing the geometrical characteristics of the array. Finally, the absorption level depends on the volume of the absorbent material used [28]. All these peaks and the acoustical characteristics of the 2nd generation of SCAS designed can be seen in Fig 13b. Note that this kind of barriers allows the inclusion in their acoustic design of different noise control mechanisms separately and their design can be shifted according to the type of noise that is needed to be controlled. Thus, the designer can choose the frequency range in which each of the noise control mechanisms must act, allowing the design of customized SCAS for each type of noise. This tunability of the attenuation capabilities of the SCAS makes them highly competitive respect to the classical ABs and it makes possible to construct barriers on demand.

Moreover, SCAS are formed by periodically distributing multi-physical phenomena scatterers, and the separation between the scatterers allows the wind to pass through decreasing the efforts that are transmitted. This characteristic makes possible the reduction on the foundations of the device. Furthermore, this characteristic can solve some structural problems when classical ABs are placed, due to the heavy wind load supported by the structure.

Another advantage is the constructive possibilities of these barriers, which allows creating barriers with important aesthetic components. In fact, the first idea of use SC technology for SCAS is given by a minimalist sculpture by Eusebio Sempere made of steel cylinders in air [12]. Thus, the aesthetic aspects are improved giving visual continuity to the urban landscape and reducing the physical isolation of the protected areas.

4.1.6.- Conclusions

In this paper, we present new open noise barriers based on sonic crystal called "Sonic Crystal Acoustics Screens" (SCAS). At SCAS, there are three noise control mechanisms

BG, absorption and resonances. These new SCAS introduce an important technological procedure in the field of the acoustic barriers.

These new devices have shown a very good acoustical response, in view of the standardization results obtained, showing that they can compete acoustically with classical ABs.

For that reason SCAS can be used in noise control to reduce the most important type of noise that appears in cities: the transport noise. The sculpture origin, its open design and its versatile to be projected for specific noises are aesthetic already appeared on the noise control market because of all advantages that this SCAS offers.

One example of the use of SCAS can be seen in Eindhoven A2 ring road by Van Campen Industries [29], where a semi-SCAS have installed following the new technology presented in this paper. Nowadays their use is at an intermediate point between the basic research of its physical properties and its widespread use as noise control devices.

4.1.7.- References

[1] EC Directive, Directive 2002/49/EC of the European Parliament and of the Council of 25 June 2002 relating to the assessment and management of environmental Noise, Official J. Eur. Communities L 189 (2002) 0012e0026 (18.7.2002), Brussels.

[2] Kotzen, B., & English, C. (2014). Environmental noise barriers: a guide to their acoustic and visual design. CRC Press.

[3] Platon, S. N., Hionis, C. A., (2014). Preventing risk of noise exposure in working environment using noise mapping. Environmental Engineering & Management Journal (EEMJ), 13(6).

[4] Schafer, R. M., (1977). The tuning of the world. Alfred A. Knopf.

[5] Harris, C. M. (1991). Handbook of acoustical measurements and noise control (pp. 30-15). New York: McGraw-Hill.

[6] FHWA U.S.A (2011). Keeping the Noise Down. Highway Traffic Noise Barriers, On line at: <http://journalofcommerce.com/Home/News/2007/7/Keeping-the-noise-down---highway-traffic-noisebarriers-JOC023547W/>.

[7] Mak, C. M., Leung, W. S. (2013). Traffic noise measurement and prediction of the barrier effect on traffic noise at different building levels. Environmental Engineering & Management Journal (EEMJ), 12(3).

[8] Okubo, T., Fujiwara, K. (1999). Efficiency of a noise barrier with an acoustically soft cylindrical edge for practical use. The Journal of the Acoustical Society of America, 105(6), 3326-3335.

[9] Watts, G. R. (1996). Acoustic performance of a multiple edge noise barrier profile at motorway sites. Applied Acoustics, 47(1), 47-66.

-
- [10] Watts, G. R., Morgan, P. A., Surgand, M. (2004). Assessment of the diffraction efficiency of novel barrier profiles using an MLS-based approach. *Journal of Sound and Vibration*, 274(3), 669-683.
- [11] Luo, J., Yang, Z. (2010). Research on the noise barrier height change of the monoline viaduct affecting the aerodynamic characteristic of high speed train. In *Intelligent Computation Technology and Automation (ICICTA), 2010 International Conference on* (Vol. 3, pp. 161-164). IEEE.
- [12] Martinez-Sala, R., Sancho, J., Sánchez, J. V., Gómez, V., Llinares, J., Meseguer, F. (1995). Sound-attenuation by sculpture. *Nature*, 378(6554), 241-241.
- [13] Chen, Y. Y., Ye, Z. (2001). Theoretical analysis of acoustic stop bands in two-dimensional periodic scattering arrays. *Physical Review E*, 64(3), 036616.
- [14] Sigalas, M. M., Economou, E. N. (1992). Elastic and acoustic wave band structure. *Journal of sound and vibration*, 158(2), 377-382.
- [15] Sánchez-Pérez, J. V., Caballero, D., Martinez-Sala, R., Rubio, C., Sánchez-Dehesa, J., Meseguer, F., Llinares J., Gálvez, F. (1998). Sound attenuation by a two-dimensional array of rigid cylinders. *Physical Review Letters*, 80(24), 5325.
- [16] Sanchez-Perez, J. V., Rubio, C., Martinez-Sala, R., Sanchez-Grandia, R., Gomez, V. (2002). Acoustic barriers based on periodic arrays of scatterers. *Applied Physics Letters*, 81(27), 5240-5242.
- [17] Kushwaha, M. S. (1997). Stop-bands for periodic metallic rods: Sculptures that can filter the noise. *Applied Physics Letters*, 70(24), 3218-3220.
- [18] Romero-García, V., Sánchez-Pérez, J. V., Garcia-Raffi, L. M. (2011). Tunable wideband bandstop acoustic filter based on two-dimensional multiphysical phenomena periodic systems. *Journal of applied physics*, 110(1), 014904.
- [19] Maekawa, Z., 1968. Noise reduction by screens. *Applied acoustics*, 1(3), 157-173.
- [20] Sánchez-Pérez J.V., Martínez-Sala R., Rubio C., Derqui M. (2003). Acoustic Barrier, Spanish Patent, No. P200200398(X)
- [21] Sánchez-Pérez J.V., Garcia-Raffi L.M., Romero-Garcia V., Castiñeira-Ibáñez S. (2009). Acoustic Barrier, Spanish Patent. No. P200902074.
- [22] European Committee for Standardisation, EN 1793-1 (1997). Road Traffic Noise Reducing Devices – Test Method for Determining the Acoustic Performance – Par 1: Intrinsic characteristics of sound absorption, CEN, Brussels, Belgium.
- [23] European Committee for Standardisation, EN 1793-2 (1997). Road Traffic Noise Reducing Devices – Test Method for Determining the Acoustic Performance – Par 2: Intrinsic characteristics of airborne sound insulation under diffuse sound field conditions, CEN, Brussels, Belgium.

-
- [24] European Committee for Standardisation, EN 1793-3 (1997). Road Traffic Noise Reducing Devices – Test Method for Determining the Acoustic Performance – Par 3: Normalised Traffic Noise Spectrum, CEN, Brussels, Belgium.
- [25] International Organization for Standardization (ISO) 10140:2010 (2010) – Acoustics – Laboratory measurement of sound insulation of building elements.
- [26] Castiñeira-Ibáñez, S., Romero-García, V., Sánchez-Pérez, J. V., García-Raffi, L. M. (2015). Periodic systems as road traffic noise reducing devices: Prototype and standardization. *Environmental Engineering & Management Journal (EEMJ)*, 14(12).
- [27] SMD (2006). Spanish Ministry of Development, Spanish Technical Building Code, SE-AE Actions in Construction, R.D. 314/2006, Official Gazette, March 28, 2006, Madrid, Spain.
- [28] Romero-García, V., Krynkin, A., Garcia-Raffi, L. M., Umnova, O., Sánchez-Pérez, J. V., (2013). Multi-resonant scatterers in sonic crystals: Locally multi-resonant acoustic metamaterial. *Journal of Sound and Vibration*, 332(1), 184-198.
- [29] Van Campen Industries, (2009). [On Line] Available in <http://www.campen.nl/albumsound-absorbent-noise-barriers> [7 September, 2009].

4.2.- Interferences in locally resonant Sonic metamaterials formed from Helmholtz resonators.

4.2.1.- Abstract

The emergence of materials artificially designed to control the transmission of waves, generally called metamaterials, has been a hot topic in the field of acoustics for several years. The design of these metamaterials is usually carried out by overlapping different wave control mechanisms. An example of this trend is the so-called Locally Resonant Sonic Materials, being one of them the Phononic Crystals with a local resonant structure. These metamaterials are formed by sets of isolated resonators in such a way that the control of the waves is carried out by resonances and by the existence of Bragg bandgaps, which appear due to the ordered distribution of the resonators. Their use is based on the creation of resonance peaks to form additional nontransmission bands mainly in the low frequency regime, usually below the first Bragg frequency. The coupling of both gaps has been made in some cases, but it is not always so. In this work, using a periodic structure formed by Helmholtz resonators, we report the existence of interferences between the resonances and the Bragg bandgaps when they are working in nearby frequency ranges, so that they prevent the coupling of both gaps. We explain their physical principles and present possible solutions to mitigate them. To this end, we have developed numerical models based on the finite element method, and the results have been verified by means of accurate experimental results obtained under controlled conditions.

4.2.2.- Discussion

Acoustic metamaterials are defined as artificial structures with physical effective properties, related to the control of elastic waves, not found in nature. In the past decade, a great effort has been made in order to analyze their rich physics and the large number of potential applications [1–16]. An important kind of acoustic metamaterial is that formed by Phononic Crystals (PCs) with a locally resonant structure, formed by periodic arrays of Helmholtz Resonators (HRs) [17–22]. These metamaterials are included inside the well-known Locally Resonant Sonic Materials (LRSMs) [11, 23–25]. In these crystalline metamaterials, the existence of Bragg gaps (BGs) in the low frequency regime is restricted due to the requirement of dimensional similarity between wavelengths and the lattice constant of PC. Nevertheless, this limitation is overcome with the creation of subwavelength Locally Resonant bandgaps (LRGs), through the inclusion of HR in the array. Although BG and LRG are usually far from each other in the domain of frequencies, in some cases, the coupling of both gaps is interesting to obtain a broadband transmission loss. This possibility has already been analyzed for other LRSM configurations [26] different from those analyzed here. However, in the case of using HR, there are some different interactions between BG and LRG that, having been reported by some authors [18, 27] as a part of papers focused on other purposes, have not yet been analyzed in depth.

In this work, we study the underlying Physics in BG/LRG interactions using a simplified two-dimensional (2D) numerical model based on the Finite Element Method (FEM) and supporting the obtained results with accurate experiments carried out under

controlled conditions. This study is focused on the case of 2DPC formed by rigid scatterers in air, usually called Sonic Crystals [28, 29].

To analyze these interactions, we have developed the geometry shown at the top of Fig. 17(a). The considered 2D domain of length $L=1$ m is formed by 3 scatterers with external (internal) radius, r_{ext} (r_{int}), and separated by the lattice constant of the array formed, a . The scatterers can work as closed cylinders or cylindrical HR with a cross-sectional area of the neck, A_n , and length of the neck, L_n . HR can be placed in the numerical domain with the necks oriented in any direction, but for the sake of brevity, we will analyze here only two cases: 0° and 180° with respect to the direction of propagation of an incident plane wave traveling from left to right, calling hereinafter $HR0^\circ$ and 180° , respectively. In all cases, the scatterers are confined between two linear boundaries separated by the lattice constant of the array, a . The measurement point is located at $d \approx 0.2$ m from the center of the last scatterer, far enough to avoid near-field effects behind the sample. The vertical boundaries are surrounded by Perfectly Matched Layers (PMLs) [30] to simulate the Sommerfeld radiation conditions. In the horizontal boundaries of the model, we have imposed periodic boundary conditions. Considering these conditions, the incident wave is not reflected by the horizontal boundaries, but the scattered waves reproduce the effect of a semi-infinite 2D Sonic Crystal formed by 3 rows of scatterers arranged in a square array. Finally, since we have considered all types of scatterers to be acoustically rigid, the Neumann boundary condition (zero sound velocity) is applied to their surfaces.

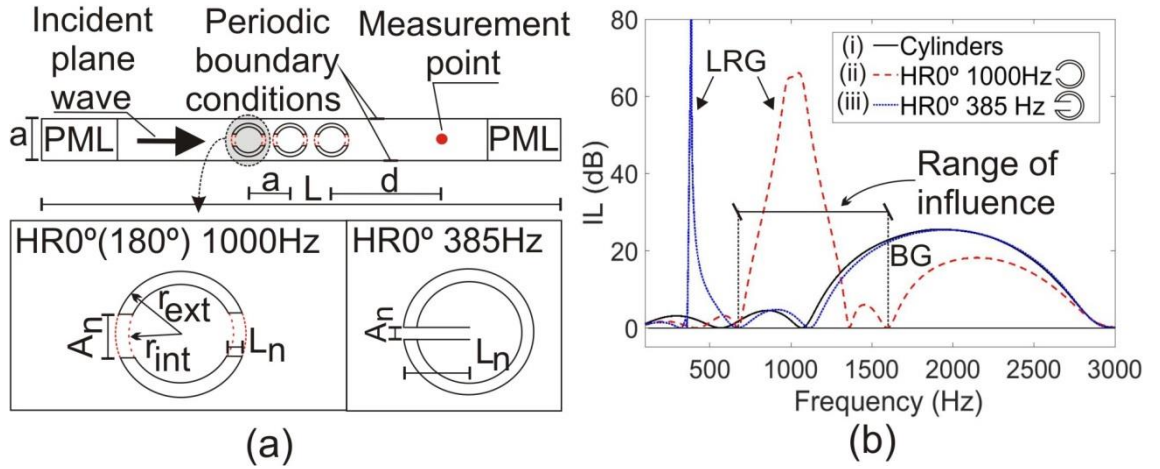


Figure 17: (a) Numerical 2D model to analyze the BG/LRG interactions. The typology of the scatterers is shown at the bottom; (b) IL spectra for the three considered arrays..

To visualize first the LRG/BG acoustic interactions, we have considered an array with a BG centered at 2000Hz with three different kinds of scatterers: (i) cylinders; (ii) $HR0^\circ$ with a LRG centered at 1000 Hz; and (iii) $HR0^\circ$ with a LRG at 385 Hz. The values of the general parameters of the array are $a=0.08$ m, $r_{ext}=0.0315$ m, and $r_{int}=0.0257$ m, being the particular values for each $HR0^\circ$ $L_n=0.0058$ m (0.04 m) and $A_n=0.02$ m (0.004 m) for the second and the third cases, respectively. The details are presented at the bottom of Fig. 17(a). In all cases, the attenuation spectrum, usually called Insertion Loss (IL), has been calculated. The obtained results are presented in Fig. 17(b). It can be observed that when the LRG is far from the BG in the frequency domain [array (i) vs array (iii)], the size of the BG is almost equal, being the BG/LRG interaction almost negligible. However, when BG and

LRG are close [array (i) vs array (ii)], a reduction in the BG appears, which would be greater if LRG and BG are closer. In the latter case, the range of influence of the interference extends to a larger frequency range than that occupied by the LRG itself.

The interference produced in the transmitted field considering only a single scatterer has been analyzed first. Three would be the potential mechanisms involved: (i) the absorption, (ii) a change in directivity, or (iii) a phase shift. The first and third mechanisms have been analyzed using a numerical model that simulates an impedance tube with anechoic ends, as can be seen in the inset of Fig. 18(a), while the scheme shown at the top of Fig. 18(b), which consists of a typical anechoic configuration used to measure the directivity of the scattered field, has been numerically developed to analyze the change in the directivity. In the latter model, a plane wave traveling from left to right impinges on each of the considered scatterers located in the center of the domain, allowing us to estimate the scattered field in the circular measurement zone.

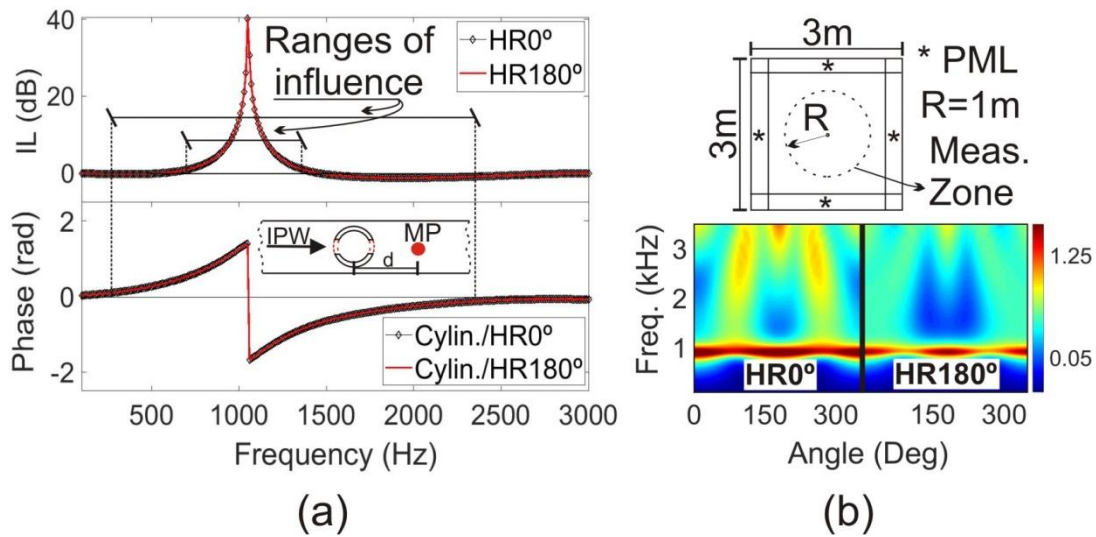


Figure 18: Analysis of the influence of the three possible mechanisms responsible for interference in the case of single scatterers; (a) absorption spectra (upper part) and phase shift spectra (lower part) for HR0° and HR180°. In the inset, you can see a schematic of the numerical model used; (b) an outline of the anechoic model used to simulate the directivity of both HR (upper part); the directivity results can be seen at the bottom.

Concerning the absorption, at the top of Fig. 18(a), it can be seen that the IL spectra for a single HR0° (HR180°) are exactly the same, showing the resonance peak centered at 1000Hz. But its range of affectation in the frequency domain does not correspond to the interference phenomenon to be analyzed, which affects a larger frequency range outside the absorption itself, as can be seen in Fig. 17(b) for the HR0° 1000 Hz case. This result allows us to rule out absorption as the main mechanism responsible for interference. In the case of the change in the directivity, the results are shown at the bottom of Fig. 18(b), where the sound pressure scattered by both HR0° and HR180° is presented. It can be seen that both sound fields are completely different being their IL spectra exactly the same, as stated above. That means that the directivity does not affect the attenuation produced by HR, and this result allows us to discard the directivity mechanism as well. Finally, the results of the Cylinder/ HR0° and Cylindier/ HR180° phase shifts are shown at the bottom of Fig. 18(b). One can observe that both spectra are equal, being this mechanism compatible with the

range of influence shown in Fig. 17(b). Then, we can conclude that the phase shift could be the main responsible for this interference.

Next, we will focus our analysis on the physics involved in the phase shift mechanism for a single scatterer, considering first the phenomenon of resonance in isolation, without scattering. For this, we use the numerical model presented at the top of Fig. 19(a), which considers a single HR not located in the transmitted wave path. The numerical domain consists of a rectangle with rigid boundaries, and an HR with dimensions $a=0.04$ m, $b=0.03$ m, $c=0.01$ m, and $d=0.01$ m, which supposes a resonance peak at 1000Hz, is considered. An incident plane wave traveling from left to right is reflected at the rigid right boundary, and the sound pressure level is measured in a point located at $e=0.85$ m from this boundary. The results can be seen at the bottom of Fig. 19(a). In the absence of the HR, the eigenmodes would appear for frequencies given by

$$f = nc/(2L) \quad (3)$$

where n is an integer, c is the speed of sound, and L is the length of the domain. However, in the presence of HR, the eigenmodes are displaced within a frequency range around the resonance frequency of the HR. Thus, within the range of influence of the HR, the modes are shifted forward or backward for frequencies below or above the resonance frequency, respectively.

The next step is the analysis of the resonance along with the scattering by adapting the model of Fig. 17(a) to the case of a single scatterer [top of Fig. 19(b)] and determining the phase shift of the transmitted wave at the measurement point. The phase shift is presented at the middle of Fig. 19(b), and one can check that the range of influence is similar to both the previous case and the one shown in Fig. 17(b). Note that the interference phenomenon reported here would exist in the frequency range in which the phase shift exists. This range is indicated in the lower part of Fig. 18(b) for the case of a single resonator (called "range of influence") and in Fig. 19(d) for the case of LRSM (from below 100Hz to above 3000Hz). This phase shift can be interpreted as a difference of distances, in which the transmitted wave in both HR 0° and cylinder cases would have the same phase state. Thus, a distance shift, Δx , can be easily calculated as a function of the frequency, f , and the phase shift previously obtained, φ , as follows:

$$\Delta x = \varphi c / 2\pi f \quad (4)$$

The absolute value of Δx has a maximum at the resonance frequency and decreases as we move away from it, maintaining in a range of influence at both higher and lower frequencies, as shown at the bottom of Fig. 19(b).

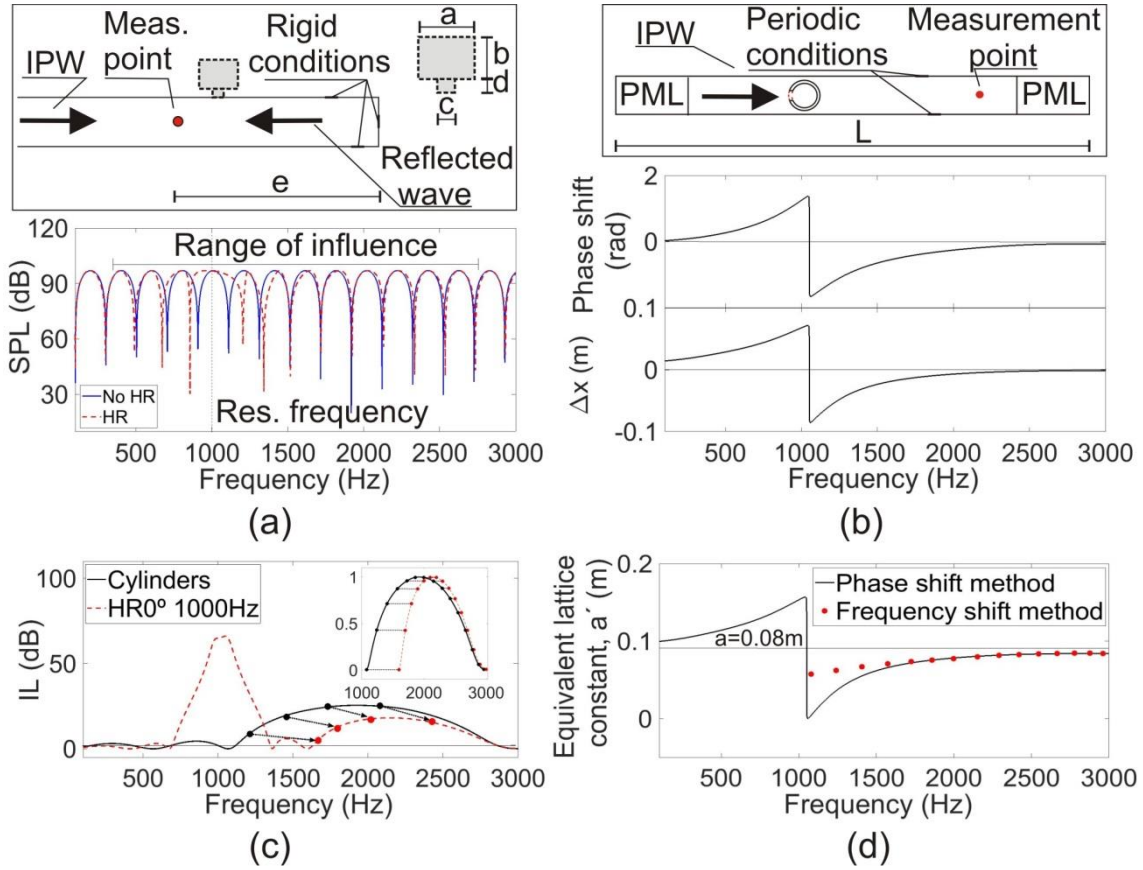


Figure 19: Analysis of the influence of the phase shift on the BG/LRG interference; (a) Phase shift for the pure resonance case for a single HR. An outline of the model is presented at the top. The variation of Sound Pressure Level (SPL) is presented at the bottom; (b) phase shift for the case of resonance plus scattering for a single scatterer. The numerical model is presented at the upper part. At the center, the phase shift Cylinder/ $HR0^\circ$ is shown. The lower part represents the distance displacement, Δx , associated with the phase shift; (c) BG/LRG interference, showing with arrows the displacement of frequencies in the BG. The normalization to 1 of the BG for both arrays formed either by cylinders or by $HR0^\circ$ can be seen in the inset; (d) ELC as a function of frequency, calculated from the phase shift (continuous black line) and frequency shift (red dotted line).

The concept of distance shift becomes important when applied to the case of PC, where the BG appears. In these devices, the location of the BG depends on the lattice constant of the array, which in turn determines the position of the scatterers. Due to the phase shift induced by the HR, the waves would arrive to the scatterers in a different state of phase, and Δx could be understood as if the lattice constants considering either $HR0^\circ$ or cylinders were different. In other words, the BG/LRG interference makes the distance between scatterers seen by the wave, a' , different from the real one, a . This means that the BG is not destroyed, but shifted to another range of frequencies. If we consider the $HR0^\circ$ 1000Hz array with $a=0.08m$, where the BG/LRG interference is more noticeable, this fact is presented in Fig. 19(c) where the displacement of frequencies in the BG is marked with arrows. In the following, we will name a' as the "Equivalent Lattice Constant" (ELC).

Two different methods to estimate the trend of variation of the ELC as a function of frequency have been considered. The first is the phase shift method, already used in the case of a single scatterer, applied to the case of the considered PC. The second is the frequency shift method, in which both BG are normalized to 1 [see the inset of Fig. 19(c)], and from the frequency shift between both BG, the corresponding ELC is estimated. The results for

some frequencies above the resonance peak are presented in Fig. 19(d) on the basis of the starting value of a ($a=0.08$ m). The same trend is observed with both methods, equal to the case of a single scatterer, where there is a variation in the ELC in the range of influence of the HR. In the example considered, the BG of the HR 0° array moves toward high frequencies because $a' < a$ since the BG is above the LRG. Due to the fact that a' depends on the frequency, an increase in the real lattice constant would compensate the effect of the phase shift induced by HR 0° and would produce a displacement of the BG again toward low frequencies. Similarly, if the BG were located below the resonance peak, $a' > a$, and the BG would shift to low frequencies. To correct this, the value of the real lattice constant should be decreased.

To validate these numerical predictions, we have carried out accurate experiments in an anechoic chamber using a directional white sound source (S) and measuring at a distance $d=1$ m behind the sample. In the inset of Fig. 20, we show an outline of the experimental setup used. A comparison between the numerical and experimental IL results for three cases can be seen in Fig. 20: At the top, a PC with closed cylinders with $a=0.08$ m, where the first BG is centered at 2000Hz and starting around 1050Hz, is observed. At the middle, a PC made of HR 0° 1000Hz, where the displacement of the first BG, which now starts around 1550Hz, is observed. At the bottom, one can see a PC with HR 0° but with a higher lattice constant ($a=0.09$ m), where the first BG has moved toward low frequencies, starting at 1450Hz. In the latter case, the size of the starting BG has not been completely recovered, and only its position in the frequency range due to the increase in the lattice constant that reduces the filling fraction of the PC is recovered. The experimental results are in quite good agreement with the numerical simulations, considering the use of an ideal numerical model. Note that although the ELC is a function of frequency, a single variation of the lattice constant produces the displacement of the BG.

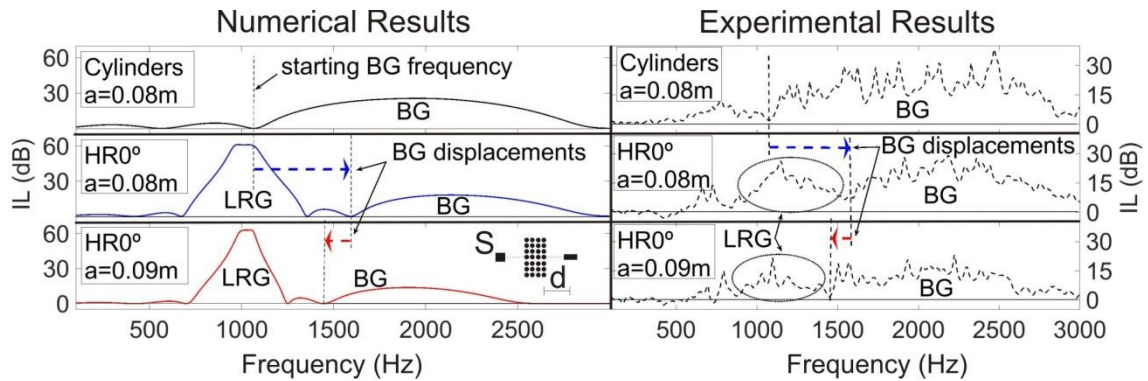


Figure 20: Numerical (continuous line) vs experimental (dashed line) IL results for three PC cases: Cylinders with $a=0.08$ m, HR 0° with $a=0.08$ m, and HR 0° with $a=0.09$ m. An outline of the experimental setup is shown at the bottom left.

In summary, in this work, we have analyzed in depth the BG/LRG interference phenomenon in PC formed by HR. We have performed numerical simulations validated with accurate experiments carried out under controlled conditions. The placement of HR as scatterers, when the LRG is close to BG, induces a phase shift in the transmitted wave that can be understood as a virtual change in the lattice constant of the array, which is greater or smaller than the real one depending on the relative position of the BG with respect to the LRG in the frequency domain. This virtual lattice constant has been named the Equivalent Lattice Constant (ELC) by us.

4.2.3.- References

- [1] Fok, L., Ambati, M., & Zhang, X. (2008). Acoustic metamaterials. *MRS bulletin*, 33(10), 931-934.
- [2] Christensen, J., Romero-García, V., Picó, R., & Cebrecos, A. FG De abajo, NA Mortensen, M. Willatzen, and V. Sánchez-Morcillo, *Sci. Rep.* 4, 4674 (2014).
- [3] Liang, Z., Willatzen, M., Li, J., & Christensen, J. (2012). Tunable acoustic double negativity metamaterial. *Scientific reports*, 2, 859.
- [4] Mei, J., Ma, G., Yang, M., Yang, Z., Wen, W., & Sheng, P. (2012). Dark acoustic metamaterials as super absorbers for low-frequency sound. *Nature communications*, 3(1), 1-7.
- [5] Lee, S. H., Park, C. M., Seo, Y. M., Wang, Z. G., & Kim, C. K. (2010). Composite acoustic medium with simultaneously negative density and modulus. *Physical review letters*, 104(5), 054301.
- [6] Fleury, R., Sounas, D. L., Sieck, C. F., Haberman, M. R., & Alù, A. (2014). Sound isolation and giant linear nonreciprocity in a compact acoustic circulator. *Science*, 343(6170), 516-519.
- [7] Cheng, Y., Xu, J. Y., & Liu, X. J. (2008). One-dimensional structured ultrasonic metamaterials with simultaneously negative dynamic density and modulus. *Physical Review B*, 77(4), 045134.
- [8] Cheng, Y., Yang, F., Xu, J. Y., & Liu, X. J. (2008). A multilayer structured acoustic cloak with homogeneous isotropic materials. *Applied Physics Letters*, 92(15), 151913.
- [9] Sanchis, L., García-Chocano, V. M., Llopis-Pontiveros, R., Climente, A., Martínez-Pastor, J., Cervera, F., & Sánchez-Dehesa, J. (2013). Three-dimensional axisymmetric cloak based on the cancellation of acoustic scattering from a sphere. *Physical review letters*, 110(12), 124301.
- [10] Farhat, M., Chen, P. Y., Bağcı, H., Enoch, S., Guenneau, S., & Alu, A. (2014). Platonic scattering cancellation for bending waves in a thin plate. *Scientific reports*, 4, 4644.
- [11] Fang N, Xi D, Xu J, Ambati M, Srituravanich W, Sun C, Zhang X. (2006). Ultrasonic metamaterials with negative modulus. *Nat Mater.* Jun;5(6):452-6. doi: 10.1038/nmat1644. Epub 2006 Apr 30. PMID: 16648856.
- [12] Shen, C., Xu, J., Fang, N. X., & Jing, Y. (2014). Anisotropic complementary acoustic metamaterial for canceling out aberrating layers. *Physical Review X*, 4(4), 041033.
- [13] Li, Y., Liang, B., Zou, X. Y., & Cheng, J. C. (2013). Extraordinary acoustic transmission through ultrathin acoustic metamaterials by coiling up space. *Applied Physics Letters*, 103(6), 063509.

-
- [14] Tang, K., Qiu, C., Lu, J., Ke, M., & Liu, Z. (2015). Focusing and directional beaming effects of airborne sound through a planar lens with zigzag slits. *Journal of Applied Physics*, 117(2), 024503.
- [15] Cai, X., Guo, Q., Hu, G., & Yang, J. (2014). Ultrathin low-frequency sound absorbing panels based on coplanar spiral tubes or coplanar Helmholtz resonators. *Applied Physics Letters*, 105(12), 121901.
- [16] Leroy, V., Strybulevych, A., Lanoy, M., Lemoult, F., Tourin, A., & Page, J. H. (2015). Superabsorption of acoustic waves with bubble metascreens. *Physical Review B*, 91(2), 020301.
- [17] Hu, X., Chan, C. T., & Zi, J. (2005). Two-dimensional sonic crystals with Helmholtz resonators. *Physical Review E*, 71(5), 055601.
- [18] Karimi, M., Croaker, P., & Kessissoglou, N. (2017). Acoustic scattering for 3D multi-directional periodic structures using the boundary element method. *The Journal of the Acoustical Society of America*, 141(1), 313-323.
- [19] Yang, X. W., Lee, J. S., & Kim, Y. Y. (2016). Effective mass density based topology optimization of locally resonant acoustic metamaterials for bandgap maximization. *Journal of Sound and Vibration*, 383, 89-107.
- [20] Chen, Y., & Wang, L. (2014). Periodic co-continuous acoustic metamaterials with overlapping locally resonant and Bragg band gaps. *Applied Physics Letters*, 105(19), 191907.
- [21] Theocharis, G., Richoux, O., García, V. R., Merkel, A., & Tournat, V. (2014). Limits of slow sound propagation and transparency in lossy, locally resonant periodic structures. *New Journal of Physics*, 16(9), 093017.
- [22] Lardeau, A., Groby, J. P., & Romero-García, V. (2016). Broadband transmission loss using the overlap of resonances in 3D sonic crystals. *Crystals*, 6(5), 51.
- [23] Liu, Z., Zhang, X., Mao, Y., Zhu, Y. Y., Yang, Z., Chan, C. T., & Sheng, P. (2000). Locally resonant sonic materials. *science*, 289(5485), 1734-1736.
- [24] Park, C. M., & Lee, S. H. (2013). Propagation of acoustic waves in a metamaterial with a refractive index of near zero. *Applied Physics Letters*, 102(24), 241906.
- [25] Wang, T. T., Wang, Y. F., Wang, Y. S., & Laude, V. (2018). Evanescent-wave tuning of a locally resonant sonic crystal. *Applied Physics Letters*, 113(23), 231901.
- [26] Yuan, B., Humphrey, V. F., Wen, J., & Wen, X. (2013). On the coupling of resonance and Bragg scattering effects in three-dimensional locally resonant sonic materials. *Ultrasonics*, 53(7), 1332-1343.
- [27] Montiel, F., Chung, H., Karimi, M., & Kessissoglou, N. (2017). An analytical and numerical investigation of acoustic attenuation by a finite sonic crystal. *Wave Motion*, 70, 135-151.

[28] Sigalas, M. M., Economou, E. N., & Kafesaki, M. (1994). Spectral gaps for electromagnetic and scalar waves: Possible explanation for certain differences. *Physical Review B*, 50(5), 3393.

[29] Economou, E. N., & Sigalas, M. M. (1993). Classical wave propagation in periodic structures: Cermet versus network topology. *Physical Review B*, 48(18), 13434.

[30] Berenguer, J.P. (1994) A perfectly matched layer for the absorption of electromagnetic waves. *Journal of Computational Physics* 114(2), 185-200.

4.3.- Sonic Crystals Acoustic Screens and Diffusers.

4.3.1.- Abstract

This article presents the use of advanced tools applied to the design of devices that can solve specific acoustic problems, improving the already existing devices based on classic technologies. Specifically, we have used two different configurations of a material called Sonic Crystals, which is formed by arrays of acoustic scatterers, to obtain acoustic screens with high diffusion properties by means of an optimization process. This design procedure has been carried out using a multiobjective evolutionary algorithm along to an acoustic simulation model developed with the numerical method called Finite Difference Time Domain. The results obtained are discussed in terms of both the acoustic performance and the robustness of the devices achieved.

4.3.2.- Introduction

Environmental noise can be defined as an unwanted or harmful outdoor sound created by human activities, and is one of the main environmental problems all over the world [1]. Among all types, traffic noise caused by cars and duty vehicles is one of the most important and annoying, making the greatest contribution to total noise pollution (around 90%) [2]. Traffic is behind the high noise levels experienced by European citizens, as according to the EU, noise levels above 55 dBA at night and 65 dBA during daylight hours should not be exceeded to ensure the comfort of citizens. However, EU-Eurostat states that 20% of EU citizens during the day and 30% at night suffer from higher noise levels. These high grades of exposure are linked with some health problems such as stress, sleep disturbance, fatigue, cardiovascular disorders or hearing loss [3,4].

Generally speaking, environmental noise can be mitigated (i) at the source, reducing the radiated sound power emitted by vehicles; (ii) during its propagation, reducing the noise level during its propagation from the source to the receiver or (iii) in the receiver, improving the isolation of the dwellings and preventing its transmission through the exterior walls. When the noise control is carried out in its propagation phase, the most used solution is the placement of acoustic barriers (AB) [5], which are located between the noise source and the receiver. Classical AB are generally made of continuous flat walls of different materials such as concrete, wood or methacrylate, and have to meet a certain number of standards in terms of their density and geometry to be acoustically effective [6]. The performance of AB can be explained as follows (Fig. 21(a)): noise is propagated from the source to the receiver following a straight line. AB are placed between them, and an important quantity of the noise energy is reflected specularly while other parts are diffracted from the edge of the barrier, transmitted through it or dissipated by the material that forms the barrier.

If we focus on the energy of specularly reflected noise, some unwanted problems can arise when placing AB to protect predetermined areas. Thus, sometimes the site where AB is located to acoustically protect a receiver can increase the noise level in other locations that also need protection. This situation is illustrated in Fig. 21(b) as an example, where the building A is protected by the AB A. However, the installation of another AB B to protect the building B may produce some reflected sound between the two barriers that may cause

reductions in AB A performance from 2 to 6 dB [3,4,7]. This situation is quite common as show in Fig. 21 (c), where the picture has been taken at one of the entrances to the city of Cádiz (Spain). The same problem of double reflections can be produced by high-sided vehicles.

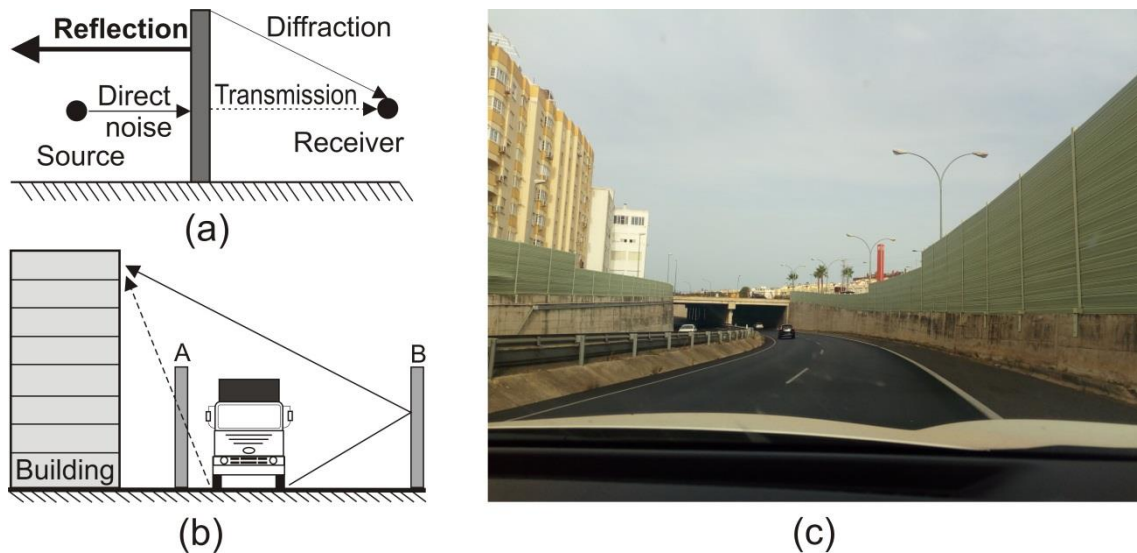


Figure 21: (a) Scheme of the acoustic performance of AB; (b) Scheme of the problems created by the specularly reflected noise; (c) A picture taken at one of the entrances to the city of Cádiz (Spain) to illustrate the described situation.

In order to minimize these specular reflections, several solutions have been proposed, the most common of which are (i) the use of absorbent materials in AB; (ii) the construction of inclined AB, in such a way that the specularly reflected sound is diverted outside the areas to be protected; or (iii) the scattering of the reflected noise on AB, avoiding specular reflection [8]. However, the first two solutions present some problems related to their cost: the use of absorbent materials in AB could increase their price reducing their competitiveness and can be highly degraded by exposure to weathering agents, and the use of tilted AB can be even more expensive and their installation technically complicated for some sites.

Regarding the solution based on scattering the reflected noise, some new proposals have been made in recent years. One of the most widely accepted is the use of new devices based on technologically advanced materials devoted to noise control. Sonic Crystals (SC), generally defined as heterogeneous materials formed by arrangements of acoustic scatterers embedded in air, is one of these materials [9,10]. There are many proposed applications for these materials, including acting as metamaterials [11,12], but in this work we will use two in particular. On one hand their use as AB [13,14], usually called Sonic Crystals Acoustic Screens (SCAS). In this application SC provide a new noise control mechanism by structuring the scatterers, which provides the existence of bandgaps, defined as ranges of frequency where the propagation of the waves is forbidden [15,16]. The existence of bandgaps is the result of the interference of waves due to a Bragg scattering within the SC. These new barriers present aesthetic and technological advantages thanks to their open structure and their versatility to be designed for specific noises, among others properties. However, SCAS also present the specularly reflection of noise, as classical AB.

On the other hand, the use of sound diffusers in room acoustics to increase the sound diffuseness is generally accepted for four decades ago, when Schroeder presented the first proposal of such devices [17]. Since then, several designs have been proposed [18–21] but again, SC seem good candidates to obtain high diffusion levels, even at low frequency range, using smaller device depths than in the case of conventional diffusers [22]. These technologically advanced devices, generally called Acoustic Sonic Crystal Diffusers (SCAD), as is the case with diffusers in general, do prevent specular reflection of noise.

In addition, in recent years it has been possible the increasing of the acoustic performance of some devices based on SC, as SCAS or SCAD, through the use of evolutionary algorithms. Specifically, an elitist Multiobjective Evolutionary Algorithm (MOEA), called ev-MOGA [23], has been used to go a step further in designing technologically advanced noise control devices based on SC, creating SCAS [24] and SCAD [25,26] with high acoustic control properties.

Following this research line, in this work we present the process of designing new devices based on SC that work simultaneously as SCAS and SCAD. To obtain this goal, we have varied the radii of the cylindrical scatterers that form a pre-selected SC module using a MOEA as a tool. Although the idea of designing devices with this double function – protecting against direct noise and avoiding specularly reflected noise – is not new [28] and it is generally carry out by adding a sound diffuser to classic AB [29,30] or designing classic AB with a corrugated side [3], our procedure is far away from these designs since we use advanced materials and new designing tools. These new devices will work fundamentally as AB but with a low level of specularly reflection, minimizing the disturbance that sometimes appears when AB are used to control transport noise. Hereafter we will refer to these new devices as SCASAD (Sonic Crystals Acoustics Screens and Diffusers). Finally, a robustness study related to the manufacturing process of the analyzed devices has been carried out.

The paper is organized as follows: in Section 4.3.3 we describe the optimization process, explaining both the optimization tool and the simulation model used. The results obtained in the optimization process from two initial modulus of SC are analyzed and discussed in Section 4.3.4. The last section, Section 4.3.5, contains the closing remarks, where the main conclusions are summarized.

4.3.3.- Theoretical considerations

Description of the optimization process

In this section we briefly explain the main characteristics of the MOEA used in this work as well as the optimization procedure carried out. There are certain types of optimization problems in which is necessary to achieve solutions that satisfy several objectives simultaneously. Obviously, the natural tendency is to search the best solution for each one of the considered objectives. However, if the objectives are in conflict, usually an improvement in one of them means a worsening in others, and this means that there is not a single optimal solution. These kind of problems, where several conflicting objectives have to be simultaneously optimized are known in the literature as multiobjective optimization

problems, and they may be solved using MOEA [31]. A general basic multiobjective problem can be formulated as follows:

$$\min J(\theta) = \min [J_1(\theta), J_2(\theta), \dots, J_s(\theta)] \quad (5)$$

$$\text{Subject to } \theta_{li} \leq \theta_i \leq \theta_{ui} (1 \leq i \leq L)$$

where $J_i(\theta)$, $i \in B: [1 \dots s]$ are the objectives to be minimized, θ is a solution inside the L -dimensional solution space $D \subseteq R^L$, and θ_{li} and θ_{ui} are the lower and the upper constraints that defined the solution space D .

The general way to solve such problems using MOEA is the localization of a set of infinite optimal solutions in the objective space, which is mapped as the Pareto front. This front shows the best individuals, in some sense, obtained in the optimization process and classified according to the values achieved in the functions to be optimized. The basic concept to obtain the Pareto set is known as Pareto dominance, which is defined as follows: a solution θ^1 dominates another solution θ^2 , denoted by $\theta^1 \succ \theta^2$, if $\forall i \in B, J_i(\theta^1) \leq J_i(\theta^2) \wedge \exists k \in B: J_k(\theta^1) < J_k(\theta^2)$. The Pareto set Θ_p is composed by all the non-dominated solutions, and the associated Pareto front is denoted as $J(\Theta_p)$. Due to the difficulties appeared in real problems to get the exact Pareto front, we have used here an elitist multi-objective evolutionary algorithm based on the concept of e-dominance [32] named ev-MOGA [23]. A complete explanation of the foundations and functioning of this algorithm as well as its applications in the field of SC can be found in references [23–25].

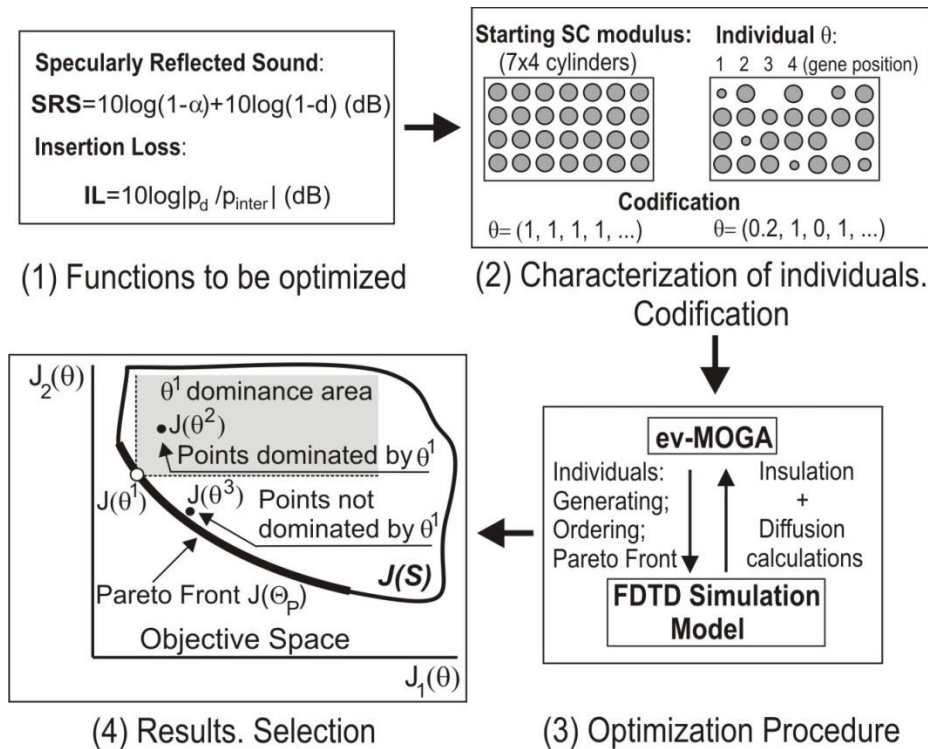


Figure 22: Scheme of the steps followed in the optimization process.

An outline of the optimization procedure is shown in Fig. 22. First (step 1), it is necessary to define the functions to be optimized, generally referred to as optimization objectives or cost functions. In our case, we want to design devices with high levels of

acoustic insulation and diffusion. This means a bi-objective optimization procedure and we have to carefully define two cost functions, related to these properties, to characterize the effectiveness of our devices. Its definition must take into account the characteristics of the ev-MOGA algorithm, which works minimizing cost functions.

The first cost function we have chosen, related to the acoustic insulation capabilities of different individuals, is related to the Insertion Loss (IL) index, defined as the difference in sound pressure at a point or area with and without the sample. Note that the goal is to achieve a high level of acoustic insulation and therefore, in the optimization process we will work minimizing – IL. Thus, for a solution (individual) θ .

$$J_{-IL}(\theta) = -10\log\left|\frac{P_d}{P_{inter}}\right| (dB) \quad (6)$$

where P_d is the direct acoustic pressure (without device), and P_{inter} is the acoustic pressure interfered (with device), both calculated at the same point or area.

The second cost function concerns the capability of the individuals to reduce the specularly reflected sound. Thus, we define the second cost function as a new index called Specular Reflection Sound (SRS). For an individual h is defined as:

$$J_{SRS}(\theta) = -10\log(1 - \alpha) + 10\log(1 - d)(dB) \quad (7)$$

where α and d are for each individual the coefficients of absorption and diffusion respectively. Note that the SRS index is a function of α and d , (where a is defined as usual, i.e. one minus reflected sound and incident sound). This is because we have taken into account in our analysis that the surface of the scatterers is slightly absorbent, with $a = 0.02$. In addition, for frequencies outside the bandgaps, the sound passes through the SC, increasing the amount of energy that is not reflected. Both effects can cause the absorption coefficient to be greater than 0 and must be considered in this second cost function.

These two cost functions determine the performance of individuals as both SCAS and as SCAD in the predetermined range of frequencies established by us. In this work we have selected a range of frequencies formed by the octaves bands whose central frequencies are 500 Hz, 1000 Hz and 2000 Hz, i.e. a range of frequencies from 355 Hz to 2828 Hz. The reason for this selection is related with the nature of the noise that our devices will deal with, which is given by the normalized spectral traffic noise defined in the norm EN 1793-3:1998 [27], where more relevant frequencies are covered by our selected range.

Once the cost functions have been defined, the next step of the optimization procedure (step 2) is twofold: (i) the characterization of the shape of the individuals – including the initial population with which the optimization process begin – in such a way that the population will be formed by a variable set of individuals, all of them based on a predetermined SC module, and (ii) their codification. In this work we have selected a module formed by 28 cylindrical rigid scatterers arranged in 4 rows. The reason for this choice is related to the characteristics of the SCAS and SCAD designed and/or optimized up to now: SCAS are usually formed by 3 or 4 rows [13,14] and, at the same time, SCAD are formed by 4 rows [25]. Taking these results into account, an optimized SCASAD should

consist of at least 7–8 rows, adding the necessary rows for an optimal performance as SCAS and SCAD. However, our design proposal aims to force the acoustic performance of the CS to produce a very compact device made up by the fewest number of rows, set by us at 4, in order to obtain an occupancy similar to that of the classic ABs at road shoulders that is around 0.50 m. In addition, the number of scatterers in each row ensures a reasonable genetic variation of the population taking into account the tool selected to obtain new individuals from the initial population, as we explain below. This initial module does not have a high performance as either SCAS or SCAD, due to the low number of rows that compose it, and its insulation and diffusion properties will be greatly improved in the optimization process to be carried out.

On the other hand, in order to provide enough genetic variation to the initial population necessary to create new individuals with a high variability in the values of their cost functions, we have used as a tool the variation of the radii of the cylindrical scatterers of the individuals formed from the module previously defined (7 x 4 cylinders). To characterize each individual of the population it is necessary to establish a gene codification, encoding each one of them by means of a set of genes that represents the set of the 28 (7 x 4) normalized cylinders radii. Each radius can take any value from 0 to 0.9. If the value is 0, the cylinder does not exist and, if the value is 0.9, the cylinder has almost the maximum possible radius, which is equal to the half lattice constant. In this way, any individual θ can be represented by a genotype given by a vector of length 28 elements, varying each one from 0 to 0.9. Two examples of the genetic coding are shown in Fig. 22.

Once the cost functions and the codification of individuals have been defined, the optimization procedure can be initiated. This process works using together ev-MOGA and an acoustic simulation model developed by us, which will be presented in next section. ev-MOGA leads the process (i) generating new individuals by mixing, following the rules of genetics including mutations, the genotypes of the individuals from the initial population generated by us; (ii) ordering and representing the different individuals in the objective space according to the values of each of the defined cost functions and (iii) stablishing the Pareto Front in the objective space. On the other hand, the simulation model evaluates the acoustic performance of each individual generated by ev-MOGA, calculating the values of its cost functions (-IL and SRS) and providing them to ev-MOGA. Finally, the optimization procedure ends when an optimal solution belonging to the Pareto Front obtained is selected according to designer preferences.

Simulation model: Finite Difference Time Domain

To acoustically characterize the different individuals obtained in the optimization process, we have developed a simulation model based on the numerical technique called Finite Difference Time Domain (FDTD). This model works together with ev-MOGA and performs the necessary calculations to obtain the values, for each individual, of the previously defined cost functions. FDTD is often used in acoustic simulations of different devices. In particular, it has been already used successfully to quantify the acoustic performance of SC in some optimization processes, working together with ev-MOGA [25]. Further details about the characteristics of this numerical setup can be found in reference [33].

The model developed specifically for this paper is shown in Fig. 23. The rectangular calculation domain is formed by two parallel lines with periodic boundary conditions in order to simulate a semi-infinite SC. Furthermore, to avoid unwanted reflections, a Perfectly Matched Layer (PML) is located at the right of the domain.

With these boundary conditions, the numerical scheme is excited by a line source placed at the left hand side of the integration area (see Fig. 23(a)). As FDTD works in the time domain it is extremely important to use excitations signals as short in time as possible in order to minimize the computational cost. In this work we have used a Dirac delta filtered with the normalized traffic noise spectra defined in the EN 1793-3:1998 norm [27]. Part of this generated signal is transmitted through the device and another part is reflected to the left. The insulation performance of each individual, given by the -IL cost function, is calculated behind the SC, on the right area of the model (measurement area in Fig. 23). To do that, we have obtained the acoustic pressure every 0.02 m in this area, with and without the sample, to obtain the -IL value at each point in 1/3 octave band for the selected range. Then a spatial average has been carried out to obtain a single -IL value for each individual. Note that this measurement area is approximately 0.2 m away from the device to avoid the near field area behind the SC.

On the other hand, to estimate the SRS index we need to estimate both the absorption and the diffusion coefficients. The absorption coefficient can be easily obtained by comparing the incident and reflected sound. The diffusion coefficient is obtained according to the guidelines of ISO 17497-2 [34] but derived from a near-field to far-field transformation used to reduce the cost of calculation in our numerical model. Note that otherwise it would be necessary to simulate a large anechoic space on the left side.

According to the characteristics of the numerical model explained, the optimization process is developed only for the normal incidence of the wave on the SC.

4.3.4.- Results and discussion

To obtain high performance devices that act simultaneously as SCAS and as SCAD we have used in this work the combination of ev-MOGA and FDTD, as we have commented above. One of the main problems of this optimization procedure is that the joint use of both algorithms implies large computational cost. In our case, the FDTD simulation for each device takes about 240 s on an Intel Core i7-3632QM 2.20 GHz (Santa Clara, CA). To calculate the total runtime, it is necessary to take into account that the total number of calculations in the optimization process is estimated as the number of new individuals plus the number of individuals in the initial population. Once the Pareto set is obtained for each generation, it is used as part of the initial population for the next optimization. In the process of optimization developed in this work, the initial population is formed by 2000 individuals, and in each generation 8 new individuals are added. Under these conditions, the total execution time of the entire process is 7 days, considering 1000 generations.

Two different arrangements, based on the module described in Section 4.3.3, have been considered in the optimization carried out. These configurations have been called mono-crystal and bicrystal by us. The specific characteristics of each configuration as well as the reasons for the choice of both of them will be explained in the following sections.

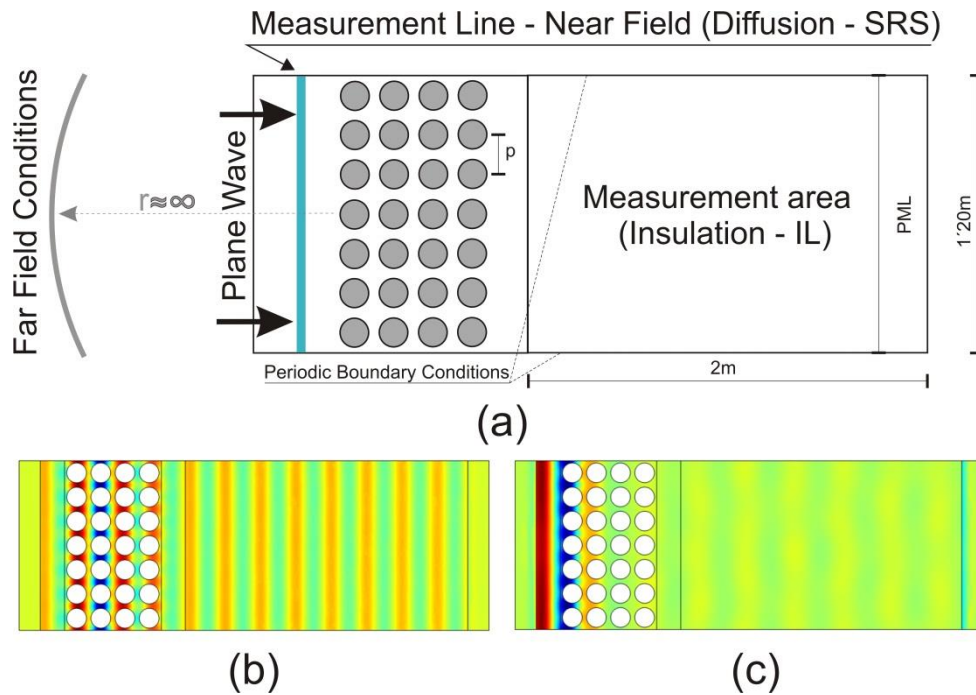


Figure. 23. (a) Scheme of the simulation model, based on FDTD, used to acoustically characterize the individuals generated by ev-MOGA; (b) and (c) Examples of acoustic pressure fields, in Pa, for frequencies outside (1370 Hz) and inside (1000 Hz) the bandgap respectively.

SCASAD of individual with a single lattice constant (mono-crystal)

The first configuration (mono-crystal) is formed by the initial module defined in Section 4.3.3 but arranging the cylindrical scatterers using only one lattice constant. That means that the existing bandgaps in the region of interest are due to only one periodicity. Specifically, and taking into account the normalized spectral traffic noise defined in the norm EN 1793-3:1998 [27], we have set the value of the considered single lattice constant in $p = 0.17$ m, which corresponds to a first bandgap centered at 1000 Hz for an incidence of 0° on the SC, the most critical frequency of the normalized spectral traffic noise. Additionally, the following bandgaps (second and third) would be located at 2000 Hz and 3000 Hz respectively, within the frequency range of interest. With these geometrical conditions, the objective in this first optimization process is to design a SCASAD device with high performance, simultaneously, as SCAS and SCAD around the same global target frequency, 1000 Hz. Note that with this lattice constant the width of the devices is about half a meter, depending on the radius of the cylinders considered, and is close to those of the classic AB.

The results of the optimization process are shown in Fig. 24(a), where the objective space is represented. The black dots represent the individuals of the initial population according to their single values of both cost functions considered, -IL and SRS (abscissa and ordinate axes respectively) calculated as shown in Section 4.3.3. The individual belonging to the initial population, which is formed by cylinders of equal radius corresponding to a filling fraction of 75%, ($r = 0.08$ m), is represented in the Figure by a blue diamond and is called by us “reference individual”. The position of this non-optimized individual in the objective space serves as a reference for the improvement achieved in the optimization process. The Pareto Front is formed in the Fig. 24(a) by the individuals marked as red squares. Among all the individuals that form the Pareto Front, we have selected as designers

the individual marked with a green square due to its balanced values of both cost functions, and we have named it “selected individual”. Fig. 24(b) shows the individuals considered, the reference (top) and the selected one (below).

The acoustic performance of both individuals (the reference in continuous blue line and the one selected in dashed green line) can be seen in Fig. 24(c) as a function of frequency, where the range of interest of the study is also indicated. Note that the IL and -SRS indexes, instead -IL and SRS, are represented here for better understanding. The insulation (IL) spectra for both individuals are shown at the top of Fig. 24(c), where the higher global performance trend as SCAS of the reference individual compared with the selected one (15,7 dB versus 12 dB in Fig. 24(a)) can be checked. In addition, the first bandgap of the mono-crystal arrangement at 1000 Hz, corresponding to the considered lattice constant, can be easily observed for both individuals, wider in the case of the reference individual and smaller for the selected one. On the other hand, the diffusion properties of both individuals, given here by the -SRS index, are shown in the center of Fig. 24(c). As can be seen, the -SRS values are generally higher for the selected individual and lower for the reference, confirming the trend shown in Fig. 24(a) (3 dB versus 0.8 dB).

Interesting conclusions can be drawn from the previous results for this first optimization process. Firstly, the increase in diffusion properties in the optimization is achieved at the expense of loss of attenuation capability. Thus, in the case of the selected individual, an increase of 2.1 dB in the SRS cost function implies a loss of 3.7 dB in the -IL index with respect to the corresponding values obtained by the reference individual (see Fig. 24(a)). Second, it seems that the increase of the diffusion capabilities of the optimized individuals is quite small compared with the SRS values that the initial population has. However, this conclusion seems a consequence of the selected cost function (SRS). Indeed, if in the frequency range considered we analyze the value of the diffusion coefficient d , used to measure the diffusion capability according to current standards and represented at the bottom of Fig. 24(c), we can conclude that the mean value of the diffusion coefficient of the selected individual compared to the reference increases considerably (0.3 versus 0.02). Finally, analyzing the -SRS and IL spectra represented in Fig. 24(c), it can be concluded that the higher the insulation value, the lower the -SRS value. This fact can be seen for the two individuals analyzed, although it is more remarkable in the case of the selected individual: around the bandgap frequency (1000 Hz), where the insulation values are maximum, minimum values of -SRS and d appear. This result is of great importance for the design of SC-based devices, SCASAD in this case: it is not possible to create SC with high performance as an insulator and as a diffuser in the same frequency target, since a high attenuation implies low diffusion. The explanation of this fact could be related to the small number of SC rows considered. We think that we have pushed the SC to the limit of their acoustic performance, demanding that they work as insulators and diffusers with only 4 rows, a very small number. Perhaps with more rows their acoustic performance could be increased. But the initial requirements force us to maintain that number of rows so that these devices are competitive with respect to the existing ones.

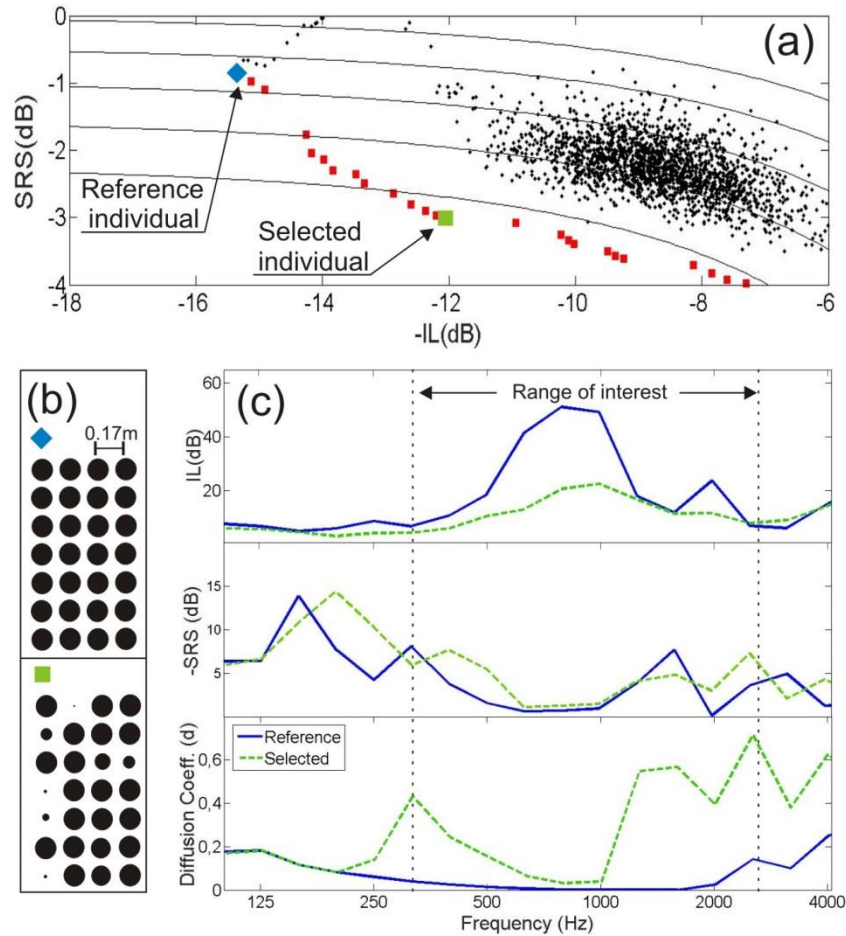


Figure 24. Optimization results for the mono-crystal case. (a) Objective space where the initial population, the Pareto Front and the selected and the reference individuals are remarked; (b) Analyzed devices; (c) Acoustic performance of both individuals, reference (blue continuous line) and selected (green dashed line). IL, -SRS and d spectra are shown in the target frequency range.

SCASAD from individual with a double lattice constant (bi-crystal)

Taking into account the conclusions obtained in the previous section, we have proposed the design of a new SCASAD arrangement based on the initial module defined in Section 4.3.3. Again, the idea is to obtain, through an optimization process, a SCASAD for the previously predefined frequency range, working simultaneously as SCAS and SCAD around the target frequency of 1000 Hz. In this case the initial module, which still has 4 rows of cylinders, is formed by two sets of two rows with different lattice constant ($p_1 = 0.24$ m and $p_2 = 0.17$ m). Both sets are separated by a distance $p_3 = 0.38$ m (see the top of the Fig. 25(b)). The first set of cylinders ($p_1 = 0.24$ m) presents its two first bandgaps centered at 700 Hz and 1400 Hz for the incidence on the SC considered through the entire study. Thus, this first set of cylinders works as a SCAD, designed in such a way that its bandgaps (maximum insulation, minimum diffusion) do not match with the target frequency of design (1000 Hz), and thereby obtain maximum diffusion in it.

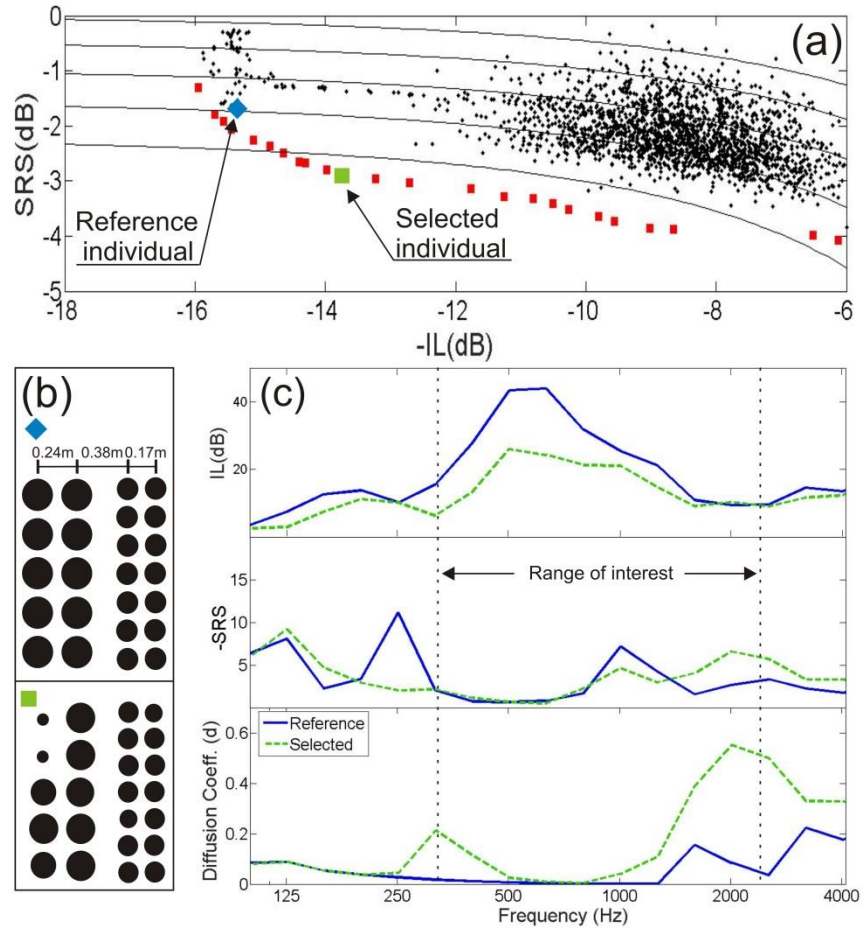


Figure. 25. Optimization results for the bi-crystal case. (a) Objective space where the initial population, the Pareto Front and both the selected and the reference individuals are remarked; (b) Devices considered, the selected individual and the reference one (c) Acoustic performance of both individuals, reference (blue continuous line) and selected (green dashed line). IL, -SRS and d spectra are shown in the frequency range targeted.

On the other hand, the second set of cylinders ($p_2 = 1000$ Hz) works as SCAS since its first bandgap match with the target frequency of design. Moreover, due to the existence of two different lattice constant in the initial module, more bandgaps exist in the frequency range of interest, and a higher global attenuation in this range should appear. Finally, the separation between both set of rows is $p_3 = 0.38$ m that corresponds to bandgaps at 400 Hz, 800 Hz and 1200 Hz, which are away from the target frequency, contributing in addition to the overall isolation obtained by the device. With this starting design, separating the rows that will work as SCAS or SCAD instead of the previous (mono-crystal) case where all rows works as SCAS and SCAD simultaneously, we are forcing much more the acoustic capabilities of SC, generally assigning only two rows to diffusion and two more to insulation, where the usual number of rows in these devices is 4 for SCAD and 3–4 for SCAS, as we have indicated above [13,14,24]. This design has developed, as in the mono-crystal case, considering the normalized spectral traffic noise defined in the EN 1793-3:1998 [27] standard. Note that in this case the width of the devices is about 0.80 m, slightly wider than a classic screen.

The results of the optimization process can be seen in Fig. 25(a), where the objective space is represented. The performance of the initial population (black dots in Figure) with

respect to defined cost functions is represented. The blue diamond represents the “reference individual”, formed with the geometrical parameters defined above, being its filling fraction fixed at 75%, which corresponds to a radius $r_1 = 0.12$ m and $r_2 = 0.08$ m for the lattices constant $p_1 = 0.24$ m and $p_2 = 0.17$ m respectively. The best individuals obtained in the optimization process, which form the Pareto Front, are represented as red squares in the Figure. Among all the individuals forming the Pareto Front we have chosen, as designers, the one represented by a green square (“selected Individual”), which is an individual with a balanced acoustic performance. Note the variability of the radii of the cylinders that form the selected individual obtained in the optimization process (see the bottom of Fig. 25(b)).

Again, the acoustic performance of both individuals (the reference individual in continuous blue line and the selected one in dashed green line) can be seen in Fig. 25(c) as a function of frequency. In the upper part of Fig. 25(c) the IL spectra for both individuals are shown, and it can be observed that the trend follows the results shown in Fig. 25(a), where the overall insulation performance of the reference individual is greater than that of the selected one (15.7 dB vs. 13.8 dB in Fig. 25(a)), as in the case of mono-crystal. On the other hand, the analysis of the -SRS spectra, shown in the center of Fig. 25(c), confirm a small increasing of the overall diffusion properties of the selected individual in front of the reference one (3 dB versus 1.6 dB in Fig. 25(a)), but instead the frequencies with lower diffusion capabilities in the selected range are below the global target frequency (1000 Hz), which have an increasing of its SRS value (4.8 dB). Thus, one of the goals of this new design has been achieved: to obtain high values of both insulation and diffusion at the global target frequency (1000 Hz).

Finally, the conclusions about the diffusion properties obtained analyzing the SRS index are confirmed by the results shown at the bottom of Fig. 25(c), where it can be seen that the target frequency is outside of the frequency range with low values of the diffusion coefficient, d . Furthermore, an increasing in the values of d in the entire frequency range considered for the selected individual is achieved, compared with the ones obtained by the reference. Specifically, as shown in the bottom of Fig. 25(c), for the frequencies range considered the mean d value of the selected individual is quite higher than the one of the reference.

An interesting analysis can be made by comparing the acoustic performance of both considered configurations. Firstly, it can be observed that the values of the -IL index are similar for reference individuals (15.7 dB) and higher than the values of the individuals selected for both analyzed configurations. This conclusion is related to the fact that both reference individuals have been designed with a high filling fraction and, as a consequence, their insulation properties must be high. However, when comparing global -IL values for both selected individuals, the bi-crystal presents a higher insulation than the mono-crystal (13.8 dB versus 12 dB). In this sense, the bi-crystal configuration has a better performance than the mono-crystal. On the other hand, the reference individual of the bi-crystal arrangement has higher global SRS value than the mono-crystal (1.6 dB versus 0.8 dB), which means that the bi-crystal is a better starting point, in terms of specular reflection reduction for the optimization process. However, the results obtained are similar for both configurations: the selected individuals for mono-crystal and bi-crystal configurations have similar values of both the global SRS index (3 dB) and the diffusion coefficient. This means

that the optimization carried out with both configurations provides individuals with better diffusion properties at the expense of reducing insulating performance.

Study of the robustness of the selected devices

Another interesting parameter used to help decision maker to choose the most appropriate individual in the optimization process is the robustness of the selected devices. This concept has been previously introduced by some of us, and is defined as the degree to which the values of cost functions are affected by small changes in the values of the parameters that vary in the optimization process [25]. In our case, we have studied the robustness of the devices related to the variation of the cylinder radius that may appear due to possible errors in the manufacturing process. The low robustness of an individual means that it may not be the right choice, as some small unwanted and uncontrolled variations in cylinder radii can result in a significant reduction in the acoustic performance of devices.

The robustness of individuals is represented by a vector that provides information on each individual according to the following rules: (i) the size of the vector indicates how robust an individual is according to the following rule of thumb: the larger the size of the vector, the less robust it is; (ii) Also, the size of vector components along the axes that represent the cost functions indicates how robust the individual is relative to each of them. To obtain the robustness vectors, each individual of the Pareto Front has been recalculated 200 times producing small random variations in the radii of the cylinders that form it. To simulate some defects in this manufacturing process, we have modified the radius of all cylinders by 5%. In doing so, we obtain in the objectives space a cloud of points around each initial Pareto point. This cloud is averaged at a single point and, finally, the robustness vector, whose origin is the point of Pareto considered and its end is this point average of the modified individuals, is plotted.

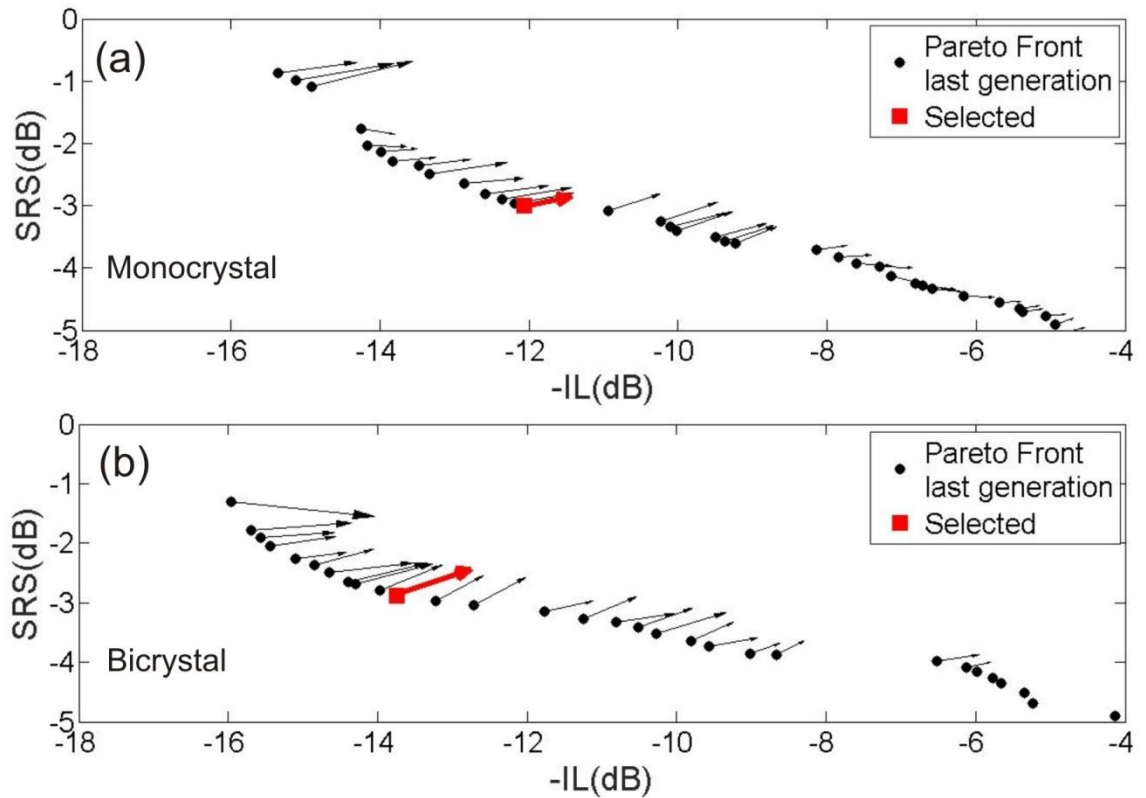


Figure 26. Pareto front with the robustness vectors of the radii for both cases analyzed. Both selected individuals are represented by a red square, and the particular robustness of both individuals is shown by a thick red vector. (a) mono-crystal; (b) bi-crystal.

Fig. 26 shows the robustness vectors of the individuals forming the Pareto Front, including the selected ones, in both optimizations carried out. It can be seen in the Figure that the trend is similar in both analyzed arrangements according to vector length: robustness is greater in the Pareto points with high SRS and low IL, and lower when Pareto individuals present low SRS and high IL. Another interesting conclusion that can be drawn from Fig. 26 is that the horizontal component of the vectors robustness (component according to IL) is generally greater than the component according to the vertical axis (component according to SRS). This fact indicates that the IL variable is less robust than the SRS variable. Moreover, from Fig. 26 it can be concluded that all the robustness vectors represented indicate that any variation in the radii of the scatterers would produce individuals with lower acoustic performance than those belonging to the Pareto front. This is a good indicator that the optimization process has been carried out to the end. Finally, the devices selected in both optimizations, represented with a red square in Fig. 26, have a robustness in line of what was previously mentioned, being more robust the individual in the case of mono-crystal optimization.

4.3.5.- Conclusions

In this work we have used a specific Multiobjective evolutionary algorithm, called ev-MOGA, together with a simulation acoustic model based on the numerical technique called Finite Difference Time Domain (FDTD) in a bi-objective optimization process.

With these tools we have designed technologically advanced devices based on Sonic Crystals. Specifically, we have solved an environmental noise problem related to the performance of classical noise barriers. These barriers, generally formed by straight walls, reflect noise specularly, so that these reflections can cause nuisance on the opposite side of the place where the barriers are located. To solve this problem we have carried out an optimization with two cost functions related to the insulation and the reduction of specular reflections of the devices, represented by the IL and SRS indexes respectively. The starting point of our designs is the use of a minimum number of rows of the SC, four, to obtain a new acoustic screen with diffusion properties and the lowest possible thickness so that it can be installed on the roadside shoulders without space problems. Even with this important restriction, the results obtained are successful, in terms of both acoustic performance and robustness.

To avoid some problems related to the acoustic behaviour of Sonic Crystals, in particular the fact that the frequency ranges with maximum attenuation (bandgap) correspond to the minimum diffusion, we have tested two different configurations of cylinders, called mono-crystal and bi-crystal. Although the acoustic performance of both arrangements is similar in terms of diffusion, in the case of the insulation the bi-crystal arrangement works better than the mono-crystal one. The resultant devices have been called Sonic Crystals Acoustic Screens and Diffusers (SCASAD) by us, and provide a high technological design process to solve an environmental problem with the help of new materials and tools.

4.3.6.- References

[1] EC Directive. Directive 2002/49/EC of the European Parliament and of the Council of 25 June 2002 relating to the assessment and management of environmental noise. Official J Eur Communities L 2002;189. 0012e0026 (18.7.2002), Brussels.

[2] den Boer LC, Schrotten A. Traffic noise reduction in Europe. CE Delft; 2007. p. 2057–68.

[3] (a) Kotzen B, English C. Environmental noise barriers: a guide to their acoustic and visual design. London: E&FN Spon; 1999; (b) Kotzen B, English C. Environmental noise barriers: a guide to their acoustic and visual design. CRC Press; 2009.

[4] Platon SN, Hionis CA. Preventing risk of noise exposure in working environment using noise mapping. Environ Eng Manage J 2014;13 (6):1349–54.

[5] Harris CM. Handbook of acoustical measurements and noise control. McGraw- Hill Companies; 1991. 30-15.

[6] U.S. Dept. of Transportation. Keeping the noise down: highway traffic noise barriers. Federal Highway Administration. U.S. Dept. of Transportation; 2018 (accessed 01 March 2018)

https://www.fhwa.dot.gov/environment/noise/noise_barriers/design_construction/keep_down.cfm.

[7] Lee CS, Fleming GG. Measurement of highway-related noise (No. FHWA-PD- 96-046). Federal Highway Administration; 1996.

-
- [8] Pigasse G, Kragh J. Optimised Noise barriers-a State-of-the-art report. Danish Road Directorate; 2011.
- [9] Kushwaha MS, Halevi P, Dobrzynski L, Djafari-Rouhani B. Acoustic band structure of periodic elastic composites. *Phys Rev Lett* 1993;71(13):2022–5.
- [10] Martínez-Sala R, Sancho J, Sánchez-Pérez JV, Gómez V, Llinares J, Meseguer F. Sound attenuation by sculpture. *Nature* 1995;378(6554):241.
- [11] Torrent D, Sánchez-Dehesa J. Acoustic metamaterials for new twodimensional sonic devices. *New J Phys* 2007;9(9):323. <https://doi.org/10.1088/1367-2630/9/9/323>.
- [12] Romero-Garcia V, Krynkin A, Garcia-Raffi L, Umnova O, Sánchez-Pérez JV. Multi-resonant scatterers in sonic crystals: locally multi-resonant acoustic metamaterial. *J Sound Vib* 2013;332(1):184–98. <https://doi.org/10.1016/j.jsv.2012.08.003>.
- [13] Romero-García V, Sanchez-Perez JV, Garcia-Raffi LM. Tunable wideband bandstop acoustic filter based on two-dimensional multiphysical phenomena periodic systems. *J Appl Phys* 2011;110(1):. <https://doi.org/10.1063/1.3599886014904>.
- [14] Morandi F, Miniaci M, Marzani A, Barbaresi L, Garai M. Standardised acoustic characterization of sonic crystals noise barriers: sound insulation and reflection properties. *Appl Acoust* 2016;114:294–306. <https://doi.org/10.1016/j.apacoust.2016.07.028>.
- [15] Sánchez-Pérez JV, Caballero D, Martínez-Sala R, Rubio C, Sánchez-Dehesa J, Meseguer F, et al. Sound attenuation by a two-dimensional array of rigid cylinders. *Phys Rev Lett* 1998;80(24):5325–8. <https://doi.org/10.1103/PhysRevLett.80.5325>.
- [16] Sigalas MM, Economou EN. Elastic and acoustic wave band structure. *J Sound Vib* 1992;158(2):377–82. [https://doi.org/10.1016/0022-460X\(92\)90059-7](https://doi.org/10.1016/0022-460X(92)90059-7).
- [17] Schröder MR. Diffuse sound reflection by maximum length sequences. *J Acoust Soc Am* 1975;57(1):149–50. <https://doi.org/10.1121/1.380425>.
- [18] Cox TJ. Designing curved diffusers for performance spaces. *J Audio Eng Soc* 1996;44(5):354–64.
- [19] Schroeder MR. Towards better acoustics for concert halls. *Phys Today* 1980;33:24–30.
- [20] Angus J. Sound diffusers using reactive absorption gratings. Audio engineering society convention 98. Audio Engineering Society; 1995.
- [21] Jiménez N, Cox TJ, Romero-García V, Groby JP. Metadiffusers: deepsubwavelength sound diffusers. *Sci Rep* 2017;7(1):5389. <https://doi.org/10.1038/s41598-017-05710-5>.
- [22] Redondo J, Picó Vila R, Sánchez-Morcillo V, Woszczyk W. Sound diffusers based on sonic crystals. *J Acoust Soc Am* 2013;134(6):4412–7. <https://doi.org/10.1121/1.4828826>.
- [23] Herrero JM. Non-linear Robust identification using evolutionary algorithms [Doctoral dissertation Ph.D. Thesis]. Spain: Polytechnic University of Valencia; 2006.

-
- [24] Herrero JM, García-Nieto S, Blasco X, Romero-García V, Sánchez-Pérez JV, Garcia-Raffi LM. Optimization of sonic crystal attenuation properties by ev-MOGA multiobjective evolutionary algorithm. *Struct Multidiscip Optim* 2009;39(2):203–15. <https://doi.org/10.1007/s00158-008-0323-7>.
- [25] Redondo J, Sánchez-Pérez JV, Blasco X, Herrero JM, Vorländer M. Optimized sound diffusers based on sonic crystals using a multiobjective evolutionary algorithm. *J Acoust Soc Am* 2016;139(5). <https://doi.org/10.1121/1.4948580>.
- [26] Hughes RJ, Angus JA, Cox TJ, Umnova O, Gehring GA, Pogson M, et al. Volumetric diffusers: pseudorandom cylinder arrays on a periodic lattice. *J Acoust Soc Am* 2010;128(5):2847–56. <https://doi.org/10.1121/1.3493455>.
- [27] ES BN 1793-3:1998 Road traffic noise reducing devices. Test method for determining the acoustic performance. Normalized traffic noise spectrum.
- [28] Monazzam MR, Lam YW. Performance of profiled single noise barriers covered with quadratic residue diffusers. *Appl Acoust* 2005;66(6):709–30. <https://doi.org/10.1016/j.apacoust.2004.08.008>.
- [29] Kamisin' ski T, Kinasz R, Szela_g A, Rubacha J, Pilch A, Flach A, et al. The comprehensive research of the road acoustic screen with absorbing and diffusing surface. *Arch Acoust* 2015;40(1):137–44. <https://doi.org/10.1515/aoa-2015-0016>.
- [30] Koussa F, Defrance J, Jean P, Blanc-Benon P. Acoustical efficiency of a sonic crystal assisted noise barrier. *Acta Acustica United Acustica* 2013;99 (3):399–409. <https://doi.org/10.3813/AAA.918621>.
- [31] Back T. Evolutionary algorithms in theory and practice: evolution strategies, evolutionary programming, genetic algorithms. Oxford University Press; 1996.
- [32] Laumanns M, Thiele L, Deb K, Zitzler E. Combining convergence and diversity in evolutionary multiobjective optimization. *Evol Comput* 2002;10(3):263–82. <https://doi.org/10.1162/106365602760234108>.
- [33] Redondo J, Picó R, Roig B, Avis MR. Time domain simulation of sound diffusers using finite-difference schemes. *Acta Acustica United Acustica* 2007;93 (4):611.-.622.
- [34] ISO 17497-2. Measurement of sound scattering properties of surfaces. Part 2: Measurement of the directional diffusion coefficient in a free field.

4.4.- Insertion loss provided by Sonic crystal acoustic screen – assessment of different estimation methods.

4.4.1.- Abstract

Sonic crystal acoustic screens have been in progressive research and development in the last two decades as a technical solution for mitigating traffic noise. Their behaviour is quite different from that observed in classical barriers, with the latter being based on physically blocking the direct sound propagation path (only allowing diffracted noise to reach sensible receivers), and sonic crystals providing attenuation efficiency based on the creation of “band-gaps” at specific frequency ranges, due to the Bragg’s interference phenomenon. The distinct physical mechanisms of these two types of noise barriers make it impossible to use the classical simplified or even numerical models developed for traditional barriers to simulate and predict the attenuation performance of a sonic crystal, and alternative methods become thus required. In the acoustics scientific literature, several authors have proposed estimation and simulation methods based on different numerical tools to predict the insertion loss provided by these new noise abatement solutions. In the present paper, a comparative assessment of some of these methods is presented, with particular emphasis to the assessment of their accuracy vs. computational cost. The main objective is to provide researchers and engineers with objective information for a good choice of prediction and simulation tools.

4.4.2.- Introduction

Noise pollution is a major environmental problem affecting urban areas close to transportation infrastructures and reducing its impact on citizens is an important challenge to be faced. Actions can be taken at both emission or transmission phases; and probably the most used devices to reduce the sound transmission of outdoor noise sources are the acoustic barriers placed between the source and the area to be protected. Since the efficiency of noise reduction by means of barriers depends directly on their height, appropriate implementations are sometimes intrinsically linked to a heavy environmental, urban, visual or aesthetic impact. In recent decades, a solution based on Sonic Crystal Acoustic Screens (SCAS) has been applied to reduce these impacts, with an acceptable acoustic performance. Sonic crystals are defined as heterogeneous materials embedded in air, formed by periodic arrangements of acoustic scatterers separated by a predetermined lattice constant [1]. These structures provide a noise control mechanism related with the fact that the multiple sound wave scattering process generates the existence of frequency ranges, called band gaps, in which the wave propagation is restricted [2], as formulated by the “Bragg’s interference” principle. There are several studies that show the application of these concepts in the development of Noise Reducing Devices (NRD) as Sonic Crystal Acoustic Screens (SCAS) [3, 4]. The most recent advances on these devices have been achieved mainly thanks to the application of numerical methods in their design and analysis processes.

The importance of correctly predicting the acoustic performance of new NRDs, even before prototyping them, has led the scientific community to develop and validate several methods that evaluate the acoustic performance of these devices. In fact, these numerical

methods have led to the improvement of technology in the field of acoustics and the development of new NRD, as in the case of sonic crystals.

To optimize the acoustic performance of sonic crystals noise barriers, an accurate and low computation cost simulation method is needed to tackle a complex optimization process that requires multiple iterations and obtaining precise acoustic performance data of the different proposed designs [5]. The current work aims to study the relationship between the accuracy of several numerical methods, and their associated computation cost. In order to compare the accuracy of the different methodologies in a simple manner, objective parameters describing the performance of the noise barrier predicted by each method need to be compared, preferably making use of single number descriptors. The standards EN 1793-2 and EN 1793-5 [6, 7] describe test methodologies for measuring the airborne sound insulation of NRDs, depending on whether or not the device will be installed in reverberant areas, and define single valued figures of merit called DL_R or DL_{SI} , which weigh the insulation measured in one-third octave bands. In this paper, we will define a parameter analogous to the above-mentioned "figures of merit", referred as Insertion Loss index ($IL_{A,tr}$), which will be used to compare the accuracy of the numerical methods under study.

The paper is developed as follows. First, the numerical methods used in this study will be briefly reviewed, as well as the variables on which their accuracy and computation cost depend. Secondly, the simulation scheme used for all methods will be described and the methodology used to calculate a global airborne insertion loss index for all simulation methods will be presented. Then, the results of the simulations for each of the methods will also be illustrated and a systematic study of the uncertainty and the associated computational cost is carried out. And, finally, the conclusions and discussions of the study will be presented.

4.4.3.- Simulation Methods Under Study

Several methods have been used to evaluate the performance of periodic structures in acoustics. One of the first proposed methods was Multiple Scattering (MS). This numerical method simulates the propagation and interaction of wave fields with obstacles. In the classical MS formulation, applied to sound waves interacting with rigid scatterers, the total acoustic field is calculated taking into account that the reflected field by one obstacle induces further reflected or scattered fields to all the other obstacles, in an iterative manner. In the particular case of cylinders, the reflected field can be evaluated analytically. As a result, MS is a semi-analytical method.

In 1913, Zaviska [8] described the MS method for studying the scattering behaviour of finite arrays in 2D acoustic fields. Moreover, Ignatowsky applied this method to research the physical phenomenon of normal incidence in an infinite row of cylinders, in 1914 [9]. Subsequently, several authors [10, 11] presented extensions of those works applied to the case of oblique incidence.

The main parameter that determines the accuracy and computational cost of this method is the number of iterations or reflections that are taken into account in calculations, commonly called the order of the approach. Periodic boundary conditions are not used in

this method, so a unit cell is defined and repeated several times. The number of repetitions also determines the computational cost.

As an alternative to semi-analytic methods, there are domain discretization methods, such as Finite Element Method (FEM) or Finite-Difference Time-Domain (FDTD) Method. The FEM analysed in the present paper is a mesh based method with second-order Lagrangian elements that resolves problems by turning a differential problem into an algebraic one by discretizing a continuous medium into several finite elements connected to each other at nodal points. All elements are delimited by sides of other elements or by the contour of the domain. The shape functions define the elemental stiffness matrix of each element which, when assembled, generate the global stiffness matrix. The system of equations is solved by establishing the appropriate boundary conditions, obtaining solutions for each mesh node.

There are many papers concerning the use of the FEM to evaluate the performance of periodic structures. As an example, in [12] the FEM has been used to analyse periodic structures and the generation of band-gaps. M. Liu et al used a wavelet-based FEM to investigate the band structure of 1D phononic crystals [13], and, more recently, Sánchez-Perez et al [14] used a 2D FEM model for the design of a SCAS.

In this case, the accuracy and computational cost of calculation is majorly associated with the mesh size. This dimension depends on geometrical parameters, such as the maximum and minimum size of the elements, which in turn depends on the excitation frequency. It is known that for the FEM discretization, usually, 8 to 10 nodes per wavelength should be used to allow adequate accuracy.

Another domain-based method is the so-called Finite-Difference Time-Domain (FDTD). This method, originating from electromagnetism [15], was adapted to acoustics about two decades ago [16]. In the case of sound waves in fluids, conservation of momentum and continuity equations are converted to two linked update equations for sound pressure and particle velocity, allowing the impulsive response of a system, and therefore its transfer function, to be obtained. The main advantage is that, being a technique that works in the time domain, a single simulation can cover a large frequency range, while its main disadvantage, as in other volumetric methods, is that the computational cost increases enormously when the integration domain is large compared to the wavelength.

We can cite, as precursor works on the use of FDTD for the study of sonic crystals, the works of Cao et al [17] and Miyashita [18]. In the first one, it was demonstrated that this technique allows the band-structure calculations in a very effective way, while the second one is focused in the study of wave guides based on sonic crystals

In the case of FDTD, the accuracy and computational cost will depend almost exclusively on the size of the elements. For the sake of simplicity other aspects, such as the type of perfectly matched layer (PML), the use of non-cartesian grids or conformal techniques will not be considered here. The Courant number has been set to 1, in order to ensure the stability of the numerical technique.

Differently from the FEM and FDTD, the Boundary Element Method (BEM) is based on the discretization of the boundaries of the analysis domain. Mathematically, the BEM is based on the application of the boundary integral equation at a set of nodes defined along a discretized boundary, allowing for the construction of a system of equations whose solution is the acoustic pressure or the normal particle velocity at these boundary nodes. Differently from previous methods, the BEM requires the a priori knowledge of the Green's function for the problem under study.

Some works can also be found regarding the application of the Boundary Element Method (BEM), such as the work of Li et al. [19], in which the BEM is used to perform band-gap calculations of solid sonic crystals, and the work by Koussa et al. [20], in which the BEM is used to study the efficiency of an acoustic barrier complemented by a sonic crystal. Gao et al. [21] also analyzed the band structure using the BEM together with the block SS method. According to the authors, this approach was shown to be effective, allowing the numerical eigenfrequency analyses of periodic phononic structures. An interesting approach was proposed by Karimi et al. [22], who developed a specific BEM algorithm tailored for the analysis of periodic systems, which exploits the periodicity of the geometry to reduce the computational cost.

In recent decades, a new class of numerical methods has emerged, namely meshless methods, which have been in progressive development, aiming mostly at a reduction of computational costs and of the effort involved in the discretization of the problem geometry. Within this class, the Method of Fundamental Solutions (MFS) has deserved attention for acoustic problems, since, as happens with the BEM, it makes use of Green's functions that can directly account for infinite or semi-infinite spaces. However, its mathematical formulation and implementation are much simpler, since it is based on a collocation approach without requiring any numerical or analytical integration. In fact, the method is simply based on a linear superposition of fundamental solutions to approximate the solution of the problem, assuming sources located outside of the computational domain to avoid singularities in the solution. There is extensive literature regarding the MFS and its application to acoustic scattering and/or radiation problems, such as the early works of Fairweather et al. [23].

There are only a few examples in the literature regarding the application of the MFS to the study of Sonic Crystals. The first application of the MFS in this field is due to Martins et al. [24], who proposed the use of the MFS to evaluate the insertion loss provided by a periodic structure made of rigid scatterers. Santos et al. [25], extended the formulation to allow considering elastic shell scatterers. However, in both works, the classic formulation of the MFS was used, involving the discretization of all scatterers, and disregarding the periodicity of the structure. More recently, Godinho et al [26] successfully used an improved version of the MFS, developed for finite periodic structures. In Godinho et al [27], further developed the method, in order to allow accounting for infinite periodic structures along one direction, in a very efficient manner.

4.4.4.- Simulation Scheme and calculations

As aforementioned, the main aim of this work is to evaluate the performance and accuracy of different methods for the simulation of sonic crystal structures. Usually, it can

be said that the best methods are those that offer high precision at the lowest possible computational cost. Since these two objectives are usually opposed, a systematic evaluation, consisting of obtaining a quantitative accuracy indicator for a series of computational cost values, is here proposed for all methods. This computational cost depends on a single control parameter for each method.

In order to perform this comparison, the same scheme, consisting of sonic crystals structures with the same lattice constant and different radius of the scatterers, was simulated making use of all considered methods. The geometry of the studied configuration (Fig 27) consists of a square array of cylindrical scatterers placed in four rows, separated by the lattice constant, $a=0.17\text{m}$, so that the first band gap, usually called Bragg's gap, appears around the frequency of 1000Hz , the most relevant frequency of the normalized traffic noise spectrum, standardized by EN 1793-3 [28]. To simulate a semi-infinite screen, a unit computational 2D cell, representing the whole 3D space, is defined. Periodic boundary conditions are imposed on both lateral contours of the computational domain for all methods except MS. An incident plane wave impinges perpendicularly the screen. The measurement points are located in a square array along the measurement area, in twelve lines parallel to the plane wave-front, separated $a/4$ from each other, the first of these lines being placed $3a/2$ apart from the centre of the nearest scatterer. In order to avoid duplication of data, since the unit cell is symmetrical with respect to an axis perpendicular to the plane wave-front passing through the centre of the scatterers, the measurement points are placed between this symmetry axis and one lateral boundary.

Several scatterer diameters were tested. For the sake of brevity, we present here only three representative cases. The results will be shown for each of these three diameter values, expressed as a fraction of the lattice constant, $0.25a$, $0.5a$, $0.75a$.

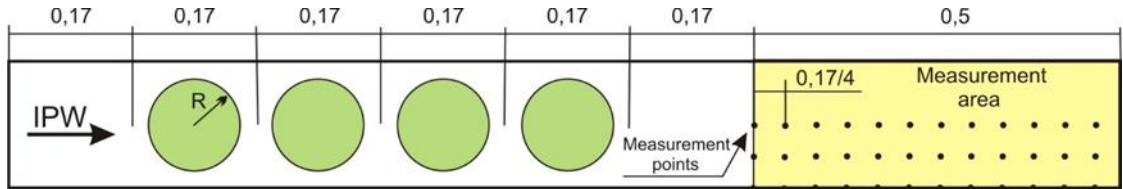


Figure. 27. Schematic representation of the system configuration used in the simulations.

With the purpose of obtaining a single figure of merit to quantify the acoustic performance of the different considered devices, a single-number rating insertion loss index ($IL_{A,tr}$) was calculated, based on the standard EN 1793-6 [29].

$$IL_{A,tr} = -10 \log \frac{\sum_{j=1}^{18} 10^{0,1L_j} 10^{-0,1IL_j}}{\sum_{j=1}^{18} 10^{0,1L_j}} \quad (7)$$

In other words, $IL_{A,tr}$ was obtained from a global transmission coefficient (τ) namely:

$$IL_{A,tr} = -10 \log \tau \quad (8)$$

being τ obtained as a weighted average of the j -th third octave values of the transmission coefficient, τ_j .

$$\tau = \sum_{j=1}^{18} C_j \tau_j \quad (9)$$

where the coefficients C_j express the normalized traffic noise spectrum with A-weighting, obtained from its normalised one-third octave band levels, L_j , by the expression:

$$C_j = \frac{10^{0,1L_j}}{\sum_{j=1}^{18} 10^{0,1L_j}} \quad (10)$$

and transmission coefficients of the j -th third octave band (τ_j) are related with the Insertion Loss index (IL_j) by

$$IL_j = -10 \log \tau_j \quad (11)$$

In time domain method (FDTD), to calculate τ_j at each measurement point, the Fourier transform of the impulse response is obtained and averaged in one third octave bands. In frequency methods, a number of frequencies for each one third octave band, separated a constant octave fraction between them, are evaluated and τ_j is obtained by averaging the results of all the frequencies inside a band. Finally, τ_j is averaged for all the measurement points.

In order to simplify the study, the number of control parameters to be considered has been reduced. To exclude some of those parameters from the study, the convergence of the results when these parameters vary was analysed. Thus, when the uncertainty is not significant (lower than 10^{-3} dB(A)) the value of this parameter is fixed. The limit value of 10^{-3} dB(A) has been defined, since these uncertainties are acceptable in the field of acoustics and high-accuracy measurement equipment provides even lower precision (10^{-2} dB(A)) [30]. This checking process is cyclic and iterative, due to the cross-dependencies between parameters.

In particular, the number of frequencies for each one-third octave band was set at 6. Similarly, the FDTD simulation time was set to 4 times the time it takes for sound to travel through the computational domain. It is noteworthy that, although these two control parameters affect the computational time, they do not significantly affect the computational cost as estimated in the present work. In the case of MS, the order was set at 5 on the recommendation of several authors [31, 32] and after verifying that the uncertainty is lower than the limit value 10^{-3} dB(A).

After the aforementioned setting of variables, the control parameters considered in the study were reduced to a unique factor per method: (i) reflection order for MS (ii) element size for FEM, FDTD and BEM and (iii) number of virtual sources in MFS.

A systematic study of the relationship between accuracy and computational cost was carried out by varying these selected control parameters. The computational cost is a common way of evaluating the efficiency of simulations [33, 34], but computational cost may depend on implementation. In this work, implementations with the minimum computational cost were applied, avoiding, for example, parallel processing of several frequencies in frequency domain methods.

4.4.5.- Results and Discussion

As a starting point, the relationship between the accuracy and the considered control parameters was studied. Figure 28 shows how the uncertainty evolves as the number of elements per wavelength increases in BEM. For the sake of brevity only the details of BEM are given. In order to calculate those uncertainties, although the literature recommends a value between 6 and 10 for this parameter [35], in this preliminary study the parameter has been varied up to 30 in order to provide an oversized simulation and obtain a value that can be used as the “true value”. Bear in mind that the uncertainty is defined as the difference between each calculated value and the “true value”.

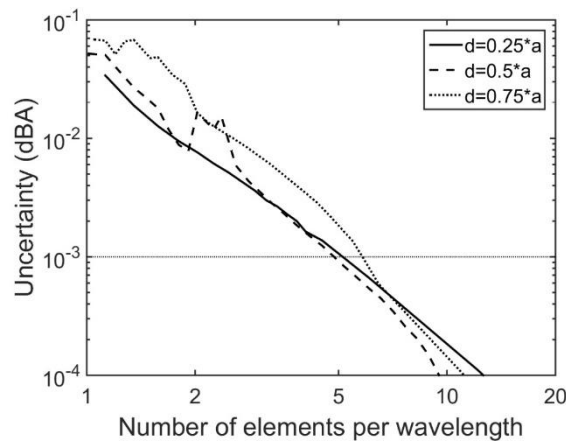


Figure. 28. Evolution of the uncertainty on $IL_{A,tr}$ (in dB(A)) with increasing number of elements for the BEM.

This study provided the values of the control parameters for which an increase in computational cost would not lead to uncertainties lower than 10^{-3} dB(A) as a baseline. These limit values of the control parameters were not exceeded in successive stages of this work since they do not affect subsequent studies.

Once found the limit values of the control parameters, the results provided by all the methods can be compared. Figure 29 shows the Insertion Loss index (IL_j) vs frequency. It can be seen that some of the lines are so close that it is very difficult to distinguish them. Small differences are observed for high values of the diameter of the scatterers in the first band gap (1kHz) for the MS method. In this case, the sound insulation is slightly underestimated. On the other hand, more evident differences appear in the second band gap (around 2kHz), particularly for the larger scatterers ($d = 0.75 a$). The underestimation of this second band gap by MS is especially noticeable.

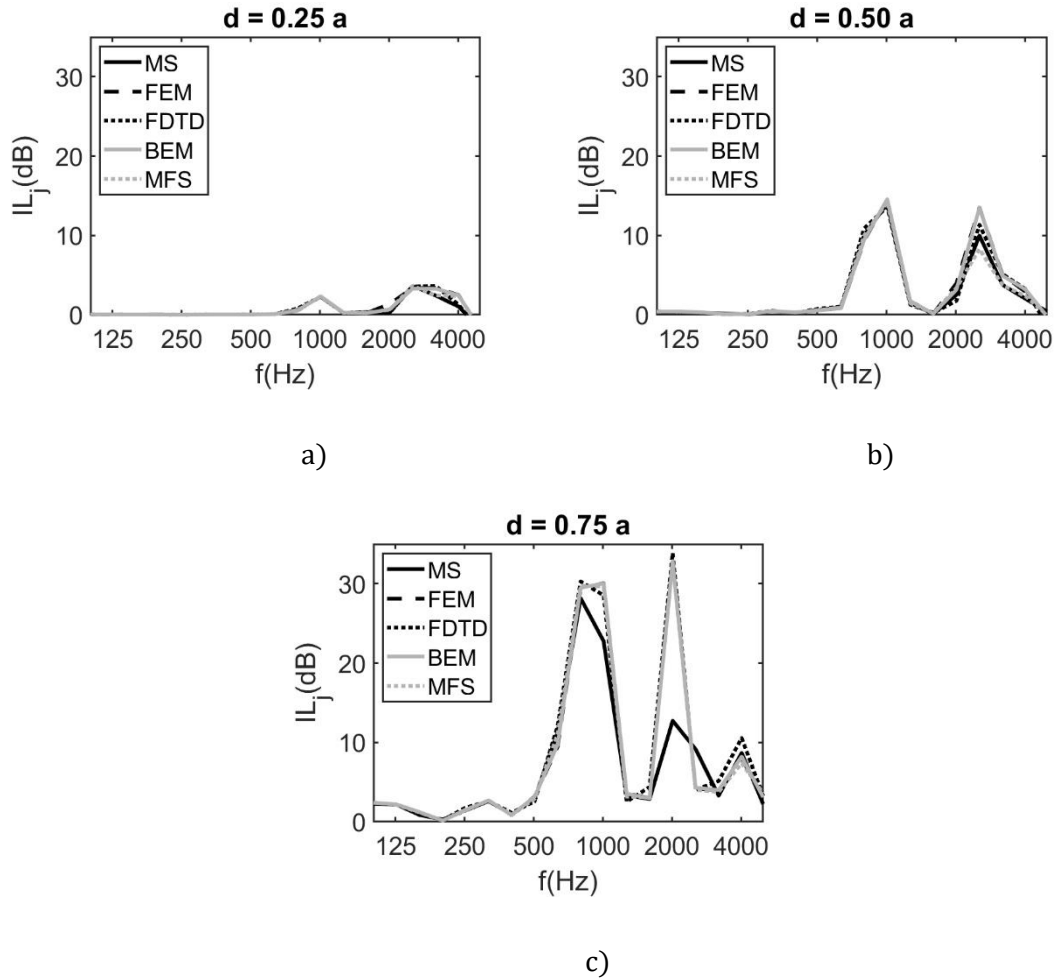


Figure. 29. IL vs frequency, in one-third octave bands, for all the considered methods: a) $d = 0.25 a$; b) $d = 0.5 a$; c) $d = 0.75 a$.

Table 1 shows the values of the single-number rating insertion loss index ($IL_{A,tr}$). The results obtained by the different methods hardly differ by one hundredth of a decibel. The $IL_{A,tr}$ uncertainty was evaluated by error propagation from the uncertainties of τ_j estimated as the difference between τ_j for each method and the average value of τ_j for the five tested methods.

$IL_{A,tr}$ (dB(A))	$d = 0.25a$	$d = 0.50a$	$d = 0.75a$
MS	$0,63 \pm 0,03$	$2,45 \pm 0,04$	$5,07 \pm 0,17$
FEM	$0,73 \pm 0,06$	$2,60 \pm 0,08$	$5,06 \pm 0,09$
FDTD	$0,66 \pm 0,04$	$2,42 \pm 0,11$	$5,15 \pm 0,22$
BEM	$0,679 \pm 0,018$	$2,56 \pm 0,04$	$5,07 \pm 0,08$
MFS	$0,678 \pm 0,016$	$2,49 \pm 0,05$	$5,01 \pm 0,05$

Table 1. $IL_{A,tr}$ values calculated with the limit values of the control parameters for each numerical method and for each of the diameters referred to.

In order to evaluate the quality of each method, the uncertainty behaviour was studied as a function of the computational cost involved. The performance for a particular diameter, method and computational cost, was quantified as a function of its uncertainty (dB(A)), obtained as the difference between its calculated $IL_{A,tr}$, and the average global $IL_{A,tr}$ found with the limit values of the control parameters accepted as “true value”. These uncertainties, depending on the computational cost entailed, are represented in figure 30 for each diameter. As expected, the higher the computational cost, the lower the uncertainty. This trend is broken in the case of data with higher computational cost, since the “true value” has been obtained as the average of all the methods, so that no uncertainty smaller than the uncertainty between methods can be found. For the highest computational cost, the uncertainty values achieved are around one hundredth of a decibel.

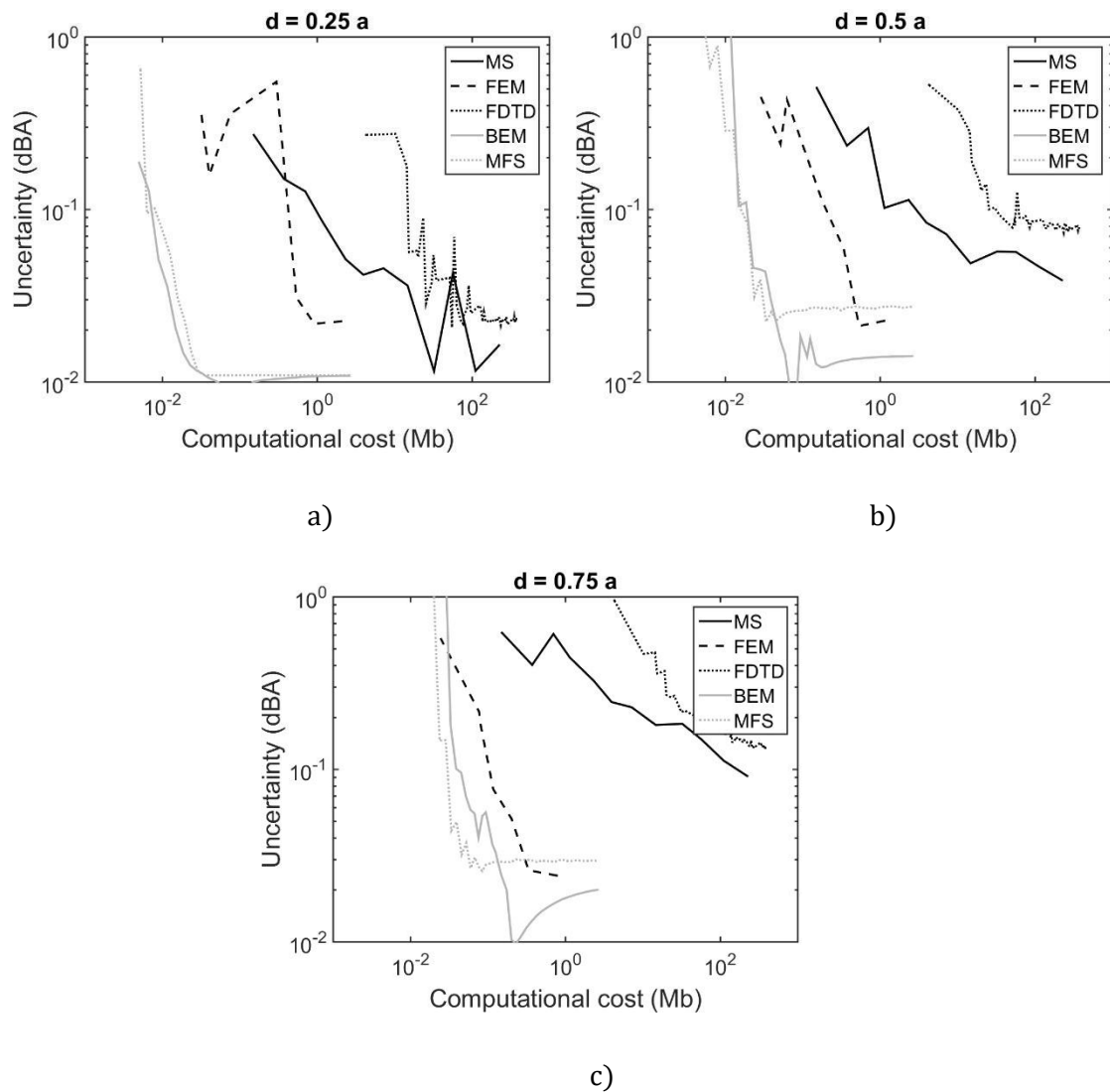


Figure. 30. Uncertainty of $IL_{A,tr}$ versus computational cost for all the studied methods: a) $d = 0.25 a$; b) $d = 0.5 a$; c) $d = 0.75 a$.

As an objective evaluation criterion, the best results are those that offer the least uncertainty involving lowest computational cost. In other words, representing the uncertainty as a function of the computational cost, the best methods are those whose curves are closest to both axes. In some cases, the curve represented by one method may

cross with the curve of another method, so there is no absolute preference between them, and the best option would depend on the aims of a particular project.

In a first analysis of the three graphs in Figure 30, there are clear performance differences between the studied methods, according to the evaluation criteria described above. BEM and MFS seem to show a much faster convergence than the rest, and FEM presents more favourable results than FDTD and MS. Furthermore, for larger scatterer diameters, FEM shows no significant differences with MFS or BEM. Indeed, for that case, the total number of elements of the BEM (or collocation points in MFS) required to discretize each scatterer is larger, and thus leads to a larger computational cost. By contrast, for these larger diameter scatterers, domain discretization methods such as FEM or FDTD benefit from a small reduction in mesh size (due to the larger void in the mesh corresponding to the scatterers), and thus have improved performance.

A deeper analysis shows that BEM and MFS methods offer very similar behaviour, as can be seen in the three graphs and in $IL_{A,tr}$ value table of the limit control parameters. Furthermore, in the case of $d=0.25$ there is almost an overlap of curves for all uncertainties, whereas in $d=0.5$ and $d=0.75$ this overlap is only for large uncertainties and is lost when the uncertainty is less than hundreds of a decibel. Although this difference could indicate an irregular behaviour of one of these two methods, they are indeed due to the fact that the "true value" has been obtained as an average of the values obtained from several methods. So, the method whose value with limit control parameters is closer to that average ("true value") will present a curve that converges better. In fact, for all methods, from uncertainties of less than 0.03 dB(A), curves can no longer be interpreted literally, since their appearance depends on the difference between the $IL_{A,tr}$ value of limit control parameters of each method and the "true value", so their accuracy is affected by the inaccuracy of the other methods.

It is also interesting to note that FEM performs better, compared to other methods, when the scatterers diameter is larger, as the graph for $d = 0.75$ in Figure 30c shows. This may be due to the way the mesh is defined. As it is the usual practice, a triangular flat mesh has been used, which adapts to the geometry and has a growth function in order to achieve the desired average size, being larger size in the areas far from the scatterers and smaller in areas close to them (see figure 31). Thus, the size gradient will be more abrupt in $d = 0.25$ than in $d = 0.75$ leading to worse behaviour for smaller radius, either because the mesh variability is an additional difficulty for the calculation or simply because of the excess computational cost needed to create the finer meshes surrounding the smaller obstacles. For this reason, the FEM curve of $d=0.25$, not only presents the worst performance with respect to its counterparts of other diameters, but it is also the one that presents a more irregular behaviour, with some increases in uncertainty when rising computational costs, in low computational costs ranges. This is basically due to the definition of small objects, small diameters of scatterers, with large size of mesh element. However, as the computational cost increases, i.e., the size of the mesh elements decreases, the representation of the elements becomes more reliable and the results present fewer uncertainties.

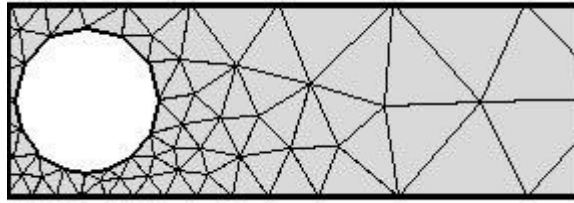


Figure. 31 FEM triangular flat mesh with a high growth factor adapted to the scatterers geometry

Thus, FEM, as a domain discretization method, varies the quality of its calculation according to the way in which the mesh elements are defined to adapt them to the domain to be simulated. However, this is not reflected in other methods. In the case of FDTD the curve that defines its uncertainty behaviour with respect to the computational cost, is shifted in the axis of the abscissa about 2-3 orders of magnitude with respect to the methods that give better results (BEM and MFS). This could be due to the fact that the mesh is Cartesian. Therefore, a large mesh element implies a poor definition of the shape of the scatterers, and a poor treatment of the wave dynamics, especially of its high frequencies. But since the method does not make an extra adaptation of the mesh to the geometry of the scatterers, its curve is not affected by the size of the scatterers.

Regarding the difference of several orders of magnitude between the computational cost of the FDTD and that of the MFS, BEM or FEM, it does not imply such a large decrease in the quality of the method, as might be apparent when observing the presented plots. It may be noted that frequency methods use a memory space multiple times, as many times as frequencies to be considered. In FDTD, on the other hand, a unique time domain simulation is made and then, by means of a Fourier transform, the transfer function is obtained. In our case, since we have taken 6 frequencies per third octave band, the number of repetitions of memory use of the frequency methods is 108.

Finally, MS is undoubtedly the worst of the frequency methods analysed as might be expected in view of the underestimation of the sound insulation observed in the band gaps (see Figure 29).

4.4.6.- Conclusions

The aim of the present work is to find a simulation tool that provides maximum precision at the lowest computational cost for the evaluation of the acoustic performance of periodic structures. It is essential to have a simulation tool with such characteristics when carrying out an optimisation process, as this process involves a large number of simulations.

For the particular case raised in the study, both BEM and MFS are the best methods for performing optimization processes and determining the acoustic performance of these periodic structures. Comparing the results offered by FDTD and FEM, both volumetric methods but with different calculation philosophy, since one is based on time domains and the other on frequency domains, we appreciate that FEM effectively gives more accurate results requiring less computation cost, but as explained above, this may be due to the way in which this computation cost is determined, and because we do not take into account to determine the quality of the calculation other factors such as computational time.

The option of using calculation time to evaluate the performance of methods was discarded because the calculation time depends strongly on the particular implementation of the method and the particular computer on which it is run. For further research, it is proposed to evaluate not only the computational cost used, but also the computational time. Shorter calculation times would shorten the iteration time in optimization processes, leading to greater efficiency of these processes and allowing them to be used as competitive design tools. It could also be interesting to include in the simulation processes absorbent materials and resonant cavities in the acoustic scatterers, which will improve the acoustic performance of the device, and to study the behaviour of the simulation tools in terms of their precision and computation cost entailed to achieve it.

The results obtained and discussed in this work cannot be extrapolated to other cases directly. It should be noted that each of the methods considered has its own peculiarities. In other words, each method has its advantages and disadvantages. This may make one method or another more suitable in other situations that have not been considered. As an example, if the propagation of the waves through elastic scatterers had been considered, significantly different results could have been obtained, and some of the methods would not be usable (such as the MS).

4.4.7.- References

- [1] Martínez-Sala R., Sancho J., Sánchez-Pérez J.V., Gómez V., Llinares J., Meseguer F. (1995), Sound attenuation by sculpture, *Nature*, London, 387, 241.
- [2] Chen Y.Y., Ye Z. (2001), Theoretical analysis of acoustic stop bands in two-dimensional periodic scattering arrays, *Physical Review E*, 64(3), 036616.
- [3] Kushwaha M.S. (1997), Stop-bands for periodic metallic rods Sculptures that can filter the noise, *Applied Physics Letters*, 70(24), 3(20)218-3220.
- [4] Sánchez-Pérez J.V., Rubio C., Martínez-Sala R., Sánchez-Grandia R., Gómez V. (2002), Acoustic barriers based on periodic arrays of scatterers, *Applied Physics Letters*, 81, 5240.
- [5] Peiró-Torres M. P., Navarro M. P., Ferri M., Bravo J. M., Sánchez-Pérez J. V., Redondo J. (2019), Sonic Crystals Acoustic Screens and Diffusers, *Applied Acoustics*, 148, 399-408.
<https://doi.org/10.1016/j.apacoust.2019.01.004>
- [6] EN 1793-2:2013 Road traffic noise reducing devices - Test method for determining the acoustic performance - Part 2: Intrinsic characteristics of airborne sound insulation under diffuse sound field conditions.
- [7] EN 1793-5:2013 Road traffic noise reducing devices -Test method for determining the acoustic performance-Part5: Intrinsic characteristics – In situ values of airborne sound insulation under direct sound field conditions.
- [8] Zavisla F. (1913), Über die beugung elektromagnetischer wellen an parallelen, unendlich langen kreisylindern, *Annalen der Physik*, 345(5), 1023-1056.
- [9] Von Ignatowsky W. (1914), Zur theorie der gitter, *Annalen der Physik*.. 349(11), 369-436.

-
- [10] Twersky V. (1962), On scattering of waves by the infinite grating of circular cylinders, *IRE Trans. on Antennas and Propagation*, 10:737.
- [11] Guenneau S., Movchan A.B. (2004), Analysis of elastic band structures for oblique incidence, *Archive for rational mechanics and analysis*, 171(1), 129-150
- [12] Wang Y. F., Wahng Y.S., Su X.X. (2011), Large bandaps of two-dimensional phononic crystals with cross-like holes, *Journal of Applied Physics*, 110 (11) 113520.
- [13] Liu M., Xiang J., Gao H., Jiang Y., Zhou Y., Li F. (2014), Research on band structure of one-dimensional phononic crystals based on wavelet finite element method, *Computer Modeling in Engineering & Sciences*, 97(5) 425-436.
- [14] Sánchez-Pérez J.V., Rubio-Michavila C., Castiñeira-Ibáñez S. (2015), Towards the development of a software to design acoustic barriers based on sonic crystals: An overlapping model, *Proceedings of Euronoise*, (Vol. 2015) 2367-2371.
- [15] Yee K.S. (1966), Numerical solution of initial boundary value problems involving Maxwell's equations in isotropic media, *IEEE Transactions on Antennas Propagation*, Vol 14, 302-307.
- [16] Maloney J.G., Cummings K.E. (1995), Adaption of FDTD techniques to acoustic modelling, *11th Annu. Rev. Prog. Applied Computational Electromagnetics*, Vol.2, 724.
- [17] Cao Y., Hou Z. Liu Y. (2004), Convergence problem of plane-wave expansion method for phononic crystals, *Physics Letters A*. 327(2) 247-253.
- [18] Miyashita T. (2005), Sonic crystals and sonic wave-guides, *Measurement Science and Technology*, 16(5), R47
- [19] Li F. L., Wang Y. S., Zhang C., Yu G. L. (2013), Band-gap calculations of two-dimensional solid-fluid phononic crystals with the boundary element method, *Wave Motion*, 50(3), 525-541.
- [20] Koussa F., Defrance J., Jean P., Blanc-Benon P. (2013), Acoustical efficiency of a sonic crystal assisted noise barrier, *Acta acustica united with Acustica*, 99(3), 399-409.
- [21] Gao H. F., Matsumoto T., Takahashi T., Isakari H. (2013), Analysis of band structure for 2D acoustic phononic structure by BEM and the block SS method, *CMES-Computer Modeling in Engineering & Sciences*, 90(4), 283-301.
- [22] Karimi M., Croaker P., Kessissoglou N. (2016), Boundary element solution for periodic acoustic problems, *Journal of Sound and Vibration*, 360, 129-139.
- [23] Fairweather G., Karageorghis A., Martin P.A. (2003), The method of fundamental solutions for scattering and radiation problems, *Engineering Analysis with Boundary Elements*, 27, 759 -69.
- [24] Martins M., Godinho L., Picado-Santos L. (2013), Numerical evaluation of sound attenuation provided by periodic structures, *Archives of Acoustics*, 38(4), p. 503-516.

-
- [25] Santos P. G., Carbajo J., Godinho L., Ramis J. (2014), Sound propagation analysis on sonic crystal elastic structures using the Method of Fundamental Solutions (MFS), *CMC: Computers, Materials & Continua*, 43(2), p. 109-136.
- [26] Godinho L., Amado-Mendes P., Pereira A., Soares Jr. D. (2018), An Efficient MFS Formulation for the Analysis of Acoustic Scattering by Periodic Structures, *Journal of Theoretical and Computational Acoustics*, 26(1), pp. 1850003-1 to -22. doi: 10.1142/S2591728518500032.
- [27] Godinho L., Redondo J., Amado-Mendes P. (2018), The Method of Fundamental Solutions for the Analysis of Infinite 3D Sonic Crystals, *Engineering Analysis with Boundary Elements*, 98, 172-183. doi: <https://doi.org/10.1016/j.enganabound.2018.09.015>
- [28] EN 1793-3:1998. Road traffic noise reducing devices. Test method for determining the acoustic performance. Normalized traffic noise spectrum.
- [29] EN 1793-6:2018. Road traffic noise reducing devices. Test method for determining the acoustic performance. Intrinsic characteristics in situ values of airborne sound insulation under direct sound field conditions.
- [30] Beyers C. (2014), Calibration methodologies and the accuracy of acoustic data. In INTER-NOISE and NOISE-CON Congress and Conference Proceedings. Institute of Noise Control Engineering, (Vol. 249, No. 5, pp. 3104-3111).
- [31] Fuster-Garcia E., Romero-García V., Sánchez-Pérez J. V., Garcia-Raffi L. M. (2007), Targeted band gap creation using mixed sonic crystal arrays including resonators and rigid scatterers, *Applied physics letters*, 90(24), 244104.
- [32] Romero-García V., Fuster E., García-Raffi L. M., Sánchez-Pérez E. A., Sopena M., Llinares J., Sánchez-Pérez J. V. (2006), Band gap creation using quasiordered structures based on sonic crystals, *Applied physics letters*, 88(17), 174104.
- [33] António J., Tadeu A., Godinho L. (2008), A three-dimensional acoustics model using the method of fundamental solutions, *Engineering Analysis with Boundary Elements* 32(6), 525-531.
- [34] Wu T.W. (2000), editor. *Boundary element acoustics: fundamentals and computer codes*, Southampton: WIT Press
- [35] Marburg S. (2008), Discretization requirements: How many elements per wavelength are necessary?, *Computational Acoustics of Noise Propagation in Fluids-Finite and Boundary Element Methods*. Springer, Berlin, Heidelberg, p. 309-332.

4.5.- Correlation between objective and subjective assessment of noise barriers.

4.5.1.- Abstract

There are several international standards that define the way to evaluate the attenuation capacity of noise reducing devices, by single-number quantities representing airborne sound insulation and insertion loss. These two single-value ratings define the quality and performance of acoustic barriers, the former being related to intrinsic and the latter to both intrinsic and extrinsic acoustic characteristics of the devices. However, not many studies can be found on whether these objective parameters correlate to the perception of annoyance reduction.

The aim of the present work is to analyze the adequacy of these objective ratings to indicate the performance of noise barriers, by comparing their values with the perception of annoyance reduction.

For this purpose, ninety individuals of two different nationalities (Spanish and Portuguese) were asked to rate the perceived annoyance reduction in a listening experimental test, in which they were exposed, under controlled conditions, to several environmental noises and acoustic screened stimuli simulated by audio filters.

The obtained results show a high correlation between objective ratings and subjective annoyance perception, with a better correlation being observed for insertion loss single-number parameter than for the airborne sound insulation single-number rating. Furthermore, significant differences were found depending on the gender and nationality of the respondents. The results, from this ongoing research work, may be of great interest for future acoustic barriers design.

4.5.2.- Introduction

During the last decades, the increasing number of vehicles in urban zones has led to excessive environmental noise pollution, which is mostly caused by road, railway and aircraft traffics. Among these, the most significant source of noise is road traffic [1], exposure to which far exceeds rail and aircraft sources combined [2]. In fact, in urban areas, road traffic is thought to account for 80% of all noise pollution [3]. It is therefore very important to achieve lower sound levels from road traffic in the process of planning urban environments [4].

Several studies have demonstrated that environmental noise is an important public health issue. The recent report “Environmental Noise Guidelines for the European Region”, from the World Health Organization (WHO) [5], provides the current state of knowledge about the non-auditory effects due to environmental noise on the population health. Noise affects cardiovascular diseases such as ischemic heart disease, hypertension or strokes, cognitive development, sleep disturbance and variables that have an adverse effect on birth and even other variables related to the decrease in quality of life and metabolic diseases. In Europe, environmental noise is assumed as an important public health issue, being among the top environmental risks to health. Its negative impacts on human health and well-being

are a growing concern among both the general public and policy-makers in Europe [6]. Being aware of this problem the WHO has, in 2018, updated the guidelines for the European Region, in order to protect human health from exposure to environmental noise [5].

In general, noise propagation can be controlled in three different ways: (i) reducing noise generation near the source; (ii) controlling noise propagation from source to receiver, and (iii) taking measures near noise reception. In the former case, acting near the noise source corresponds, for example, to reducing engines sound power, to reducing vehicles speed or to adopting noise absorbing pavements or more silent tyres. On the other hand, regarding noise reception, sound insulation of buildings and buildings facades has to be considered, although being a complex and expensive task [7].

The most commonly employed solution to reduce road traffic noise is the use of noise barriers, which mitigate noise by placing an obstacle between noise emission and reception. Some of the emitted sound energy is reflected or dispersed towards the source, some of the energy is absorbed and dissipated by the barrier material, and some energy arrives at the receiver, being diffracted from the edges of the barrier or being transmitted through this type of noise reducing device [7].

Usually, a noise barrier is a solid continuous, opaque and appropriately dense construction. The effectiveness of these devices in reducing noise is related to several factors, such as the relative position between the noise emitter and receiver, the barrier's height, length, thickness or its geometric design, the presence of top diffusive devices, or ground cover in the vicinity of the barrier [8, 9].

There are different types of barriers, namely: simple reflecting barriers, absorbing/diffusive barriers which have absorbing materials on the side facing the noise source; angled barriers which reflect sound away from the receiver with a specially designed geometry and diffusive top section; and covering barriers, such as galleries or tunnels, that offer significant noise reduction. Noise barriers can be made of a variety of materials, such as glass or plastic/acrylic thin elements, masonry blocks, pre-cast concrete elements, perforated steel or aluminum, and they may also incorporate recycled materials [10-11].

The use of classical sound barriers in urban areas can have considerable disadvantages. One of these is clearly related to the reflection of sound energy that occurs on the surface of the traditional barrier and can significantly affect receivers on the same side of the sound source. This is mitigated in the case of Sonic Crystal Acoustic Screens (SCAS) by producing a reflection with a higher diffusion index than the traditional barrier [12]. Undoubtedly, the sound absorption of the acoustic barrier is a very important factor in the design and rethinking of the barriers. However, this work will not take this into account as its main objective is the evaluation of the perceived annoyance of the noise energy passing through the barrier (either through it or by edge diffraction).

Other factors associated to this new barrier technology (SCAS) are related to the reduction of the necessary foundations due to the decrease in the effect of wind load since the barrier surfaces are much more permeable. Permeability also affects the concentration of pollutants and temperature near the ground, as traditional barriers prevent the passage

of air, they generate an increase in temperature in the environment and they constitute a physical limit that affects the natural dispersion of pollutants. However, SCAS, being permeable, do not produce such effects.

In addition, the length and height of the large opaque panels have a strong effect in relation to blocking the field of vision of citizens and reducing natural light, so they have a significant impact on the urban landscape and provide physical isolation of acoustically protected areas [13]. In general, it could be said that traditional acoustic barriers have not evolved much in recent years from a technological point of view; in fact, they are still non-tunable acoustic systems that act in the same way regardless of the spectral characteristics of the noise, and are often inefficient at low frequencies [14, 15].

In the last two decades, new devices to provide noise reduction on urban environments have been developed based on disruptive concepts. Among these are the SCAS which consist of structures built by periodic arrays of cylindrical acoustic scatterers, separated by a predetermined lattice constant [16]. In this type of structures, sound attenuation is provided for certain frequency bands, by activating a noise control mechanism based on the Bragg interferences due to a multiple scattering process [17]. The range and position of these frequency forbidden bands, also called Band Gaps (BG), can be designed by changing the geometrical properties of the arrays of scatterers [18, 19]. Nowadays, the use of SCAS is at an intermediate state between the basic research of concepts and physical properties, and their industrial production and widespread use as noise reducing devices.

The idea of using arrays of scatterers for sound attenuation was born from the artistic sculpture by Eusebio Sempere, with a periodic arrangement of steel tubes installed in the gardens of the Juan March Foundation in Madrid (Spain). Despite the improvement of aesthetic characteristics of these devices, they also enable some visual continuity to the urban landscape, since a complete interference of the optical line between emitter and receiver is not produced through the discrete scatterers forming the SCAS. Another advantage of this type of sound barrier is its permeability to wind, substantially reducing the effects of turbulence and the forces exerted on the ground, and allowing for lighter foundations during on site implementation.

In order to increase the sound attenuation provided by the SCAS, it is also possible to add other noise control mechanisms, such as absorption or resonance [20], in addition to the BG effect, allowing acoustic tuning [21] in the design of the noise barrier for each noise spectra [22]. The use of SCAS has also been explored because of its high environmental sustainability, when logs from forest thinning operations have been proposed for traffic noise abatement [23]. As a matter of fact, there is ongoing research work envisaging the increase of the range of frequency bands that can be attenuated by SACS in traffic noise mitigation, as has been described in the revision work by Fredianelli et al. [24] or as it can be seen in the recent paper by Gulia and Gupta [25], where variations of systems based on sonic crystals have been studied with the aim of extending their performance bandwidth and improving their noise attenuation efficiency.



(a)



(b)

Figure. 32. a) photograph of a traditional continuous noise barrier; b) photograph of a noise barrier based on sonyc crystals concept

The effectiveness of a sound barrier, in terms of the sound attenuation provided, can be expressed by the following parameters: two intrinsic parameters, DL_R and DL_{SI} , which characterize the attenuation of sound propagation, and an extrinsic parameter, D_{IL} , which takes into account the physical characteristics of the sound barrier, its height, thickness and the position of the barrier in relation to sound emission and reception. These parameters are given by:

- DL_R , which refers to a single-number rating of airborne sound insulation for devices designed to reduce road traffic noise under diffuse sound field conditions in the laboratory [26];
- DL_{SI} , which refers to a single-number rating of in situ airborne sound insulation of the noise reducing device for free field sound conditions [27];
- D_{IL} , which corresponds to an insertion loss value, that is evaluated by the difference, in decibels, in sound pressure levels registered at a specific receiver position before and after the installation of an outdoor noise barrier [28].

Some published works can be found that describe methodologies for in-situ measurement of sound reflection and airborne noise insulation characteristics of acoustic barriers [29, 30, 31]. Some works studied how tonal sounds are perceived by the human ear or tried to understand human auditory comfort through psychoacoustic studies [32, 33]. However, few papers have analyzed whether the objective value of sound attenuation of such devices corresponds to the subjective perception of the population. Some of these studies have been carried out indoors, by comparing traffic noise façade insulation linked to reported noise annoyance [34], by consulting a sample of the population in order to relate the users' opinion to airborne sound insulation of constructions [35] or to impact sound insulation over a concrete floor with different coverings [36]. Also some study have studied the intersensory perceptions of noise barrier performance in terms of the noise reduction combined with visual impressions [37] but in no case it has been studied whether there are significant differences that affect of the users features like gender or nationality.

The objective of the present study is to analyze the suitability of quantifying the performance of noise barriers by comparing the above mentioned objective ratings to indicators with the subjective response of the people surveyed in listening tests.

For this purpose, the acoustic characteristics of the devices performances, as well as those of the subjects, will be taken into account. Firstly, the results of the analysis of the surveyed Perceived Annoyance Reduction (PAR) and its correlation with the objective parameters of the sound barriers, intrinsic and extrinsic, will be analyzed. Secondly, that correlation is studied according to the characteristics of the population interviewed and different types of emitted sound.

The observed limits of these objective parameters are investigated, trying to address the following questions: Does it make sense to continuously improve the results of target objective indices? Does the human ear respond in a linear way to this improvement? Is there a possible saturation limit beyond which the improvement of the barriers is no longer useful, since the human ear does not perceive this improvement? In fact, if a saturation limit can be set, it would be very interesting to be able to define the range in which this saturation occurs, as this would correspond to the limit for improving the objective sound attenuation of these reducing noise devices.

In short, this work aims to address the psychoacoustic research field, by studying the human perception of noise under the influence of noise reducing devices, such as acoustic barriers, that are used to attenuate road traffic noise.

4.5.3.- Testing methodology

This section will present the design and methodology of the subjective experiment that was carried out. Then, the type of traffic noise and the adopted signal processing procedure to induce different degrees of sound attenuation will be explained. Finally, details will be given regarding the procedure followed for the collection of information through listening tests.

The listening surveys present an international character, and they were carried out at both the offices of the Department of Civil Engineering of the Universidade de Coimbra (in Portugal), and at the offices of the Sonic Crystal Technology Research Group at the Universitat Politècnica de València (in Spain).

Sample of participants

To develop the present study a sample of 90 people, from two different countries (45 in Spain and 45 in Portugal), voluntarily participated in a listening survey, defined in close agreement with the objectives already stated. The ages of the respondents ranged from 18 to 61 years old and gender-balance rules were observed. The sample of participants on this study include mainly university students, doctoral students, university professors and professionals from other sectors.

Noise stimuli

Traffic noise spectra and noise attenuation filters

Since the scope of the present study involves the assessment of noise reducing devices, representative stimuli of road traffic noise had to be monitored in real conditions. Therefore, dozens of road traffic noise samples were recorded, in the vicinity of important roadways, and, at the end, a set of 3 noise samples were selected as being representative of the most interesting types of noise for this study (city or urban traffic noise and road or motorway traffic noise), as well as one particularly annoying road traffic noise that was also included, corresponding to a motorbike noise sample. On the other hand, one of the selected traffic noise samples was registered from vehicles in an urban environment, and the other two corresponded to vehicles passing on the motorway (separately, light vehicles and motorcycles). In Figure 33, the sound spectra of the three selected traffic noise signals (A, B and C) can be observed.

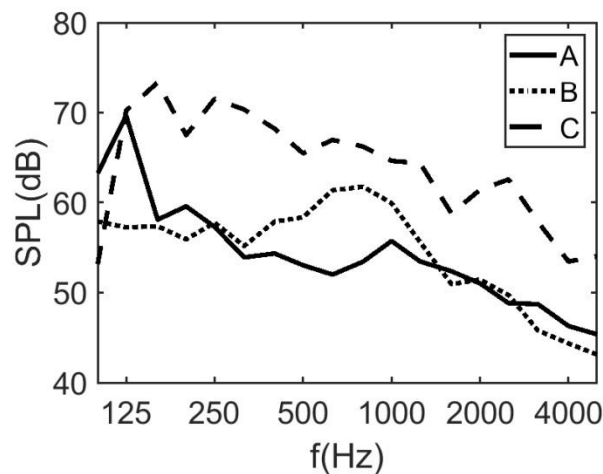


Figure. 33. Sound spectra in one-third octave frequency bands of the noise traffic recordings selected for the listening tests: (A) light vehicles at urban speed; (B) light vehicles on motorways; (C) motorcycles on motorways.

	A	B	C
SPL (dB)	71.9	69.5	79.7
SPL (dBA)	63.5	66.9	74.7

Table. 2. Global Sound Pressure Level (SPL) values for each type of traffic sound emission selected for the study, in dB and dB(A).

These traffic sounds were chosen since they exhibit sufficiently evident spectral differences between them, as can be seen in Figure 33 and in the corresponding global Sound Pressure Levels summarized in Table 2.

Once the traffic noise signals were selected, corresponding to the sound emissions, different sound attenuation filters were mathematically applied to each signal by post-processing the original signals. The attenuation filters represent the implementation of different noise reducing devices, and they were calculated from the data of the insertion loss

values of three selected noise barrier types, with distinct characteristics, namely a classic sonic crystal noise barrier, an absorbent sonic crystal noise barrier, and a traditional continuous noise barrier. The sound attenuation filters were applied in one-third octave frequency bands, in the range between 100 and 5000 Hz, since these are the limiting bands used in the standard defining the normalized traffic noise spectrum [38].

The simulated noise barriers, regardless of their type, have always been considered with a height of 3 m. The traditional noise barrier has been considered with an estimated surface weight of 21 kg/m², and the two sonic crystal noise barriers composed by three rows of dispersers, periodically organized in a square lattice mesh, with a regular spacing between the centers of the cylinders of 0.17 m and a filling factor of 40%.

Three different attenuation scenarios have been simulated for each noise barrier, with distinct relative positions between the noise emitter and the receiver with respect to the barrier (see schematic illustrations in Table 2 – I, II and III, represented in Figure 34, respectively, by continuous, dotted and dashed lines). For each noise barrier type, the three different situations (I, II and III) have been taken into account for the numerical evaluation of the insertion loss values along the frequency range, IL_i , which corresponds to a considerable number and variety of attenuation situations being simulated.

Therefore, situation I is simulating a semicircular sound wavefront being emitted from the ground level, at a distance of 2.5 m from the noise screen, and the receiver is located at a distance of 1 m from the screen and at a height of 1 m from the ground. Then, in situation II, an incident plane wave has been considered and a receiver has been simulated at a distance of 1 m from the screen and at a height of 1 m from the ground. Finally, in situation III, an emitter has been simulated as an incident plane wave and the receiver has been placed at a distance of 4.5 m from the noise barrier and at a height of 2.75 m from the ground. In short, the computed sound stimuli database includes 9 different possibilities of noise attenuation, for each selected sound signal. With all these sound stimuli, the database used to generate the attenuation filters in the listening experience has been completely and adequately generated.

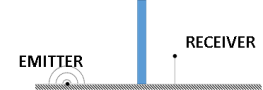
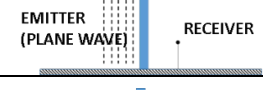
EMITTER/RECEIVER SITUATION				
		$DL_{SI} = 4,98 \text{ dB(A)}$	$DL_{SI} = 11,1 \text{ dB(A)}$	$DL_{SI} = 26,4 \text{ dB(A)}$
I		$D_{IL,Atr} = 5 \text{ dB(A)}$ Sample 3	$D_{IL,Atr} = 11 \text{ dB(A)}$ Sample 7	$D_{IL,Atr} = 22 \text{ dB(A)}$ Sample 9
II		$D_{IL,Atr} = 4.8 \text{ dB(A)}$ Sample 2	$D_{IL,Atr} = 10.5 \text{ dB(A)}$ Sample 6	$D_{IL,Atr} = 17 \text{ dB(A)}$ Sample 8
III		$D_{IL,Atr} = 3.7 \text{ dB(A)}$ Sample 1	$D_{IL,Atr} = 6.5 \text{ dB(A)}$ Sample 4	$D_{IL,Atr} = 7.8 \text{ dB(A)}$ Sample 5

Table 3. Representation of noise barriers configurations, and estimated insertion loss parameters, $D_{IL,Atr}$, obtained from the intrinsic characteristics of the three types of noise barriers (DL_{SI}) and extrinsic characteristics related to the emission and reception relative positions (situations I, II and III).

In order to obtain the attenuation filters associated to each sample, and taking into account not only the intrinsic characteristics of each noise barrier but also the particular geometry and configuration (for example, noise barrier height, type of generated sound wave, position of the emitting source and receiver), a simple methodology has been adopted, based on the Huygens-Frenel-Kirchoff principle. In fact, the portion of the acoustic energy not blocked by the noise screen has been calculated numerically, using a 2D simulation model, based on a Finite Difference in the Time Domain (FDTD) method previously developed and validated by the authors [39]. Then, the two contributions at the receiver, namely the sound traveling over the noise barrier and the sound going through the noise screen, are added assuming incoherence of both contributions. One should note that the second contribution, the sound going through the noise screen, is partially attenuated in comparison to the incident sound wave. The acoustic attenuation provided by the noise barriers is estimated from the sound reduction index of each noise barrier. Further details can be found at [40].

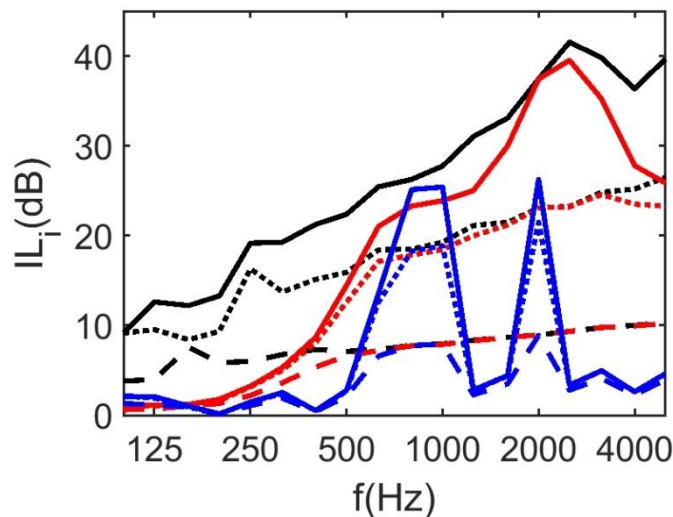


Figure. 34. Estimated insertion loss levels, IL_i , along the analyzed frequency range, for the 9 sound attenuation samples in one-third octave bands: different situations I, II, III represented, respectively, as continuous, dotted and dashed lines; on the other hand, traditional noise barrier, sonic crystal noise barrier with absorbent scatterers and classic sonic crystal noise barrier represented in lines black, red and blue, respectively.

As it can be seen in Figure 34, the classic sonic crystal noise barrier, incorporating completely rigid and reflective scatterers, acts as very selective attenuation filters, only affecting very specific ranges of frequencies. These same crystal elements, when coated with absorbent material, leads to the amplification of their attenuation capacity to the medium and high frequencies, but not in the lower range of frequencies. In reality, only traditional continuous noise barriers can present some attenuation at low frequencies, while exhibiting increasing sound reduction values with the frequency increase.

Objective parameters characterizing noise mitigation

In this study, the sound attenuation provided by noise barriers is expressed by the airborne sound reduction single parameter, DL_{St} , attending to intrinsic features of the

mitigation devices. This parameter arises by taking into account the energy losses when the sound waves crosses the barrier. On the other hand, taking also into account other extrinsic features, such as the energy that is diffracted at the top of the noise barrier or the relative position of the noise emitter and receiver, the single parameter defining the noise barrier's insertion loss, $D_{ILA, tr}$, is used too.

In both cases, the information corresponding to the frequency spectrum in one-third octave bands is weighted into single value ratings, according to the following expressions.

The airborne sound insulation rating, DL_{SI} , has been evaluated following standard [27], being weighted with the standardized traffic noise spectrum [38]:

$$DL_{SI} = -10 \log \left[\frac{\sum_{i=m}^{18} 10^{0,1L_i} 10^{-0,1SI_i}}{\sum_{i=m}^{18} 10^{0,1L_i}} \right] \quad (12)$$

where:

L_i is the A-weighted standard sound pressure level, in decibels, of road traffic noise within the i th one-third octave band of the spectrum defined in EN 1793-3 [38],

SI_i is the acoustic reduction index, in the i th one-third octave band, of the noise barrier.

This parameter has been selected to take into account the intrinsic characteristics of the noise barriers being analyzed.

Additionally, in order to quantify the acoustic performance, accounting for the different extrinsic characteristics of each noise barrier, the single rating parameter $D_{ILA, tr}$ has also been calculated, based on standards [27, 28], ensuring that both parameters are equally weighted (Table 4).

$$D_{ILA, tr} = -10 \log \frac{\sum_{i=1}^{18} 10^{0,1L_i} 10^{-0,1IL_i}}{\sum_{i=1}^{18} 10^{0,1L_i}} \quad (13)$$

where:

IL_i is Insertion Loss of the noise barrier, in the i th one-third octave band.

Therefore, in both cases, the noise barriers sound attenuation ratings were weighted by the A-weighting curve and the normalized traffic noise spectrum [38] and evaluated by single-number indices as already mentioned (Table 4). The computed single-number ratings characterizing the three types of noise barriers and the three situations being analyzed are presented in Table 3, ranging from 3.7 dB(A), for the classic sonic crystal noise barrier under situation III, to a maximum attenuation performance of 22 dB(A), corresponding to the traditional noise barrier under situation I.

SI_i IL_i Frequency parameters. One value for each i^{th} one-third octave band.

DL_{SI}	$D_{IL,Atr}$	Single-number ratings, weighted by the A-weighting curve and the normalized traffic noise spectrum.
-----------	--------------	---

Table. 4. Objective parameters used in the study

Listening survey procedure

The present study was developed in two South European countries and therefore in two different sites. In order to ensure analogous environments in both countries for performing the listening tests, the use of a dedicated headphone system in the survey, connected to a laptop computer from which the sound emission was controlled, was considered to be more appropriate for the accuracy of the responses. The conditions and environments where the listening tests took place were controlled to ensure that the conditions during all experiments were similar. In fact, working with the same laptop and a dedicated headphone system ensured that the conditions were equivalent, given that the same devices were used in both cases.

An application was designed and implemented in MATLAB R2019 to control and perform the listening survey. It allowed for the clear presentation of the purpose of the survey and operational instructions, then, the ordered emission and listening of the noise signals followed. At the same time, the answers given to the listening tests have been collected and successfully stored. Some degree of versatility was given to the participants, being able to repeat each played signal before answering or moving to the next sound. The sound events were sorted and played randomly.

The computer application was designed to allow the rating of perceived attenuation provided by the different noise barriers, based on six possible responses given by the listening test respondents. Therefore, when each test respondent was asked about his Perceived Annoyance Reduction (PAR), compared to the original sound (the emitted traffic noise without attenuation). Below you can see the possible answers that the user could choose to evaluate the PAR value in relation to the numerical value that has subsequently been used in the analysis of results (Nothing=0. Very Little=2. Little=4. Enough=6 Much=8. A lot=10.)

Since the survey participants were either Portuguese or Spanish native speakers, the application was designed in English language to serve all participants equally and avoid misinterpretations related to the question formulation.

The procedure followed during each listening survey carried out is described below. The different steps that have been followed with each interviewed individual are here detailed:

1. First of all, an audiometric test was performed, to rule out individuals with any type of hearing defect.

2. After the audiometric test, the procedure of the listening survey was explained. A presentation was used to ensure that all test respondents received the same information.

3. The listening survey began when the individual was comfortably installed and the dedicated headphone systems correctly put on. The noise signals were reproduced, for the first time they were played, in pairs (i.e the unfiltered traffic noise sample followed by the noise attenuated by the noise reducing device) so that the test listeners had to select one of the above mentioned options to evaluate the effectiveness of the device, before moving on to the next sound event.

The complete listening test (audiometry, presentation with explanation and noise reduction listening survey) did not take longer than approximately 20 minutes, depending on the number of repetitions of the same sound event that was selected by the respondent.

Respondents were exposed to four series of ten pairs of sounds (first, the unfiltered noise and, then, the attenuated noise). Therefore, each test respondent listened to a total of 40 pairs of noise events. Firstly, they heard all the attenuation combinations referred to noise signal A, then those to noise signal B, and then those to noise signal C. Finally, they listened for a second time to the noise signal of A series. The first series of noise signal A was not registered because the respondents needed some training time to adapt to the listening survey and the computer application they were using for responding.

An analysis of the response times was carried out to check that the familiarization and training phase was long enough, and the average answering delays from all respondents can be observed in Figure 35. The evident stabilization in the average response time, approximately after the first group of 10 questions, seems to indicate that the first part of the listening test, with the first hearing of noise signals A, has been sufficient to adequately train the survey respondents.

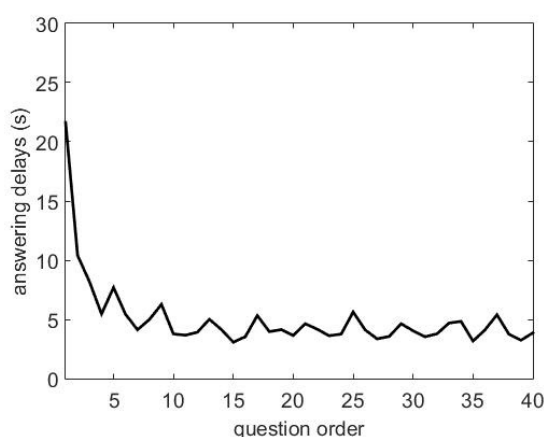


Figure. 35. Average response time of the 40 questions asked.

Within each series of noise signals, as mentioned above, the noise events were played in random order, but always starting with the most attenuated noise signal, i.e. the one with the highest $D_{IL,Atr}$ value. Accordingly, each survey respondent was informed of this

circumstance, allowing this reference noise signal to be taken by the listener as an "anchor" of the survey within each series noise.

Analysis methodology

Once the database was compiled, a statistical analysis of the collected data was carried out. For this purpose, the SPSS statistics software was used, enabling the application of different known statistical evaluations, in two separate phases, as briefly described on Table 5 (the reader who wishes to explore the use of the software and the set of applied statistical techniques can consult Field 2005 [41]).

Phase	Techniques	Expected result
a	- Spearman correlation	Correlation between objective parameters ($DL_{L,Atr}$ and DL_{SI}) and subjective assessment (PAR)
		Correlation between objective parameters ($DL_{L,Atr}$ and DL_{SI}) and subjective assessment (PAR), differentiating by noise type
		Correlation between objective parameters ($DL_{L,Atr}$ and DL_{SI}) and subjective assessment (PAR), differentiating by respondent characteristics
b	- Mean analysis - Kruskal-Wallis test/ Mann-Whitney test - Mean analysis - Friedman test and Wilcoxon's post-hoc analysis	Significant differences in subjective assessment (PAR), according to the age, gender and country of the respondent
		Significant differences in subjective assessment (PAR), according to noise type

Table. 5. Data treatment phases, statistical techniques and expected results.

4.5.4.- Results of the listening test

The analysis of the data collected from the listening survey followed the methodology listed in summary in Table 5. Firstly, the results regarding the main objective of this work are presented, corresponding to the relationship between objective parameters used for noise barriers characterization and the subjective assessment perceived by the respondents to the listening tests. Secondly, significant differences observed in the subjective assessment, detected in the Perceived Annoyance Reduction (PAR) responses, are analysed.

Correlation between objective parameters ($D_{IL,Atr}$ and DL_{SI}) and subjective assessment (PAR)

In this section, the correlation between the objective indicators measuring the acoustic performance of noise reducing devices and the respondents' subjective assessment is analyzed, obtaining a first general correlation, and then distinguishing between the acoustic characteristics and the characteristics of the respondents themselves.

The statistical treatment for this analysis depended on the normality of the data for each variable. Kolmogorov-Smirnov (K-S) test were used to examine the normality of data. The data corresponding to the objective single-number indicators ($D_{IL,Atr}$ and DL_{SI}) and the subjective assessment variable (PAR) follow a non-normal distribution (K-S test, $p < 0.05$), so the Spearman rank-order correlation (non-parametric test) is used.

Correlation between $D_{IL,Atr}$ and DL_{SI} and subjective assessment (PAR)

The Spearman correlation coefficient, significant at $p < 0.05$, between the subjective assessment variable (PAR) and the objective indicators ($D_{IL,Atr}$ and DL_{SI}) are analysed, respectively, in Figure 36 and Figure 37, taking into account all the answers by the test respondents. A high value of the Spearman's correlation coefficient (rho), approaching +1, and a significance level of 0.000, indicates significant and very high correlations with both indicators, especially in Figure 36 with $D_{IL,Atr}$. However, it can also be observed in Figure 37 that, as the values related to the objective sound attenuation parameter (DL_{SI}) increase, the subjective perceived response does not grow proportionally, tending towards a saturation value in the annoyance reduction perception value (PAR).

Spearman's rho $D_{IL,Atr}$-PAR	
Correlation coefficient	0.812
Sig.	0.000

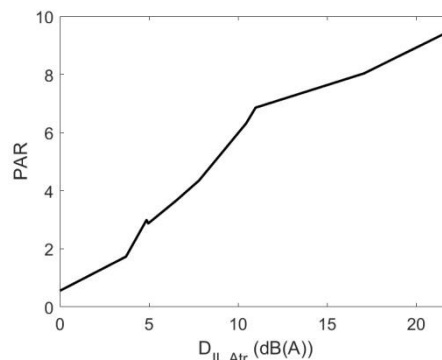


Figure. 36. Correlation between $D_{IL,Atr}$ objective parameter and subjective assessment, PAR.

Spearman's rho DL_{SI}-PAR	
Correlation coefficient	0.695
Sig.	0.000

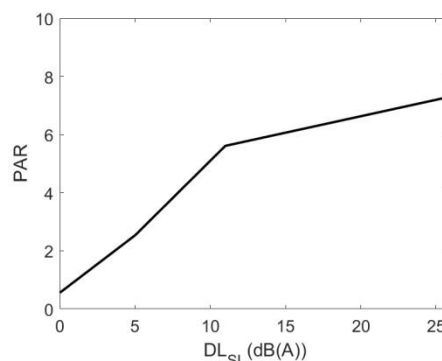


Figure. 37. Correlation between DL_{SI} objective parameter and subjective assessment, PAR.

Correlation between $D_{IL,Atr}$ and DL_{SI} and subjective assessment (PAR), differentiating by noise type

When separated by noise type (A, B and C, as described in of noise stimuli), the interesting level of correlation is still maintained (Figure 38 and Figure 39). Thus, with all three types of noise the correlations between the target indicators ($D_{IL,Atr}$ and DL_{SI}) and PAR subjective assessment are significant ($p < 0.05$) and with a high correlation coefficient (above 0.82). Analyzing both figures 38 and 39, it becomes evident that the test respondents perceive motorcycle traffic noise in a clearly differentiated way from that of light vehicles, either in urban areas or in motorways. In fact, the subjective annoyance perception of the motorbike traffic noise generates exhibit lower values of PAR, independently of the type of noise barrier being used to mitigate traffic noise. Once again, the behavior observed by the correlations of Figure 39 illustrate the presence of a saturation value when dealing with the single-number rating related to the insertion loss provided by the noise barriers ($D_{IL,Atr}$).

Spearman's rho	NOISE TYPE ($D_{IL,Atr}$ -PAR)		
	Urban (A)	Motorway (B)	Motorbike (C)
Correlation coefficient	0.833	0.826	0.821
Sig.	0.000	0.000	0.000

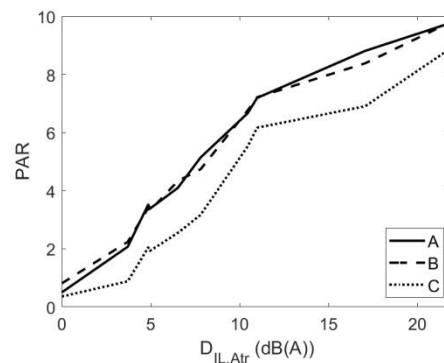


Figure 38. Correlation between $D_{IL,Atr}$ objective parameter and PAR, separating by noise type.

Spearman's rho	NOISE TYPE (DL_{SI} -PAR)		
	Urban (A)	Motorway (B)	Motorbike (C)
Correlation coefficient	0.731	0.706	0.685
Sig.	0.000	0.000	0.000

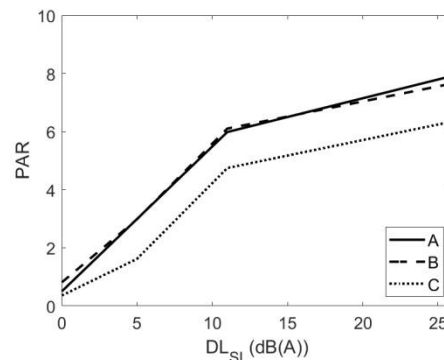


Figure 39. Correlation between DL_{SI} objective parameter and PAR, separating by noise type.

Correlation between $D_{IL,Atr}$ and DL_{SI} and subjective assessment (PAR), differentiating by respondent characteristics

Two respondent characteristics can now be considered, namely the country where each part of the listening test took place and the gender of the test respondents. Very high and significant correlations ($p < 0.05$) are observed when separating the analysis of results by country, with higher Spearman's correlation coefficients in the case of Portugal. The Portuguese individuals that participated in the listening test have perceived the changes in the annoyance reduction with slightly greater intensity than the Spanish respondents (Figure 40 and Figure 41), in terms of the effectiveness of the noise barriers, independently

of the type of the noise barrier considered. This could be an interesting result, taking into account the differences between the regulations related to environmental noise control between the two countries.

Spearman's rho	COUNTRY ($D_{IL,Atr}$ -PAR)	
	Spain	Portugal
Correlation coefficient	0.807	0.823
Sig.	0.000	0.000

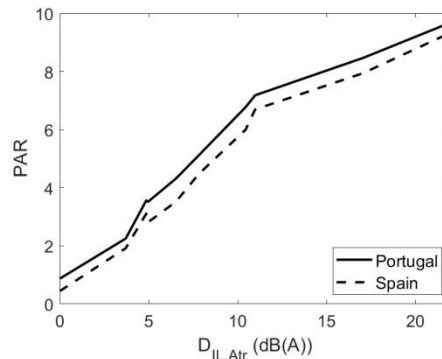


Figure. 40. Correlation between $D_{IL,Atr}$ objective parameter and PAR, separating by country

Spearman's rho	COUNTRY (DL_{SI} -PAR)	
	Spain	Portugal
Correlation coefficient	0.689	0.707
Sig.	0.000	0.000

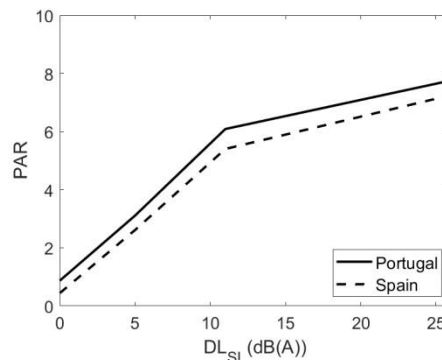


Figure. 41. Correlation between DL_{SI} objective parameter and PAR, separating by country

Performing the statistical analysis while separating the listening test sample between men and women respondents, a strong correlation is still maintained (cf. Figure 42 and Figure 43). In general, women have higher Spearman's coefficient correlations with both objective indicators, $D_{IL,Atr}$ and DL_{SI} . The graphic representations demonstrate that the female respondents are more sensitive to noise or, in other words, that there is less reduction in the perception of noise annoyance by women, in any of the situations herein studied.

Spearman's rho	GENDER ($D_{IL,Atr}$ -PAR)	
	Male	Female
Correlation coefficient	0.808	0.837
Sig.	0.000	0.000

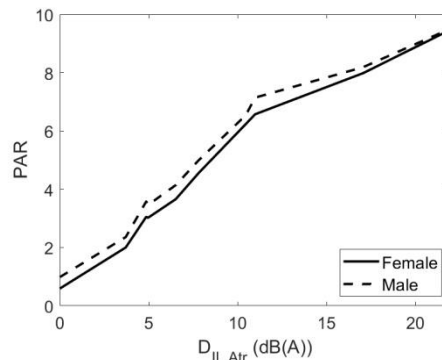


Figure. 42. Correlation between $D_{IL,Atr}$ objective parameter and PAR, separating by gender

Spearman's rho	GENDER (DL_{SI} -PAR)	
	Male	Female
Correlation coefficient	0.690	0.718
Sig.	0.000	0.000

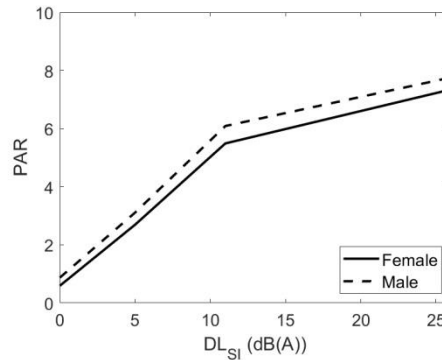


Figure. 43. Correlation between DL_{SI} objective parameter and PAR, separating by gender

The analysis of the collected data, differentiating by the age of the respondents is not here presented because, as it will be seen in Section of analysis of significant differences in assessment, there are no significant differences in the subjective parameter PAR, depending on the age of the respondents ($p=0.113$)

Analysis of significant differences in assessment

In this section, possible significant differences in the Perceived Annoyance Reduction assessment (PAR) by all participants are now analyzed according to their own characteristics (for instance, age, gender and country) and the acoustic characteristics of the traffic noise being mitigated by the devices (the three noise types).

Since the collected data representing subjective perception (PAR) do not follow a normal distribution (K-S test, $p<0.05$), different non-parametric tests are adopted for the following statistical analyses: Mann-Whitney and Kruskal-Wallis tests, respectively comparing 2 (for country or gender characteristics) or k (for respondents age) independent samples; and Friedman test comparing k (noise type) dependent samples).

Significant differences in subjective assessment (PAR), according to the age, gender and country of the respondents

Through the application of the Kruskal-Wallis test it is possible to verify that there are no significant differences in the subjective evaluation PAR depending on age of the respondents (Chi square=5.964; $df=3$; $p=0.113$). Therefore, and since the population responds homogeneously in terms of age, this variable does not segment the sample in the rest of the analysis.

On the other hand, the application of the Mann-Whitney test highlights significant differences in the degree of the perceived annoyance reduction, depending on the respondent gender (Mann-Whitney $U=488492.500$; $p=0.000$) and country (Mann-Whitney $U=574146.000$; $p=0.000$). In terms of gender, Figure 44 shows that men present higher PAR values than women. With regard to the country, the subjective evaluations of the listening tests in Portugal, in relation to PAR, correspond to slightly higher values than those carried out in Spain.

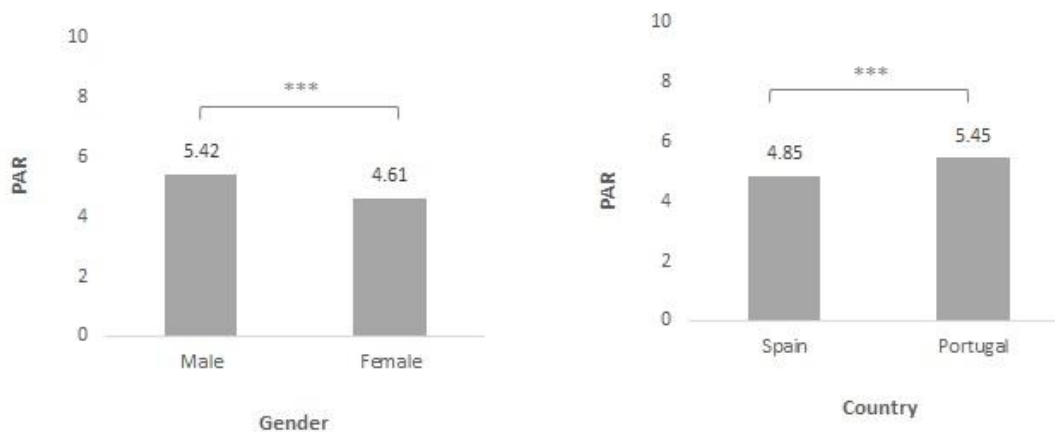


Figure. 44. Average levels of PAR by gender and by country. Keys indicate the comparisons and asterisks the significance level (* $p < 0.05$, ** $p < 0.01$, *** $p < 0.001$).

Significant differences in subjective assessment (PAR), according to the emitted traffic noise type

The application of the non-parametric Friedman statistical test indicates that there are significant differences in the subjective evaluation PAR, depending on the type of the traffic noise emitted (Chi square= 385. 334; $df=2$; $p=0.000$). By performing a post-hoc analysis with Wilcoxon signed-rank tests, important correlations are observed between motorbike traffic noise and the other two types of traffic noise, urban traffic noise ($p=0.000$) and motorway traffic noise ($p=0.000$). In Figure 45, a lower level of the subjective evaluation PAR can be noticed, in the case of motorbike induced traffic noise, in comparison to PAR values for light vehicles both in urban and motorway environments.

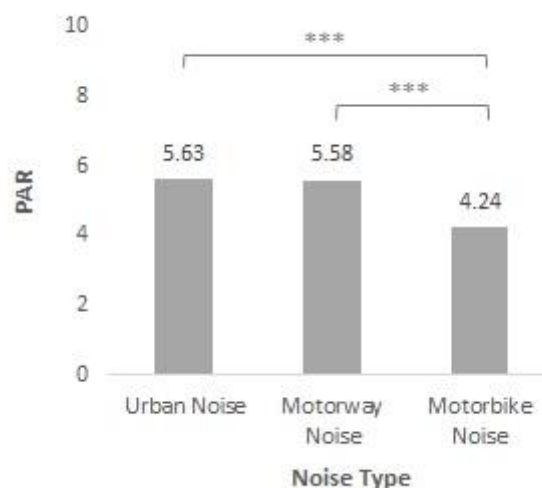


Figure. 45. Average levels of PAR by emitted traffic noise type. Keys indicate the comparisons and asterisks the significance level (* $p < 0.05$, ** $p < 0.01$, *** $p < 0.001$).

Finally, when separating the responses to the listening test by gender and by country, an analogous situation can be observed, with higher subjective PAR ratings for

male respondents and Portuguese tests (Figure 46). The application of the non-parametric Friedman statistical test enables detecting significant differences in PAR values, depending on the type of emitted traffic noise in male (Chi square=132.831; df=2; p=0.000) and female (Chi square=251.034; df=2; p=0.000) test respondents, and in the Spanish (Chi square=227.752; df=2; p=0.000) and Portuguese (Chi-square=160.018; df=2; p=0.000) parts of the listening test performed. Additionally, by using post-hoc analyses with Wilcoxon signed-rank tests, it is possible to see that, in all cases, these differences occur once again between the motorbike traffic noise and the other two types of emitted traffic noise.

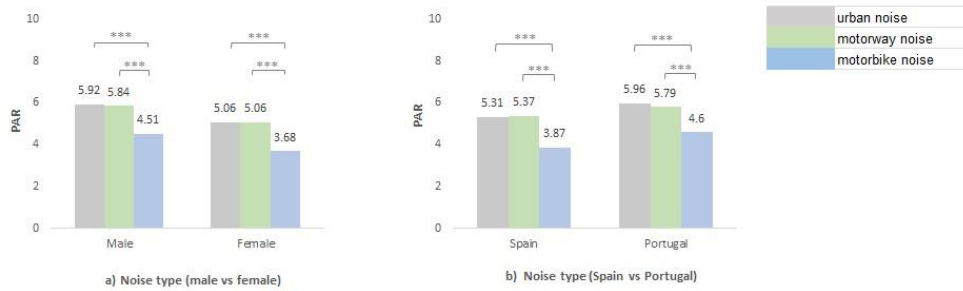


Figure. 46. Average levels of PAR by emitted traffic noise type, according to gender and country. Keys indicate the comparisons and asterisks the significance level (* $p < 0.05$, ** $p < 0.01$, *** $p < 0.001$).

4.5.5.- Discussion

Different research studies have been developed on the effectiveness of some devices that provide acoustic insulation, both in terms of airborne sound reduction and impact sound insulation in building acoustics context [35, 36, 32, 43]. Also, some perception studies have been carried out on the acoustic comfort provided by noise reducing devices installed close to transport infrastructures (roads and railways) [44, 45], where either acoustic performance of noise barriers and their relation with the subjective annoyance reduction were studied, or predictions of annoyance and exposure-response curves (in L_{den}) were compared searching for significant correspondences.

However, the adequacy of the objective parameters used with respect to the annoyance in environmental noise situations has not been sufficiently studied. The effects of audio-visual variations on the perception of the acoustic performance of noise barriers have been considered by Hong and Jeon [37], but not its correlation with objective parameters. In fact, technical interventions for reducing noise levels may not lead to proportional impacts on annoyance reduction [46], according to the objective indices with which they are assessed. Therefore, all of this justifies the interest of the present work.

Currently, in order to evaluate the acoustic performance of a noise barrier, the most frequently used target indices are the above described intrinsic parameters, DL_R and DL_{SI} , depending whether they are measured on diffuse sound field or direct sound field conditions. It is common to use only the single number DL_R or DL_{SI} to determine the quality

of a noise barrier. In fact, some recent technical publications even establish requirements of a minimum sound insulation (DL_{SI}) value of 28 dB [47]. But, as we have seen, there is another single number index that considers, not only the intrinsic conditions of the noise barrier itself, but also the extrinsic conditions of the implemented noise barrier and the measurement environment, representing an Insertion Loss rating, standardized in ISO 10847 [28]. Based on this standard, a single-number quantity for rating the insertion loss weighted by standardized traffic noise spectrum has been defined, $D_{IL,A,tr}$.

In the present study, the correlation between these objective indices that characterize the acoustic barriers (DL_{SI} and $D_{IL,A,tr}$) and the perception of annoyance reduction (PAR) felt by respondents of a listening test is analyzed. In fact, a high correlation between these objective and subjective indices has been observed.

Previous studies have shown that the configuration of the urban environment determines the effectiveness of noise barriers, thus demonstrating the importance of their extrinsic characteristics [48]. In the present work, it can be verified that, indeed, there is a better correlation between the subjective evaluation PAR and the objective index which considers the insertion loss achieved by the noise barrier and its extrinsic characteristics ($D_{IL,A,tr}$) than the single-number rating that considers intrinsic characteristics as the airborne sound reduction (DL_{SI}).

Another interesting aspect extracted from the described results is that, for both objective indices, the subjective evaluation PAR is getting saturated above certain values of attenuation; in other words, the increase of attenuation provided by the noise reduction devices, does not lead to a relevant increase of the subjective reduction PAR. In fact, above certain values of airborne noise reduction, the perceived acoustic comfort hardly improves at all. In 1968, Maekawa [49] already pointed out that it was not possible to achieve noise barrier attenuation above a certain value. This limit, verified experimentally, depends on the particular thickness of the noise barrier and ranges between 20 and 25 dB. The results of the present psychoacoustic test confirm this conclusion. This is an important factor to bear in mind when designing noise reduction devices, since efforts should not focus on increasing attenuation performance above certain values, but once these values are reached, research efforts should better be focused on obtaining lighter devices, that require less foundations, smaller areas occupied at the sides of the infrastructures and better acceptance by citizens.

Concerning secondary objectives of the study, although previous studies have found that demographic variables such as age, gender and type of housing are unimportant noise annoyance modifiers in steady state noise conditions [50, 51], after the analysis of the results with respect to the characteristics of the test respondents in the present study it can be seen that the correlation between subjective and objective data is present in all cases, but there are significant differences with respect to the gender and nationality of those surveyed. Thus, comparing the results between men and women, female respondents were more demanding than male respondents when it comes to evaluating acoustic comfort. The same happens in the case of Spanish respondents as compared to Portuguese ones, being the Spaniards more demanding in their answers than the Portuguese. Then, in view of the results, gender and nationality are relevant factors to consider when evaluating the effectiveness of noise reduction devices.

Significant differences were also observed with respect to the traffic noise used as emission source. The level of correlation is very similar in all three cases; however, the motorbike traffic noise has been shown to have a smaller reduction in annoyance perception than the rest. These differences in the perceived annoyance reduction as a function of emitted and attenuated noise are in accordance with what has been found in previous studies [42].

The results obtained in this work are very interesting, especially from the point of view of non-proportionality and the observed trend to saturation of the perceived reduction of traffic noise annoyance. This should encourage further studies aimed at finding the best noise barrier characterization index and clearly verifying what attenuation limits may exist.

The data analysed in this paper enables the identification of an interesting trend, that requires further research in order to get its consolidation, when considering different frequency weightings from the A-weighting curve. In Figure 47, the results already presented in Figure 36 are now being compared to alternative results obtained by replacing the A-weighting with other frequency weighting curves. Bear in mind that the weighting curves A, B, C, and others, were established to be use at different average sound levels. In fact, the A-weighting curve was originally introduced to deal with lower sound levels (around 40 phon). On the other hand, the B-weighting curve corresponds approximately to 60 phon, and it is appropriate to deal with intermediate sound levels. In addition, we have also computed and introduced in the present analysis the -weighting curve inspired in the equal loudness of 10 phon, which has been designated as "alpha" in Figure 47, allowing for the representation of very low sound levels. Attention should also be drawn to the fact that the A-weighting curve is nowadays widely used due to its good correlation between the pollution measurements and industrial noise, in relation to the occupational deafness and human hearing annoyance. Therefore, Figure 47 illustrates that the higher the loudness level considered in phon, the relationship between both objective and subjective indices represented in this figure become less linear. It should be noted that the main difference between the "alpha", A and B-weightings is the relevance level of the low frequencies sound components. This observed trend seems to indicate that the usual procedures could be overestimating the relevance of low frequencies in the evaluation of noise barriers for reducing road traffic noise. Further research in this area will be necessary to reach conclusions.

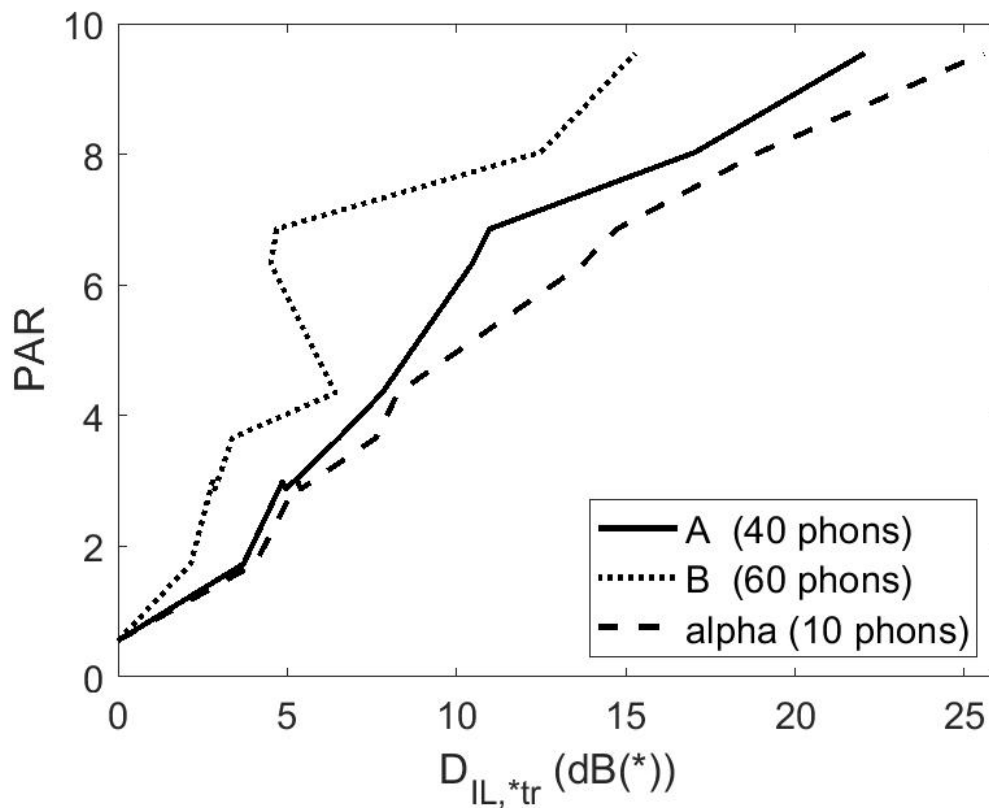


Figure. 47. Perceived annoyance reduction (PAR) versus three different possible frequency weighting curves applied for computing objective indices $D_{IL,*tr}$.

4.5.6.- Conclusions

Results have been presented regarding a psychoacoustic study where the response of a group of individuals has been studied in relation to the reduction of perceived sound annoyance when traffic noise is attenuated by using a noise barrier. The study was based on sound stimuli using traffic noise, with two stimuli related to light vehicles (driving in urban areas and on motorways) and one related to motorcycles traffic noise emission. On the other hand, these sound stimuli have been filtered taking into account 9 possible attenuations of greater or lesser objective value.

Two particularly interesting results have been obtained from the analysis of the data obtained. Firstly, it is observed that the reduction of perceived annoyance does not increase proportionally to the attenuation of the noise reducing device. A relatively proportional growth is observed in the range of the first 10 dB of noise attenuation, but from that point onwards the slope grows less and with a certain trend to a saturation level. This seems to indicate that the improvement in noise attenuation, estimated by the introduction of a noise barrier has an upper limit value.

On the other hand, significant differences have been noticed between the opinion of individuals consulted on the basis of their gender and place of origin, observing that, in general, female respondents are more sensitive to noise, or, in other words, the level of perceived annoyance reduction are always lower than those of male respondents. Regarding the place of listening test accomplishment, a greater level of sensitivity

corresponds to the sample of respondents from Portugal, i.e., the Spaniards seem to detect a greater reduction in perceived noise annoyance, which could possibly indicate a lower hearing sensitivity. Besides the interest of the present research study, more listening tests should be carried out taking into account these significant differences and expanding the database of noise attenuation filters in order to more accurately assess the maximum perceived reduction saturation values

Additionally, it shall be also mentioned that the presence of a saturation limit on the perceived annoyance reduction provided by noise barriers could be very relevant if other objectives are included in the design process, widening the study to supplemental characteristics, such as, increasing fluid permeability to wind, reducing visual impact, minimizing space occupied by the noise barriers, reducing the foundation structural requirements or improving aesthetics in the design of innovative noise barriers. In this case, the use of multi-objective evolutionary optimization techniques can be applied. A number of published works already propose the use of such techniques, to increase the performance of sonic crystals noise reducing devices, mainly due to the simplicity of the genetic algorithmic codification [11, 52, 53]. The presence of the above mentioned saturation limit would lead to a convex Pareto front that makes search for compromise solutions with good performance while attending to all cost functions easier.

Both acoustic and landscape issues need to be taken into consideration to design effective noise barriers in urban environments [37]. For this reason, following these conclusions, further research could be carrying out of audiovisual perception tests to measure the effective performance of traditional barriers and SCAS.

4.5.7.- References

- [1] European Environment Agency (2014) Noise in Europe 2014.
- [2] Murphy, E. and King, E.A. (2014) Environmental Noise Pollution. Elsevier.
- [3] The SMILE Consortium (2003) Guidelines for road traffic noise abatement.
- [4] Gidlöf-Gunnarsson, A., & Öhrström, E. (2007). Noise and well-being in urban residential environments: The potential role of perceived availability to nearby green areas. *Landscape and urban planning*, 83(2-3), 115-126.
- [5] WHO, 2018. Environmental Noise Guidelines for the European Region. World Health Organization. Regional Office for Europe, Copenhagen.
- [6] EC Directive, Directive 2002/49/EC of the European Parliament and of the Council of 25 June 2002 relating to the assessment and management of environmental Noise, Official
- [7] Department of Transportation, Federal Highway Administration U.S.A., Keeping the Noise Down, Highway Traffic Noise Barriers, Washington, 2001, 2001 FHWA-EP-01e004 HEPN/2-01 (10M) E.
- [8]. D. C. Hothersall, S. N. Chandler-Wilde and M. N. Hajmirzae, Efficiency of single noise barriers, *J. Sound Vibr.* 146 (1991) 303–322.

-
- [9] R. L. Wayson, A. MacDonald, A. El-Aassar and W. Arner, Continued evaluation of noise barriers in Florida, Florida Dept. Transportation (2002).
- [10] Kloth, M., Vancluyesen, K., Clement, F. & Lars Ellebjerg, P. (2008) Practitioner Handbook for Local Noise Action Plans: Recommendations from the SILENCE project.
- [11] Van Renterghem, T. Forssén, J. ; Attenborough, K. et al. (2015) "Using natural means to reduce surface transport noise during propagation outdoors". *Applied Acoustics*, vol. 92 pp. 86-101. <https://doi.org/10.1016/j.apacoust.2015.01.004>
- [12] Peiró-Torres, M. P., Navarro, M. P., Ferri, M., Bravo, J. M., Sánchez-Pérez, J. V., & Redondo, J. (2019). Sonic Crystals Acoustic Screens and Diffusers. *Applied Acoustics*, 148, 399-408.
- [13] FHWA U.S.A, 2011. Keeping the Noise Down. Highway Traffic Noise Barriers, On line at: <http://journalofcommerce.com/Home/News/2007/7/Keeping-the-noise-down---highway-traffic-noisebarriers-JOC023547W/>.
- [14] M.P. Peiró-Torres , J. Redondo , J.M. Bravo , J.V. Sánchez Pérez , Open noise barriers based on sonic crystals. *Advances in noise control in transport infrastructures, Transportation Research Procedia* 18 (2016) 392 – 398, doi: 10.1016/j.trpro.2016.12.051.
- [15] Sergio Castiñeira-Ibañez, Constanza Rubio, Juan Vicente Sanchez-Perez Environmental noise control during its transmission phase to protect buildings. Design model for acoustic barriers based on arrays of isolated scatterers, *Building and Environment* 93 (2015) 179-185 <http://dx.doi.org/10.1016/j.buildenv.2015.07.002>.
- [16] Martínez-Sala, R. ; Sancho, J. ; Sánchez, J.V. ; Gómez, V. ; Llinares, J. ; Meseguer, F. Sound attenuation by sculpture, *Nature*, 378, 1995, pp. 241. <http://dx.doi.org/10.1038/378241a0>.
- [17] Chen, Y. Y., Ye, Z., 2001. Theoretical analysis of acoustic stop bands in two-dimensional periodic scattering arrays. *Physical Review E*, 64(3), 036616.
- [18] Sigalas, M. M., Economou, E. N., 1992. Elastic and acoustic wave band structure. *Journal of sound and vibration*, 158(2), 377-382.
- [19] Sánchez-Pérez, J. V., Caballero, D., Martínez-Sala, R., Rubio, C., Sánchez-Dehesa, J., Meseguer, F., Llinares J., Gálvez, F., 1998. Sound attenuation by a two-dimensional array of rigid cylinders. *Physical Review Letters*, 80(24), 5325.
- [20] García-Chocano, V.M.; Cabrera, S.; Sánchez-Dehesa, J. Broadband sound absorption by lattices of microperforated cylindrical shell, *Appl. Phys. Lett.*, vol. 101 (18), 2012, 184101.
- [21] Romero-García, V., Sánchez-Pérez, J. V., Garcia-Raffi, L. M., 2011. Tunable wideband bandstop acoustic filter based on two-dimensional multiphysical phenomena periodic systems. *Journal of applied physics*, 110(1), 014904.
- [22] Castiñeira-Ibañez, S.; Rubio, C.; Romero-García, V.; Sánchez-Pérez, J.V.; García-Raffi, L.M. Design, Manufacture and Characterization of an Acoustic Barrier Made of Multi-

Phenomena Cylindrical Scatterers Arranged in a Fractal-Based Geometry, *Archives of Acoustics*, vol. 37 (4), 2012, pp. 455–462.

[23] Godinho, L.; Santos, P.G.; Amado Mendes, P.; Pereira, A.; Martins, M., 2016, Experimental and numerical analysis of sustainable sonic crystal barriers based on timber logs, in *EuroRegio 2016 - TECNIACÚSTICA 2016*, ISBN: 978-84-87985-27-0.

[24] Fredianelli, L., Del Pizzo, A., & Licitra, G. (2019). Recent developments in sonic crystals as barriers for road traffic noise mitigation. *Environments*, 6(2), 14.

[25] Gulia P., Gupta A. (2020) Multi-directional Sound Reduction by Slitted Sonic Crystal. In: Biswal B., Sarkar B., Mahanta P. (eds) *Advances in Mechanical Engineering*. (pp. 1099-1108) *Lecture Notes in Mechanical Engineering*. Springer, Singapore

[26] EN 1793-2 - Road traffic noise reducing devices - Test method for determining the acoustic performance - Part 2: Intrinsic characteristics of airborne sound insulation under diffuse sound field conditions, 2012.

[27] EN 1793-6 - Road traffic noise reducing devices - Test method for determining the acoustic performance - Part 6: Intrinsic characteristics - In situ values of airborne sound insulation under direct sound field conditions, 2012.

[28] ISO 10847 – Acoustics – In-situ determination of insertion loss of outdoor noise barriers of all types, 1997.

[29] P. Guidorzi and M. Garai, "Advancements in Sound Reflection and Airborne Sound Insulation Measurement on Noise Barriers," *Open Journal of Acoustics*, Vol. 3 No. 2A, 2013, pp. 25-38. doi: 10.4236/oja.2013.32A004.

[30] Morandi, F., Miniaci, M., Marzani, A., Barbaresi, L., & Garai, M. (2016). Standardised acoustic characterisation of sonic crystals noise barriers: Sound insulation and reflection properties. *Applied Acoustics*, 114, 294-306.

[31] Dimitrijević, S. M., García-Chocano, V. M., Cervera, F., Roth, E., & Sánchez-Dehesa, J. (2019). Sound Insulation and Reflection Properties of Sonic Crystal Barrier Based on Micro-Perforated Cylinders. *Materials*, 12(17), 2806

[32] Oliva, D., Hongisto, V., & Haapakangas, A. (2017). Annoyance of low-level tonal sounds—Factors affecting the penalty. *Building and Environment*, 123, 404-414.

[33] Hongisto, V., Oliva, D., & Rekola, L. (2015). Subjective and objective rating of spectrally different pseudorandom noises—Implications for speech masking design. *The Journal of the Acoustical Society of America*, 137(3), 1344-1355.

[34] Van Renterghem, T., & Botteldooren, D. (2016). View on outdoor vegetation reduces noise annoyance for dwellers near busy roads. *Landscape and urban planning*, 148, 203-215.

[35] Virjonen, P., Hongisto, V., & Oliva, D. (2016). Optimized single-number quantity for rating the airborne sound insulation of constructions: Living sounds. *The Journal of the Acoustical Society of America*, 140(6), 4428-4436.

-
- [36] Kylliäinen, M., Hongisto, V., Oliva, D., & Rekola, L. (2017). Subjective and objective rating of impact sound insulation of a concrete floor with various coverings. *Acta Acustica united with Acustica*, 103(2), 236-251.
- [37] Hong, J. Y., & Jeon, J. Y. (2014). The effects of audio-visual factors on perceptions of environmental noise barrier performance. *Landscape and Urban Planning*, 125, 28-37.
- [38] EN 1793-3 - Road traffic noise reducing devices - Test method for determining the acoustic performance - Part 3: Normalized traffic noise spectrum
- [39] J. Redondo, R. Picó, B. Roig, M.R. Avis. Time domain simulation of sound diffusers using finite-difference schemes. *Acta Acustica united with Acustica* 93(4) July 2007
- [40] Redondo, J., Godinho, L., & Amado-Mendes, P. (2019, September). Simple method to predict the performance of Noise Barriers. In *INTER-NOISE and NOISE-CON Congress and Conference Proceedings (Vol. 259, No. 6, pp. 3467-3474)*. Institute of Noise Control Engineering.
- [41] Field, A.P., 2005. *Discovering statistics using SPSS*. Sage Publications, London.
- [42] Hongisto, V., Oliva, D., & Keränen, J. (2014). Subjective and objective rating of airborne sound insulation-living sounds. *Acta Acustica united with Acustica*, 100(5), 848-863.
- [43] Kylliäinen, M., Takala, J., Oliva, D., & Hongisto, V. (2016). Justification of standardized level differences in rating of airborne sound insulation between dwellings. *Applied Acoustics*, 102, 12-18.
- [44] Torija, A. J., & Flindell, I. H. (2014). Listening laboratory study of low height roadside noise barrier performance compared against in-situ field data. *Building and environment*, 81, 216-225. <https://doi.org/10.1016/j.buildenv.2014.07.006>
- [45] Nilsson, M. E., & Berglund, B. (2006). Noise annoyance and activity disturbance before and after the erection of a roadside noise barrier. *The Journal of the Acoustical Society of America*, 119(4), 2178-2188. <https://doi.org/10.1121/1.2169906>
- [46] Laszlo, H. E., McRobie, E. S., Stansfeld, S. A., & Hansell, A. L. (2012). Annoyance and other reaction measures to changes in noise exposure—A review. *Science of the total environment*, 435, 551-562. <https://doi.org/10.1016/j.scitotenv.2012.06.112>
- [47] Vanhooreweder, B., Marcocci, S., & De Leo, A. (2017). *State of the Art in Managing Road Traffic Noise: Noise Barriers (No. Technical Report 2017-02)*.
- [48] Sanchez, G. M. E., Van Renterghem, T., Thomas, P., & Botteldooren, D. (2016). The effect of street canyon design on traffic noise exposure along roads. *Building and Environment*, 97, 96-110.
- [49] Maekawa, Z. (1968). Noise reduction by screens. *Applied acoustics*, 1(3), 157-173.
- [50] Bluhm, G., Nordling, E., & Berglund, N. (2004). Road traffic noise and annoyance-An increasing environmental health problem. *Noise and Health*, 6(24), 43.

[51] Fields, J. M. (1992). Effect of personal and situational variables on noise annoyance: With special reference to implications for en route noise. U.S. Department of Commerce, National Technical Information Service

[52] Romero-García, V., Sánchez-Pérez, J. V., García-Raffi, L. M., Herrero, J. M., García-Nieto, S., & Blasco, X. (2009). Hole distribution in phononic crystals: Design and optimization. *The Journal of the Acoustical Society of America*, 125(6), 3774-3783.

[53] J. Redondo, J.V. Sánchez-Pérez, X. Blasco, J.M. Herrero, M. Vorländer. Optimized sound diffusers based on sonic crystals using a multiobjective evolutionary algorithm. *J Acoust Soc Am*, 139 (5) (2016), 10.1121/1.4948580.

5. Discussion

An article titled “Open noise barriers based on Sonic crystals. Advances in noise control in transport infrastructures” has been published in the journal *Transport Research Procedia*. The article reviews the state of the art in the field of acoustic screening and reflects the progress made using CS-based devices in transport infrastructures. Following this publication we have focused on four specific areas:

Firstly, working on understanding the physical properties of SCs and analyzing how different noise control mechanisms used in SC design interact. In particular, we have studied the appearance of destructive interference phenomena between the attenuation bands due to resonance and multiple scattering. We have determined the physical basis of this destructive interference, and have also provided possible solutions to avoid it. This study will help to design SC-based acoustic screens with greater noise control capabilities, increasing the range of attenuated frequencies. The results of this research, as well as the conclusions reached after the study, have been published in the journal *Applied Physics Letters* under the title “Interferences in locally resonant Sonic metamaterials formed from Helmholtz resonators”.

Secondly, we have developed a device that, in addition to screening, has diffusing properties in the noise incidence side in order to provide new functionalities to the SC-based acoustic screens. This new functionality can be very useful in preventing specular reflections that could direct the noise towards areas that are to be protected. To design this device we used multi-objective optimization techniques, in particular evolutionary algorithms. These techniques consist in the generation of an initial population of designs, and combine them to evolve towards designs that present better results in two established objectives. In this case the objectives were better acoustic screening and reflection of the sound towards the noise source in a diffused way. The work has been published in the *Applied Acoustics* journal with the title “Sonic crystals Acoustic Screens and Diffusers”.

Thirdly, we have performed a comparative study of the numerical methods currently used to simulate the behaviour of SC. In this study we have compared the computational costs and the accuracy of the five most commonly used numerical methods, for this type of device according to the bibliography (MS, BEM, FEM, FDTD, MFS)¹. The result of this study has been written in a paper that has been sent to the journal *Acta Acustica* under the title “Insertion loss provided by sonic crystal acoustic screens – assessment of different estimation methods”.

Finally, to complete the work we compiled the user's perception of this new type of acoustic screen. This involved a psychoacoustic study which evaluated the perceived reduction in annoyance provided by traditional acoustic barriers and this new type of screen. We have performed this study in two countries to compare the data and noting significant differences between different factors of the sample surveyed. In addition, to determine if there is correlation in the results we have compared the objective parameters for evaluating the acoustic screens described in the standards with the subjective answers of those surveyed. The most important conclusions are highlighted in an article titled “Correlation between objective and subjective assessment of noise barriers” and which has been accepted for publication in the journal *Applied Acoustics*.

6. Conclusions

In this report, we first present a state of the art review of the advances made in the field of SC-based acoustic screens and then the results of the research carried out during the PhD student's training period, which cover some of the active lines of research in the area of the application of SC to acoustic screens. The main conclusions of the different studies carried out are summarized in this section.

Following the study on the **advances made in the area of SC-based acoustic screens**, it is concluded that:

I) CS-based acoustic screens introduce an important technological advance in the field of acoustic screening, and such technology is mature enough to be used in commercial devices, as they offer multiple advantages over traditional acoustic barriers.

Regarding the study carried out on **interference detected in metamaterials formed by helmholtz resonators**, it has been observed that a reduction in BG occurs when the resonance and BG effects are located at nearby frequencies. In addition, it is also observed that the f_{Bragg} is shifted towards high or low frequencies, depending on the resonance peak frequencies being lower or higher than the f_{Bragg} respectively. Furthermore, this research has shown that:

II) The destructive interference found could be explained by three possibilities: i) the absorption produced by the resonators, ii) the change in directivity of the scattered field due to the orientation of the neck of the resonators, iii) the phase change that occurs in the transmitted wave when an array of resonators is interposed in it instead of an array of rigid cylinders. We have compared the attenuation spectrum of the array of resonators with different entrance orientations to the transmitted wavefront. The phase change produced with resonators with orientations at 0 and 180 degrees was the same, and their attenuation spectrum was equally identical. This was not the case with the other possibilities analyzed. Therefore we have concluded that the detected interference is due to the phase change that occurs in the transmitted wave.

III) Since the explanation of the phenomenon is a phase change of the transmitted wave, this variation can be interpreted as a difference of the space traveled by the wave transmitted through a SC of rigid scatterers, with respect to the wave transmitted in the array of resonators, which could be also interpreted as a change in the lattice constant. This new virtual lattice constant, which has been called "equivalent", would be lower than the real one if the BG occurs at higher frequencies than the resonance and vice versa. Therefore, this proves that the detected interference could be reduced by varying the value of the lattice constant to the "equivalent".

With regard to the study on **SC-based acoustic screens with new functionalities such as diffusion**, we have used a new design tool based on multi-objective optimization. In this case, the objectives to be optimized were acoustic screening and the diffuse reflection of the noise. Our optimization process was carried out with two different configurations, one formed by a single crystal of four rows with a specific lattice constant, and the other formed

by two adjacent crystals with different lattice constant of two rows each. After analyzing the results, it was concluded that:

IV) Both configurations were able to offer these two functionalities, screening and diffusion, in a satisfactory way with a minimum number of rows. But the configuration consisting of two crystals offered better results. We have called these new devices Sonic Crystals Acoustic Screens and Diffusers (SCASAD).

Related to design tools based on optimization, we highlighted the importance of using simulation tools which offer reasonable accuracy with low computational costs. These methods are iterative and require a large number of calculations, therefore for the methodology to be viable it needs to be, not too time-consuming and feasible without a very high-capacity hardware. Thus, we have carried out a **comparative study of the numerical methods used to estimate the acoustic performance of CS-based screens** that are currently used (MS, BEM, FEM, FDTD, MFS)ⁱ, concluding that

V) BEM and MFS are presented as the methods that provide the best accuracy with the lowest computational costs in the evaluation of the acoustic performance of periodic structures. The calculation time was discarded as a parameter to evaluate the performance of the different methods, since this parameter depends on the particular implementation of each method and on the hardware used.

Finally, we have performed a psychoacoustic study to analyze the **correlation between objective and subjective evaluation parameters** related to the work of reducing annoyance associated with this type of screen. For this purpose, we selected a sample of respondents, who were exposed to different traffic sounds attenuated by different types of acoustic barriers, including CS-based acoustic screens and then we evaluated their perception of annoyance reduction after the attenuation of traffic noise. After the statistical analysis of the data collected in the surveys, it was concluded that:

VI) The devices with sound insulation of more than 10dB did not present a linear relationship of these objective parameters with the analyzed subjective perception. This finding is very important when selecting the best screen designs, since not only the objective parameters relating to acoustic insulation should be taken into account. Also, other parameters such as permeability, and the reduction of visual impact should also be taken into account.

VIII) In addition, statistically significant differences were detected between the respondents based on nationality and gender. Portuguese users were more sensitive to the perception of noise and more demanding in terms of the reduction offered by noise-reducing devices than Spaniards. The same applied for female respondents compared to male users.

7. Further research.

Progress in SC research is proving very promising. Their early application in commercial screening should be expected in the near future. However, there are still aspects that require further research. This would make it possible for more technologically advanced devices offering better overall acoustic performance.

This thesis report presents advances in the lines of research that are currently active in this area. However, this research also opens up new possibilities for continuing investigation in this field of acoustic screening.

Thus, further studies on the interferences detected between BG and resonance would be necessary to analyse if there are more destructive interferences between the noise control mechanisms in the SC in order to minimise them and obtain wider attenuation bands.

Adding new functionalities to SC-based acoustic screens, in addition to screening, like the incorporation of diffusers seems interesting. However, the difficulty in achieving acoustic screening and diffusion in the same frequency range has been noted. A more in-depth study of the issue would make it possible to achieve devices that combine both functions more effectively.

As regards selecting the optimum simulation method to be used in each case, it would be interesting to incorporate the computational time in future studies, since less calculation time would reduce the design time, and would make these techniques more viable.

Regarding the study on the subjective evaluation of this type of device, there is still a long way to go. The perceptive studies performed during this thesis period are based only on acoustic exposures but they could also consist of exposing the respondents to visual stimuli to obtain more data from immersive experiences. This would provide real data about the likeability of this new type of screen.

Moreover, the possibilities of reducing the edge diffraction effects of this type of screen would increase significantly the attenuation provided, which opens up a field that has yet to be explored. The application of new design techniques, such as optimization, will be necessary to determine the combination of the scatterers height that best minimizes this effect, or to analyze other ways of reducing this edge diffraction in this type of screen.

So, there is still work to be done.

ⁱ MS: Multiple scattering; BEM: Boundary element method; FEM: Finite element method; FDTD: Finite difference time domain; MFS: Method of fundamental solution.